



National Library
of Canada

Bibliothèque nationale
du Canada

Canadian Theses Service

Service des thèses canadiennes

Ottawa, Canada
K1A 0N4

NOTICE

The quality of this microform is heavily dependent upon the quality of the original thesis submitted for microfilming. Every effort has been made to ensure the highest quality of reproduction possible.

If pages are missing, contact the university which granted the degree.

Some pages may have indistinct print especially if the original pages were typed with a poor typewriter ribbon or if the university sent us an inferior photocopy.

Reproduction in full or in part of this microform is governed by the Canadian Copyright Act, R.S.C. 1970, c. C-30, and subsequent amendments.

AVIS

La qualité de cette microforme dépend grandement de la qualité de la thèse soumise au microfilmage. Nous avons tout fait pour assurer une qualité supérieure de reproduction.

S'il manque des pages, veuillez communiquer avec l'université qui a conféré le grade.

La qualité d'impression de certaines pages peut laisser à désirer, surtout si les pages originales ont été dactylographiées à l'aide d'un ruban usé ou si l'université nous a fait parvenir une photocopie de qualité inférieure.

La reproduction, même partielle, de cette microforme est soumise à la Loi canadienne sur le droit d'auteur, SRC 1970, c. C-30, et ses amendements subséquents.

Body-surface Potential Mapping:
Classification of Spatial Features
Associated with an Arrhythmogenic State

by

Cheryl Lynne Kozey

Submitted in partial fulfillment of the requirements
for the degree of Doctor of Philosophy

at

Dalhousie University
Halifax, Nova Scotia, Canada
March 1992

©1992 by Cheryl Lynne Kozey



National Library
of Canada

Bibliothèque nationale
du Canada

Canadian Theses Service Service des thèses canadiennes

Ottawa, Canada
K1A 0N4

The author has granted an irrevocable non-exclusive licence allowing the National Library of Canada to reproduce, loan, distribute or sell copies of his/her thesis by any means and in any form or format, making this thesis available to interested persons.

The author retains ownership of the copyright in his/her thesis. Neither the thesis nor substantial extracts from it may be printed or otherwise reproduced without his/her permission.

L'auteur a accordé une licence irrévocable et non exclusive permettant à la Bibliothèque nationale du Canada de reproduire, prêter, distribuer ou vendre des copies de sa thèse de quelque manière et sous quelque forme que ce soit pour mettre des exemplaires de cette thèse à la disposition des personnes intéressées.

L'auteur conserve la propriété du droit d'auteur qui protège sa thèse. Ni la thèse ni des extraits substantiels de celle-ci ne doivent être imprimés ou autrement reproduits sans son autorisation.

ISBN 0-315-76689-1

Canada

To my family
John, Sarah and William
and my parents
Sally Hubley and Frederick Hubley (1915–1985)

Contents

Acknowledgements	xvi
1 Introduction	1
2 Background and rationale	8
2.1 Ventricular arrhythmias	9
2.2 Body-surface potential mapping	21
2.3 Antiarrhythmic agents	31
3 Methodology	37
3.1 Subjects	37
3.2 Body-surface potential mapping	42
3.3 Classification based on discriminant analysis	53
4 Classification of the three-group training set	54
4.1 Eigenvector analysis of QRST-integral maps	59
4.2 Nondipolar content of QRST-integral maps	62
4.3 Discriminant analysis employing KL features	64
4.4 Discriminant analysis employing KnY features	67
4.5 Summary and discussion	70
5 Classification of the two-group training set	72
5.1 Eigenvector analysis of QRST-integral maps	72
5.2 Nondipolar content of QRST-integral maps	76
5.3 Discriminant analysis employing KL features	78
5.4 Discriminant analysis employing KnY features	79
5.5 Summary and discussion	79
6 Classification of an independent test set	83
6.1 Analysis based on features from the three-group training set	84
6.2 Analysis based on features from the two-group training set	92
6.3 Summary and discussion	95
7 Classification of the posttreatment VT group	99
7.1 Analysis based on features from the three-group training set	100
7.2 Analysis based on features from the two-group training set	109
7.3 Summary and discussion	115

8	Error estimates for classification procedures	119
8.1	Eigenvector analysis of QRST-integral maps	120
8.2	Discriminant analysis employing KL features	123
8.3	Discriminant analysis employing KnY features	126
8.4	Classification of the posttreatment VT group	127
8.5	Error estimates	131
8.6	Number of features	138
8.7	Summary and discussion	139
9	Discussion and conclusions	144
9.1	Spatial reduction of QRST-integral maps	144
9.2	Nondipolar content of QRST-integral maps	147
9.3	Analysis based on features from the three-group training set	149
9.4	Analysis based on features from the two-group training set	153
9.5	Summary	168
9.6	Conclusions	169
A	Training-set groups	171
B	Test-set groups	176
C	Posttreatment group	180
D	Interpolation procedure	188
	Bibliography	192

List of Figures

3.1	Placement of body-surface electrodes	43
4.1	Percent trace vs. eigenvectors for three-group training set	60
4.2	Eigenvectors derived from three-group training set	61
4.3	Worst-case reconstruction errors for three-group training set	63
4.4	QRST-integral maps for three-group training set	65
4.5	Nondipolar content for three-group training set	66
4.6	KnY coefficients derived from three-group training set	69
5.1	Percent trace vs. eigenvectors from two-group training set	73
5.2	Eigenvectors from two-group training set	74
5.3	Worst-case reconstruction errors for two-group training set	75
5.4	Nondipolar content for two-group training set	77
5.5	KnY coefficient derived from two-group training set	80
6.1	QRST-integral maps for two-group test set	85
6.2	Worst-case reconstruction errors for two-group test set: based on eigenvectors derived from three-group training set	87
6.3	Two-group test set in feature space of KnY coefficients from three- group training set	91
6.4	Worst-case reconstruction errors for two-group test set: based on eigenvectors from two-group training set	93
6.5	Two-group test and training sets in feature space of KnY coefficient from two-group training set	96
7.1	Worst-case reconstruction errors for posttreatment VT group	102
7.2	Pre- and posttreatment QRST-integral maps for VT group	103
7.3	Nondipolar content of pre- and posttreatment QRST-integral maps for VT _{train} group	104
7.4	Nondipolar content of pre- and posttreatment QRST-integral maps for PET and nPET subgroups	105
7.5	Posttreatment VT group in feature space of KnY coefficients from three-group training set	108
7.6	Worst-case reconstruction errors for posttreatment VT group	110
7.7	Nondipolar content for pre- and posttreatment VT group	112
7.8	Nondipolar content for pre- and posttreatment PET and nPET sub- groups	113

7.9	Posttreatment PET and nPET subgroups in terms of KnY coefficient from two-group training set	116
7.10	Pre- and posttreatment PET and nPET subgroups in terms of KnY coefficient from two-group training set	117
8.1	Percent trace vs. number of eigenvectors for total patient set	121
8.2	Eigenvectors for total patient set	122
8.3	Worst-case reconstruction errors for total patient set	124
8.4	KnY coefficient for total patient set	128
8.5	Worst-case reconstruction errors for posttreatment VT group	130
8.6	Posttreatment VT group in terms of KnY coefficient from total patient set	132
D.1	Interpolation results for a VT patient	191
D.2	Interpolation results for a VT patient	192

List of Tables

2.1	Classification of antiarrhythmic agents	32
2.2	Effects of antiarrhythmic agents	33
4.1	Reconstruction errors for three-group training set	60
4.2	Classification of three-group training set: discriminant analysis based on KL features derived from this set	67
4.3	<i>SE</i> , <i>PV</i> and <i>DP</i> of classification based on KL features derived from three-group training set	67
4.4	Classification of three-group training set: discriminant analysis based on KnY features derived from this set	68
4.5	<i>SE</i> , <i>PV</i> and <i>DP</i> of classification based on KnY features derived from three-group training set	70
5.1	Reconstruction errors for two-group training set	76
5.2	Classification of two-group training set: discriminant analysis based on KL features derived from this set	78
5.3	<i>SE</i> , <i>PV</i> and <i>DP</i> of classification based on KL features derived from two-group training set	78
5.4	Classification of two-group training set: discriminant analysis based on KnY feature derived from this set	81
5.5	<i>SE</i> , <i>PV</i> and <i>DP</i> of classification based on one KnY feature derived from two-group training set	81
6.1	Reconstruction errors for test set: based on eigenvectors from three-group training set	84
6.2	Classification of test set: discriminant analysis based on KL features from three-group training set	88
6.3	<i>SE</i> , <i>PV</i> and <i>DP</i> of test-set classification based on KL features from three-group training set	88
6.4	Classification of test set: discriminant analysis based on KnY features from three-group training set	90
6.5	<i>SE</i> , <i>PV</i> and <i>DP</i> of test-set classification based on KnY features from three-group training set	90
6.6	Reconstruction errors for test set: based on 16 eigenvectors from two-group training set	92
6.7	Classification of test set: discriminant analysis based on KL features from two-group training set	94

6.8	<i>SE</i> , <i>PV</i> and <i>DP</i> of test-set classification based on KL features from two-group training set	95
6.9	Classification of test set: discriminant analysis based on KnY feature from two-group training set	97
6.10	<i>SE</i> , <i>PV</i> and <i>DP</i> of test-set classification based on KnY feature from two-group training set	97
7.1	Reconstruction errors for posttreatment VT group: based on eigenvectors from three-group training set	100
7.2	Classification for posttreatment VT group: discriminant analysis based on KL features from three-group training set	107
7.3	Reconstruction errors for posttreatment VT group: based on eigenvectors from two-group training set	109
7.4	Classification of posttreatment VT group: discriminant analysis based on KL features from two-group training set	114
7.5	Classification of posttreatment VT group: discriminant analysis based on KnY feature from two-group training set	115
8.1	Reconstruction errors for total patient set	123
8.2	Classification of total patient set: stepwise discriminant analysis based on KL features from this set	125
8.3	<i>SE</i> , <i>PV</i> and <i>DP</i> of total-patient-set classification based on KL features from this data set	125
8.4	Classification of total patient set: discriminant analysis based on KnY feature from this data set	127
8.5	<i>SE</i> , <i>PV</i> and <i>DP</i> of total-patient-set classification based on KnY feature from this data set	127
8.6	Reconstruction errors for posttreatment VT group: based on features from total patient set	129
8.7	Classification of posttreatment VT group: discriminant analysis based on KL features from total patient set	131
8.8	Classification of posttreatment VT group: discriminant analysis based on KnY feature from total patient set	133
8.9	Error and variance estimates of correct classifications obtained by bootstrap method without replacement	134
8.10	Error and variance estimates of correct classifications obtained by bootstrap method with replacement	134
8.11	Error and variance estimates of correct classifications obtained by cross-validation method	135
8.12	Error and variance estimates of correct classifications for 8- and 16-dimensional KL feature space	140
8.13	Error and variance estimates of correct classifications for one KnY feature based on 13 and 14 KL features	141
A.1	Age and gender of training-set groups	173
A.2	Training set: VT _{train} group	174

A.3	Training set: NC group	175
A.4	Training set: MI_{train} group	176
B.1	Age and gender of test-set groups	178
B.2	Test set: VT_{test} group	179
B.3	Test set: MI_{test} group	180
C.1	Summary statistics for VT_{train} group and posttreatment subgroups .	183
C.2	Clinical characteristics	184
C.3	Clinical characteristics	186
C.4	Summary statistics for ranked data	187
C.5	Transformed data	187
C.6	Summary statistics for nominal clinical data	188
D.1	Interpolation errors for a normal subject	190

Abstract

This study investigated the value of electrocardiographic (ECG) body-surface mapping during sinus rhythm for noninvasively identifying individuals at risk of life-threatening ventricular arrhythmias. Training and test sets were formed from 255 subjects — 51 normals, 102 patients with recurrent ventricular tachycardia (VT) and 102 patients with myocardial infarction (MI) but no clinical arrhythmias. Measurements analyzed for each subject consisted of 117 QRST-integral values calculated from as many ECG leads; the rationale for choosing QRST-integral maps was that they reflect the distribution of ventricular repolarization properties, any disparity of which might constitute an arrhythmogenic substrate. The Karhunen-Loeve (KL) technique was applied to represent each subject's measurements by 16 coefficients, and the Kittler and Young (KnY) method of feature selection further reduced the number of characteristic features to only one or two. Nondipolar content of QRST-integral maps, determined from higher-order KL coefficients, was significantly lower for the normal subjects than for the patient groups, but it differentiated poorly between the latter groups. A much-improved diagnostic classification was based upon discriminant analysis which used three selected KL features or, alternatively, just one KnY feature. The best classification results were achieved with one KnY feature derived from the two patient groups of the training set; the diagnostic performance (percentage of patients classified correctly) was 89% for the training set and 85% for the test set. The errors to be expected in classifying future observations were estimated by bootstrap and cross-validation methods. Furthermore, the potential clinical usefulness of all classification procedures as methods for noninvasively evaluating the effectiveness of drug therapy was assessed. The results of this study demonstrate that multiple-lead body-surface ECGs contain valuable information that, if properly extracted, can identify an arrhythmogenic substrate in the myocardium of patients at risk of malignant ventricular arrhythmias.

List of Abbreviations and Symbols

- μV \equiv microvolt
- μVs \equiv microvolt-second
- AP \equiv action potential
- APD \equiv action potential duration
- AV \equiv atrio-ventricular
- λ \equiv eigenvalue
- ϕ \equiv eigenvector
- $[A]$ \equiv matrix A
- $[A]^t$ \equiv the transpose of the matrix A
- A^{-1} \equiv the inverse of the matrix A
- BSPM \equiv body-surface potential map(ping)
- CC \equiv correlation coefficient
- DAD \equiv delayed afterdepolarization
- DP \equiv diagnostic performance
- e_{mean} \equiv mean error [μV]
- e_{rms} \equiv root-mean-square error [μVs]
- e_{rel} \equiv relative error [%]
- e_{peak} \equiv peak error [μVs]
- EAD \equiv early afterdepolarization
- ECG \equiv electrocardiogram
- EPS \equiv electrophysiological studies
- f_i \equiv weighting coefficient from the Kittler-Young space
- FFT \equiv fast Fourier transform
- KL \equiv Karhunen-Loeve
- KnY \equiv Kittler and Young
- LQTS \equiv long Q-T syndrome

- LVEF \equiv left ventricular ejection fraction
- MI \equiv myocardial infarction (diagnostic category)
- MI_{train} \equiv the training-set group of patients with previous myocardial infarction and no history of arrhythmias
- MI_{test} \equiv the test-set group of patients with previous myocardial infarction and no history of arrhythmias
- MI_{total} \equiv the entire population of patients with previous myocardial infarction and no history of arrhythmias ($MI_{\text{train}} + MI_{\text{test}}$)
- ms \equiv millisecond
- mV \equiv millivolt
- NC \equiv normal control group
- $NDPC$ \equiv nondipolar content
- nPET \equiv nonpredicted effective therapy (group)
- NPV \equiv negative predictive value
- Perr \equiv percent error [%]
- PET \equiv predicted effective therapy (group)
- PV \equiv predictive value
- rms \equiv root mean square
- s \equiv second(s)
- SA \equiv sino-atrial
- SD \equiv \pm standard deviation
- SE \equiv sensitivity
- SE_{NC} \equiv sensitivity to the NC category
- SE_{VT} \equiv sensitivity to the VT category
- SE_{MI} \equiv sensitivity to the MI category
- SVD \equiv singular value decomposition
- R_x \equiv treatment
- VA \equiv ventricular arrhythmia
- VF \equiv ventricular fibrillation

- VPD \equiv ventricular premature depolarization
- VT \equiv ventricular tachycardia (diagnostic category)
- VT_{train} \equiv the training-set group of patients
with recurrent ventricular tachycardia
- VT_{test} \equiv the test-set group of patients
with recurrent ventricular tachycardia
- VT_{total} \equiv the entire population of patients
with recurrent ventricular tachycardia (VT_{train} + VT_{test})
- WPW \equiv Wolff-Parkinson-White
- \bar{X} \equiv mean
- y_i \equiv weighting coefficient from the Karhunen-Loeve space

Acknowledgements

It is a pleasure for me to acknowledge those who have contributed to making my graduate work a positive experience. I extend my deepest gratitude to my supervisor, Dr. Milan Horacek for his guidance, patience and friendship during my graduate work, for his constant support during the preparation of this thesis and for keeping me focussed on the important issues – he is a true *mentor*. I extend my sincere appreciation to Cindy Penney for all of her efforts throughout various stages of the project – from beginning to end. Thanks to Jim Warren for his significant contribution to the statistical aspects of the project and the many thought-provoking discussions. I would also like to thank Brian Hoyt, Paul MacInnis and Bob Potter for always being willing to help me out when I ran into difficulties.

Appreciation is extended to those in the clinical community, both here at the Victoria General Hospital in Halifax and at the Foothills Hospital in Calgary, whose input and cooperation were vital to the success of this project. In particular, I am grateful to Dr. M.J. Gardner for his cooperation and constructive input and to Drs. L.B. Mitchell and E.R. Smith, who shared with us the critical patient data analyzed in this study. A special thanks to Linda Ellis for being my contact person in Calgary and for responding promptly to my numerous requests.

Financial support for this work was contributed by the Medical Research Council of Canada, the Alberta Heritage Foundation for Medical Research and the Heart and Stroke Foundations of Nova Scotia and Alberta.

A special thank you to my wonderful husband, John, for his encouragement,

friendship, support and most of all his love. To my two lovely children Sarah and William, thank you for making each day special with your sweet smiles.

Chapter 1

Introduction

Sudden cardiac death is a critical issue in cardiology and a huge research effort has been directed toward understanding the factors associated with this phenomenon. Ventricular arrhythmias and fibrillation have been shown to immediately precede sudden cardiac death and thus it is highly desirable to establish valid and clinically practical predictive measures for detecting patients who are at risk for developing these lethal arrhythmias.

Attempts have been made to identify risk factors which predispose individuals to malignant arrhythmias that cause sudden cardiac death. Clinical correlates—such as age, smoking habits, body type, cholesterol level, presence of coronary artery disease and hypertension—have been evaluated by epidemiological studies. Risk factors have been identified by means of multivariate statistical analysis and a set of factors which could potentially be altered to reduce the risk of heart disease has been established [80,100,180]. These factors alone have limited value in predicting malignant arrhythmias, but in combination with other measurements (such as those made available by radionuclide ventriculography and computerized electrocardiography) provide valuable information.

Assessment of the electrophysiological events of cardiac activation and repolarization has been intensively pursued in an attempt to extract diagnostic information. Two methods which are commonly used for diagnosing arrhythmias and for evaluating their treatment are ambulatory monitoring and programmed stimulation. In ambulatory monitoring, the electrocardiogram (ECG) is recorded over a long period of time (e.g. 24 hours) and the record is analyzed for the number of irregular beats or other abnormal features. Ambulatory monitoring has been used with varying degree of success as a predictor of vulnerability to malignant arrhythmias [23,108,198] and as a method for guiding antiarrhythmic therapy [22,130,198]. The underlying assumption is that ventricular ectopic activity is a marker for sustained arrhythmias [81,83]. The presence of ventricular premature beats in patients with myocardial infarction or coronary artery disease has been considered a risk factor for the development of malignant arrhythmias [149], but the hypothesis that there is a causal relationship between ectopic activity and the development of arrhythmias has been recently questioned [22,36]. Programmed stimulation, in conjunction with endocardial mapping, has provided a method of evaluating the stability of the electrophysiological state of the myocardium during a controlled application of extrastimuli [30,123,192]. The method is invasive, and while it has been considered the *gold standard* for predicting vulnerability to ventricular arrhythmias, it is known to have associated risks, for its objective is to attempt to induce (under clinically controlled conditions) the state which is ultimately the one to be prevented. In spite of these shortcomings, endocardial mapping and programmed stimulation constitute a valuable *in vivo* model for studying mechanisms of arrhythmias

[41,50,103,194,195] and they serve as one method of predicting successful antiarrhythmic therapy [22,60,61,203].

In recent years, ventricular activation and repolarization during sinus rhythm has been studied in search of a possible noninvasive predictor of malignant ventricular arrhythmias. This approach differs from the two discussed above in that it attempts to characterize (from noninvasive body-surface measurements) the underlying electrophysiological state of a ventricle — rather than attempting to capture or induce the abnormal rhythm *per se*. The two approaches pursued are those that examine the late phase of ventricular depolarization, and those that examine the primary repolarization properties of the ventricles. Alterations in both depolarization and repolarization properties have been associated with vulnerability to ventricular arrhythmias.

Analysis of the amplitude, frequency and, more recently, spatial characteristics of the terminal phase of the QRS complex from standard 12-lead ECGs during sinus rhythm is an attempt to quantify the late-depolarization properties of the ventricle [36]. This noninvasive method is based on the relationship between the low-level, high-frequency potentials recorded on the body surface during terminal QRS [38,40,174,175] and the late epicardial potentials which have been shown to be associated with malignant ventricular arrhythmias [28,99]. (The relationship between the late epicardial potentials and the low-level body-surface potentials with respect to the arrhythmogenic circuit was discussed by Ideker et al. [92].) The sensitivity of these techniques for detecting abnormalities in the terminal QRS complex has been very good; however, the specificity percentages have been generally low

[36,37,187]. While many statistical studies have been conducted, the need to expand the analysis beyond temporal and frequency analysis of the late QRS complex has been considered necessary from the theoretical perspective [36,39,57].

Primary repolarization properties of the ventricle have been assessed as a measure of the risk for ventricular arrhythmias [2,32,109,186]. Several ECG measurements from the body surface have been shown to reflect ventricular repolarization properties, and there is a sound experimental [6,8,9] and theoretical [71,72,155] basis for relating the QRST integral (the net area of QRST inscription) derived from body-surface ECGs to local primary repolarization properties. Therefore, assessment of QRST integrals from ECG leads should quantify disparate repolarization properties and provide diagnostically valuable information concerning the anatomical and electrophysiological substrate that predisposes the ventricles to arrhythmias.

While standard 12-lead ECGs have been used to examine both late potentials [37] and primary repolarization properties [169], the spatial distribution of these measurements, obtained by means of body-surface potential mapping (BSPM), should provide a comprehensive picture of all electrocardiographic information available on the body surface [46,59,65]. Increasing the spatial sampling of the cardiac electric field by recording from a large number of ECG leads improves the probability of detecting regional events. This is particularly important in the study of arrhythmogenesis, since there can be local disparities in repolarization properties which may not be detectable with standard methods of ECG recording [9]. Both qualitative and quantitative assessments of BSPMs suggest that the individuals who are at risk of ventricular arrhythmias have unique map characteristics [46,59,65,88,148,153].

For instance, the QRST-integral maps of individuals who are at risk for arrhythmias have a more complex spatial distribution in comparison with normal subjects [46,65]. While the ability to differentiate between individuals vulnerable to arrhythmias and normal subjects is of interest, much more desirable diagnostic distinction is between patients with an abnormal ventricle who are not vulnerable to arrhythmias and patients at risk of malignant arrhythmias. This is an important issue to address, since complications such as myocardial infarction are often present in individuals who are being assessed for vulnerability to arrhythmias. Few studies have dealt specifically with this problem, and there are indications that with better quantification of the BSPMs, the QRST integral should provide diagnostically significant information specific to an arrhythmogenic state [9,67,152,188].

The aim of this study was to evaluate whether advanced stochastic analysis applied to BSPM data acquired during sinus rhythm would extract the distinct information necessary to identify patients at risk for life-threatening arrhythmias. The spatial distribution of the QRST-integral maps was at the focus, because of its association with the primary repolarization properties of the ventricle, disparity of which is thought to constitute an arrhythmogenic substrate. Five objectives define the scope for this study:

- To reduce (without losing diagnostic information) the pattern space of the BSPM data acquired from a training set consisting of individuals who are vulnerable to ventricular arrhythmias and those who are not.
- To identify in this reduced feature space those features that best differentiate

among the constituent groups of the training set.

- To evaluate the diagnostic performance in classifying the constituents of the training set in the reduced feature space.
- To estimate the expected error in diagnostic performance for classifying future observations, based on the features and classification space derived from the training-set analysis.
- To examine the applicability of features derived from the training set in differentiating patients who were vulnerable to ventricular arrhythmias in a drug-free state from their posttreatment state (presumably some will remain vulnerable and others nonvulnerable, as assessed by programmed stimulation).

The hypothesis was that there would be quantifiable differences in the features derived from the QRST-integral distributions between patients vulnerable to ventricular arrhythmias and patients with no arrhythmias.

The background for the methodology and experimental design used in this study is provided in chapter 2, which reviews the literature dealing with ventricular arrhythmias, body-surface potential mapping and antiarrhythmic agents. Chapter 3 describes the methodology employed in the present study, including methods of acquisition, processing and analysis (feature selection and classification) of BSPM data, and description of the patient population. Chapter 4 presents the results of classification for the training set comprising a group of patients vulnerable to ventricular arrhythmias, a normal control group and a group of patients with myocardial infarction, but no clinical arrhythmias. Chapter 5 presents the results of

classification for a two-group training set, made up of only the two patient groups from chapter 4. The test-set results are presented in chapter 6, with the two groups of the test set being an independent group of patients vulnerable to arrhythmias and an independent group of patients with myocardial infarctions and no arrhythmias. The results for the treatment group are presented in chapter 7; the treatment group consists of the group of patients vulnerable to ventricular arrhythmias from the training set, after treatment with an antiarrhythmic agent (quinidine). Chapters 8 deals with error estimates for classification procedures and chapter 9 contains a general discussion of results and conclusions.

Chapter 2

Background and rationale

The heart normally undergoes highly synchronized electrical processes of activation and repolarization before it begins its contractile action [19]. Macroscopically, myocardium behaves as a syncytium, but microscopic examination reveals that it is comprised of distinct myocardial cells which are connected by tight junctions [147,177]. The transmembrane action potential of each cell is the result of ion transport across the cell membrane; the action potentials of various types of myocardial cells differ, but they all have a much longer repolarization phase than do those of other excitable cells [63]. During the prolonged repolarization, the myocardial cell is in an absolute refractory period, and is unable to respond to an additional stimulus; this property ensures that the wave of propagated activation in the heart is unidirectional [63]. The normal electrophysiological matrix is maintained by a complex feedback system [63] and of importance to this study are the processes of ventricular activation and repolarization. In the ventricular myocardium, the wave of activation follows a distinct pattern (progressing from endocardium to epicardium and from apex to base), whereas the repolarization process takes place in approximately the opposite order [63].

These electrophysiological processes are reflected by distinct electrocardiographic patterns measured at the body surface. Therefore, the electrocardiogram (ECG) noninvasively provides information on cardiac electrical activity and has been valuable as a clinical diagnostic tool [63]. The QRS complex reflects the ventricular activation process and the T wave reflects ventricular repolarization process. Normally, in most ECG leads, the T wave is concordant with the R wave; this is explained by the fact that the order of repolarization is essentially opposite to that of depolarization [33,159]. Primary and secondary components of the T wave can be distinguished [4,5], with the former related to the intrinsic repolarization properties of the ventricle and the latter predetermined by the ventricular activation sequence. The QRST integral, calculated from digital ECG recordings, is a lumped measure of the intrinsic ventricular repolarization properties [6,8,10].

The area of interest in this study is the association between arrhythmogenic conditions in the ventricular myocardium and their manifestations in the body-surface potential maps. The following section discusses this association with respect to ventricular arrhythmias — disturbances considered a precursor to sudden cardiac death.

2.1 Ventricular arrhythmias

Arrhythmias are the abnormal electrical events in the myocardium that are caused by disruptions in either impulse initiation or impulse conduction through the highly organized system of cardiac excitable cells [64,203]. Arrhythmogenic mechanisms have been extensively reviewed [44,64,73,95,97,202,203]. Reentry, automaticity and

triggered activity are three proposed mechanisms of ventricular arrhythmias supported by cellular studies, animal models and clinical evidence [163]. The purpose of this section is to provide an overview of the most relevant literature on ventricular arrhythmias, focussing on the methods used to classify patients at risk for these arrhythmias.

Reentry refers to an impulse that does not die out as it would normally but persists to reexcite the myocardium [56]. Two conditions are necessary for this to occur: the presence of a unidirectional block and that the wave of excitation progresses through the pathway and back to its point of origin. Janse [95] reviewed in detail the basic principles and clinical aspects related to reentry as an arrhythmogenic mechanism. The clinical support for the concept of reentry is provided by the fact that the ventricular arrhythmias can be initiated and terminated with pacing, although it is agreed that pacing alone does not distinguish reentry from all other mechanisms such as triggered activity [163,194].

Automaticity, which has been discussed in detail by Gilmore and Zipes [73], relates to the inappropriate and spontaneous depolarization caused by a pacemaker current produced by a normal or an abnormal pacemaker. For example, spontaneous discharge of the sinus node can be altered by drugs, disease and autonomic nervous system [73]. Clinical documentation of automaticity relates to the inability to initiate the arrhythmia with a premature stimulus. Gilmore and Zipes [73] cite evidence that parasystole and accelerator idioventricular rhythms are probably due to enhanced automaticity.

Triggered activity refers to the impulse being initiated in the cardiac fibers by a mechanism that is dependent on afterdepolarization [202]. Early afterdepolarization (EAD) occurs during repolarization; delayed afterdepolarization (DAD) occurs after repolarization is complete. While clinical studies have not convincingly demonstrated EAD (the clinical manifestations of this rhythm are thought to be *torsades de pointes* and triggered activity associated with the long QT syndrome), some animal studies demonstrate this mechanism [163]. DAD has been manifested *in vivo* by exercise-induced ventricular tachycardia (VT) in the absence of coronary artery disease [163]. Triggered activity has been well defined at the cellular level, with supportive evidence provided by animal models and clinical observations [56,163,202].

Since a complex interaction of factors provides the dynamic equilibrium for normal ventricular processes to occur [63], the substrate for disruptions of ventricular rhythm may be neurological, anatomical, or physiological (the latter being associated with ionic imbalances). Studies of cardiac nerve stimulation demonstrate that the sympathetic nervous system contributes significantly to arrhythmogenesis (see review by Corr et al. [44]). Long QT syndrome (LQTS) has been considered a precursor to the development of lethal arrhythmias [168,169] and the role of the autonomic nervous system in its genesis has been extensively reviewed [205]. The parasympathetic nervous system also affects cardiac function; in general, these effects are inhibitory with respect to arrhythmias and vagal stimulation was shown to mitigate to some extent the arrhythmic sympathetic effect [56,64].

Gardner and coworkers describe an anatomical substrate for arrhythmias associated with the activation wave front propagating through and around areas of

viable and damaged myocardium [68,69]. Electrograms from these areas are fractionated. Damage to the intricate structure of myocardial cells disrupts the smooth current flow, and myocardium so affected has been considered the anatomical substrate for developing arrhythmias in the ventricle [92]. The results of a ring model study by Quan and Rudy [158] showed the importance of cellular uncoupling and demonstrated that propagation itself provided the necessary unidirectional block for reentry. Neurochemical and ionic imbalances have also been associated with electrical instability of the heart and these imbalances are also considered substrates for arrhythmias [43,73,163,202,203]. All of these substrates have been shown to have an effect on the electrophysiological processes of the ventricular myocardium, but their presence alone may not be sufficient to accurately identify a ventricle at risk for arrhythmias.

Therefore, methods based on measurable electrophysiological alterations have been pursued to provide information for classifying patients at risk for developing ventricular arrhythmias. The objective of these methods is *to identify the electrophysiological substrate associated with vulnerability to ventricular arrhythmias*. Several approaches have been explored. They include ambulatory monitoring, temporal and frequency-domain analysis of signal-averaged ECGs, measures of disparate ventricular repolarization, and intracardiac electrophysiological studies involving programmed stimulation (EPS studies). Ambulatory monitoring and EPS studies are the two clinical techniques most commonly used to evaluate an individual's vulnerability to ventricular arrhythmias and to guide antiarrhythmic therapy [77,204].

Ambulatory monitoring involves recording of ECGs for long periods of time dur-

ing patient's normal activity; these records are then analyzed and various criteria for determining vulnerability to ventricular arrhythmias are applied [26,101,198]. This approach is based on the evidence that VT and ventricular fibrillation have been reported as terminal rhythms preceding sudden cardiac death [23,83,149], and that the presence of ectopic ventricular activity is a marker for VT [77,81]. It is assumed that the higher the frequency of occurrence of ectopic or complex beats, the higher the probability of developing ventricular arrhythmias [81]. The prognostic value of ambulatory monitoring for detecting vulnerability to arrhythmias and for evaluating the effectiveness of antiarrhythmic therapy has been extensively studied [22,23,26,75,77,108,130,200,204]. Ambulatory monitoring in conjunction with other measures—such as EPS, left ventricular ejection fraction and signal-averaged ECGs—provide better results for predicting vulnerability to arrhythmias than does monitoring alone [26,75,108]. The duration of the recording has been shown to be important, since it increases the chance of capturing the abnormal activity. It has been suggested that 48 hours of monitoring provides a 93% sensitivity of detecting ventricular ectopy [204]. For those patients who experience frequent ventricular arrhythmias, ambulatory monitoring has been useful for quantifying frequency and severity of the ectopy; however, for some patients with suspected VT the interval between occurrence of events may be much larger than 48 hours and thus ambulatory monitoring may be of lesser value [204]. The results from the CAST trial do not provide encouraging evidence that the suppression of ectopy is directly associated with a decrease in risk of ventricular arrhythmias [22] and *this evidence severely undermines the underlying assumptions upon which this approach was developed.*

EPS studies use programmed stimulation in an attempt to initiate the abnormal ventricular rhythm under clinically controlled conditions; this approach is based on the premise that if the substrate for ventricular arrhythmias is present, the pacing and ectopic stimuli will induce the abnormal rhythm. It has been demonstrated that a relationship exists between the patient's clinical arrhythmia and the arrhythmia induced during programmed stimulation [195]. Various efficacies have been reported for this method [23,30,77,123,149,193,204]. The discrepancies in results reported by different laboratories (sensitivities of 48–95% and specificities of 44–100% [77]) occur largely due to differences in: (a) the clinical arrhythmia itself, (b) the underlying cardiac disease [97,194,204], (c) the aggressiveness of the pacing protocol, and (d) the definition of the end point [77,91]. The aggressiveness of the protocol relates to the number of extrastimuli, the number of stimulation sites, the drive-cycle length and the strength of stimulation current. With three extrastimuli and rapid pacing, an arrhythmia was induced in 95% of patients [77]. The specificity of diagnostic classification was 90% for two extrastimuli and decreased with increasing number of stimuli used [77]. Horowitz et al. [91] reported that three or fewer extrastimuli were required to induce VT in 80–95% of the patients with clinically documented VT, and that two or less stimuli were highly specific. Therefore, there is a trade-off between sensitivity and specificity related to aggressiveness of the protocol.

Programmed stimulation has been used to guide therapy; the underlying assumptions are that pharmacological intervention results in an alteration of the electrophysiological arrhythmogenic properties of the myocardium, and that there is a parallel between the induced arrhythmia and the clinically documented arrhythmia

[91]. Evidence has been presented that supports a good prognosis for patients whose arrhythmia is inducible in the drug-free state but not inducible in the state affected by an antiarrhythmic drug [77,165]. The predictive value of programmed stimulation for accurately determining reoccurrence of arrhythmia has been cited as having a wide variability 30–100% [77,91].

Programmed stimulation studies have also been used as the standard for comparing the efficacy of other methods of predicting the presence of arrhythmias — such as ambulatory monitoring and signal-averaged ECG analysis [26,37,140,183,187]. With the exception of long-term follow up, programmed stimulation appears to provide the best level of performance among available methods for predicting vulnerability to ventricular arrhythmias. While improvements and standardization of protocols for both ambulatory monitoring and programmed stimulation may improve the classification of patients at risk for ventricular arrhythmias [204], both methods have their limitations (ambulatory monitoring is based on a hypothesis which is in doubt and programmed stimulation relies on inducing the potentially lethal rhythm and has other associated risks [164,194]). These limitations and risks provide incentive for exploring other methods for classifying high-risk groups, based on noninvasively detecting abnormal electrophysiologic events.

There is evidence that specific electrophysiologic alterations during sinus rhythm are associated with arrhythmogenesis and that these alterations are manifested in body-surface potentials. Methods that analyze body-surface ECG during sinus rhythm include (a) the analysis of high frequency, low-level signals at the terminal phase of the QRS complex, and (b) the analysis of the T-wave or QRST-integral

alterations.

The high-frequency, low-level potentials measured at the terminal portion of the QRS complex have been associated with fractionated electrograms recorded from the patchy myocardium [92,128]. These late potentials have been found in patients with ventricular arrhythmias during normal sinus rhythm [28,99]; thus, they have been associated with the anatomical substrate for ventricular arrhythmias [68,69]. (Some debate exists [92] regarding the significance of low-level potentials as predictors of ventricular arrhythmias, since there is evidence that the sites from which the late potentials are recorded do not appear to be part of the reentrant circuit [111,148]; as well, it has been recently questioned [39] that such signals would only be manifested during the terminal phase of QRS complex.) However, qualitative and quantitative examination of the frequency components of the terminal QRS portion of the body-surface ECG recordings show that patients with VT have, during their sinus rhythm, an increased content of higher-frequency low-level signals compared to those without arrhythmias [38,40,49,115,173,174,175]. A wide range of sensitivity and specificity percentages have been reported when temporal and frequency analysis of the terminal QRS complex has been used to identify post-MI patients at risk for VT and to predict successful antiarrhythmic therapy [36]. Many studies base their diagnostic discrimination upon confidence limits, but give no measure of future performance [140,201]. Vatterott et al. [187] recently developed a logistic model based on clinical measures in conjunction with signal-averaged ECG variables and validated the model by cross-validation techniques (one of the very few studies that did so). Their cross-validated sensitivity for distinguishing MI patients without

arrhythmia from patients that had arrhythmia inducible by programmed stimulation was 91% and specificity was 59%. In general, the deficiency of the present procedures that employ analysis of signal-averaged ECG is their lack of specificity; this occurs because high-frequency components at the terminal QRS complex are also associated with abnormalities other than VT [38,39,74,115]. Other reasons have been cited for the wide variation in diagnostic performance, including the technical aspects of signal processing and analysis, and considerations related to the underlying electrophysiology [29,36,39,57,92]. Further refinements of these techniques, to better identify features that are more specific to arrhythmogenic conditions, are presently being pursued [36,39].

Considerable attention has been directed toward the recovery properties of the ventricular myocardium and its association with ventricular arrhythmias. The primary T wave, a notion introduced by Abildskov [4,5], has been associated solely with ventricular repolarization properties and their distribution in the ventricular myocardium [3,35]. Dispersion of repolarization properties causes heterogeneity of excitability, with reentry as the most likely mechanism for arrhythmias facilitated by this dispersion [109]. The role of heterogeneity of ventricular repolarization properties in the genesis of ventricular arrhythmias has been discussed by Kuo et al. [109]. Not just the *presence* of nonuniform repolarization is important; the *degree* of disparity in local recovery times has been shown to lower ventricular fibrillation thresholds [82]. Therefore, methods to accurately assess ventricular repolarization properties are indispensable in identifying myocardium at risk for developing arrhythmias. As mentioned earlier, the T wave is of the same polarity as the R wave in normal ECGs,

which has been explained by the order of repolarization being essentially opposite to that of depolarization [33,159]. Alterations of the normal T-wave morphology have been demonstrated by means of experimentally induced abnormalities [34]. Several studies have demonstrated that there is a relationship between dispersion of repolarization, measured as T-wave fluctuations, and vulnerability to VT and ventricular fibrillation [11,31,32]. Simple measures such as QT duration and various temporal measures from the 12-lead ECG have been considered reflective of dispersion of repolarization properties [126] — in particular those associated with LQTS [18,168,169]. Abildskov [1] found abnormal QT lengthening in only a few patients with ventricular arrhythmias. A recent study by Benhorin et al. [18] used simple electrocardiographic measures, aimed at quantifying repolarization characteristics, in an attempt to classify patients with LQTS from normal subjects. The 95% confidence interval for their sensitivity percentage was 81.6–100%, based on five predictor variables in their model. Unfortunately, this high sensitivity reflected the low error in classifying over 300 normal subjects, while the mean error rate for classifying the LQTS patients was 9.3/37 or 25%. As well, the predictive value of this result is lessened, since the ratio of features to subjects was 1:7 (5 variables and 37 subjects). These results demonstrate the limitation of methods that rely on simple measurements to evaluate a complex phenomenon such as heterogeneity of ventricular repolarization. Since the QRST integral has been shown to reflect the distribution of ventricular repolarization properties [6,7,8,10,129], this measure could be used to assess susceptibility to ventricular arrhythmias [9]. A recent study by Kubota et al. [107] reported very high negative correlations between QRST

integrals and ventricular fibrillation thresholds after MI in a canine model (these correlations were modified by the size of the MI). In general, there is evidence supporting the value of assessing dispersion of repolarization based on measurements from the electrocardiographic waveforms associated with this process; however, local alterations in these properties would not be easily assessed using conventional ECG leads [9].

The regional disparities associated with both ventricular depolarization and repolarization processes have been a concern in assessing the ventricle at risk for arrhythmias. On the surface, these regional differences in depolarization and repolarization can be reflected in BSPM (as will be shown in the following section). Studies have demonstrated that BSPMs of individuals with ventricular rhythm disturbances have both qualitative and quantitative differences in comparison with maps of normal subjects [65,66,104,151,153]. The spatial distributions of late depolarization potentials (measured as the spatial distributions of BSPMs from the terminal QRS) appear to be much more complex in patients with ventricular arrhythmias than in terminal phases of normal ventricular activation [49,59]; these findings were corroborated in a canine model [148]. Attempts are being made to measure the spatial distribution of late depolarization potentials for detecting regional differences in ventricular depolarization associated with VT [36]. Further examination of this *spatial* aspect of late depolarization, in contradistinction to analysis limited only to selected ECG leads, may provide a more complete picture of the arrhythmogenic substrate which could improve the specificity of classification based on late potentials.

This study focussed on quantifying the spatial aspect of dispersion of ventricular repolarization properties associated with ventricular arrhythmias. Local inhomogeneities of these properties should affect spatial measurements of QRST integrals [9,88,129], and it has been suggested that multipolar body surface distributions of the QRST integral reflect heterogeneity of repolarization properties [9]. Therefore, the QRST-integral distributions calculated from signal-averaged BSPM data were interrogated for diagnostic information. The theoretical and experimental basis for evaluating regional repolarization properties to assess the arrhythmogenic state of the ventricle is sound. Lacking is the clinical evidence that these regional repolarization properties can be accurately quantified to identify ventricles at risk for arrhythmias. Many studies have been based on qualitative assessment [66] or simple quantitative measures (e.g. number of extrema) based on visual inspection of morphological features; these studies observed that the QRST-integral maps of VT patients were more complex (multipolar) than normal maps [65]. However, multipolar QRST-integral maps were also noted in patients with MI and no arrhythmias [65,129]. It turned out that it is very difficult to distinguish between MI and VT patients by means of a qualitative assessment of their maps [46], and discrepancies in results have been noted when simple quantitative measures were employed [9].

Recently, the problem of more objectively measuring and classifying spatial characteristics reflecting dispersion of ventricular repolarization properties in BSPMs has been addressed. A 2-D fast Fourier transform (FFT) of the QRST-integral maps of normal subjects, MI patients and VT patients quantified differences between the groups, but the overlap between groups indicated that this method was not spe-

cific enough for classification [153]. Higher nondipolar content, determined by an orthogonal-expansion approach to data reduction, was reported for QRST-integral maps of VT patients compared to normal subjects [9,46,151]. Again the difficulty was in separating the MI and VT patients, since there was a large overlap between the two groups for nondipolar content and the classification based on this measure was poor [151]. In a study of post-MI patients, nondipolar content was significantly higher for those patients ($n=8$) who later died suddenly than it was in those who survived [188]. In contrast to using a single measure, such as nondipolar content, De Ambroggi et al. [46] also showed that individual KL features, derived from the QRST-integral maps, differed between LQTS patients and normals; this suggests that there may be specific features that contain diagnostic information. In a recent study based on the KL features, an approach proposed by Kittler and Young [102] was used to classify normal subjects, MI patients and VT patients; the results showed that a distinct classification separating the three diagnostic groups is a real possibility [67,152]. Cumulatively, the results above indicate the need for more rigorous evaluation of the QRST-integral maps to establish the degree to which it can be used in the diagnosis of ventricular arrhythmias. The following section deals with quantitative methods for evaluating BSPMs to assess regional disparities of ventricular repolarization properties.

2.2 Body-surface potential mapping

Standard 12-lead electrocardiography uses only a small set of all measurable ECG leads and therefore misses some noninvasively accessible diagnostic information

[78,127,133,166,181]. Vectorcardiography has been shown to be inadequate in describing regional cardiac abnormalities, because its underlying assumption is that all cardiac sources can be lumped into a single, fixed-location dipole [166]. In contrast, BSPM involves the simultaneous acquisition of multiple ECG leads placed over both the anterior and posterior torso [47,116,166,181,182]. Measurements from the entire torso, with high spatial resolution in the precordial area, ensure that BSPM captures nearly all noninvasively-available electrocardiographic information [86,127,133,166]. On the other hand, there is a great deal of redundancy in the entire set of BSPM data [58,119,184] and thus an optimal number of leads and their optimal placement have been explored [58,79,17,118,120].

Heart-produced BSPMs are affected by the volume-conductor properties, such as shape and internal inhomogeneities, of the torso. The solutions to the two fundamental problems in electrocardiology—the *forward problem* [15] and the *inverse problem* [16,166]—provide the deterministic foundation for utilizing BSPMs to examine regional cardiac events *in vivo*. The ability to utilize this noninvasive method to accurately describe the regional electrical events of the heart has great clinical and physiological significance. The question addressed in this study is whether BSPMs, although distorted by volume conductor characteristics, can provide directly (i.e., without the benefit of forward/inverse calculations) the diagnostic information for differentiating the electrophysiological substrate associated with an arrhythmogenic state from the nonarrhythmogenic state.

Typically, the BSPM data have been displayed at selected time instants as isopotential maps, or as isointegral maps such as the QRS Σ -integral maps [47,90,88,116].

As identifying and differentiating the diagnostic characteristics from these maps is difficult, qualitative approaches to assess BSPMs—sometimes aided by simple quantitative measures—have prevailed. The qualitative assessment is based on the morphological features of the contour maps that can be related to some characteristic events in the heart (such as right-ventricular breakthrough). The simple quantitative measures include, e.g., locations of extrema and their trajectories in time, number of extrema in different phases of activation/repolarization, and time to characteristic events such as breakthroughs [59,114,136,138,154,181]; all such measures represent only an arbitrary (albeit judicious) selection from the total spatio-temporal information provided by BSPM. There has been some debate regarding the increased diagnostic information provided by BSPM compared to conventional ECG approaches for studying certain abnormalities, such as MI [179,185]. However, to capture body-surface information about the regional dispersion of repolarization associated with arrhythmogenic substrate, BSPM approach would seem to be clearly superior to any ECG lead system with a small number of leads.

Despite limitations of the interpretation based on the qualitative or semi-qualitative assessment, BSPM has been used successfully to locate accessory pathways in Wolff-Parkinson-White (WPW) syndrome [48,52,94], to classify patients with MI [136,138] [142,154] and coronary artery disease [78,114,117], and to identify characteristics associated with the LQTS [46] and ventricular arrhythmias [59,65,66,114,125]. In general, qualitative assessments have provided initial evidence that diagnostic information is contained in these maps, and recent studies indicate that better quantification procedures are necessary for statistical comparisons. BSPM has been explored

as a technique for identifying patients with coronary artery disease; sensitivities of 88% and 94% have been reported for correctly classifying these patients from normal subjects, by means of signal representation procedures applied to the BSPM data and statistical analysis [78,117]. Vondenbusch et al. [189] recorded BSPMs during percutaneous transluminal coronary angioplasty and reduced the data by employing a KL expansion; they were able to differentiate between BSPMs of patients who underwent balloon-inflation angioplasty of three different coronary arteries. Although the sample size was small in this latter study, the results illustrate that a small number of properly selected features can provide distinct information for diagnostic classification. Sun [178] demonstrated that spatial features derived from the QRST-integrals were more effective than other spatial and temporal information for classifying—by means of a neural network algorithm—four diagnostic groups (normal, ischemia, anterior MI and left bundle branch block). As discussed in the previous section, recent studies [9,46,67,151,152,188] suggest that improved data reduction procedures and the implementation of sophisticated statistical analysis, is a plausible approach to identifying noninvasively the BSPM features unique to VT. In general, the number of patients has been relatively small in the BSPM studies, and few have used more advanced statistical procedures for feature selection and classification.

Data reduction in body-surface potential mapping

In order to achieve a more objective selection of diagnostic features from BSPMs for diagnostic classification, successful data reduction is necessary. The problem is to

reduce the amount of BSPM data—without losing important diagnostic information. Data-reduction procedures reduce the original pattern space to a feature space of smaller dimensionality, while maintaining the important characteristics; features are then selected that are the best discriminators for classification purposes [12]. The success of the classification procedure, however, is highly dependent on the success of the feature-reduction procedure to reflect the salient features in the map.

The statistical approaches evaluate common features of the signals and these features are represented as a set of coefficients and basis functions. The limitation of these statistical approaches has been primarily with data representation. Since the data are reduced to a series of coefficients which are not easily related back to the morphological features of the pattern, the results are difficult to interpret intuitively [178].

There are various methods of statistical representation available, and two approaches that have been used with BSPM data are the 2-D FFT [134,151], and those based on orthogonal expansion. The success of the latter techniques in BSPM data reduction [58,119,151,178,184] illustrates its potential value to the problem of feature selection and diagnostic classification. The orthogonal-expansion approaches include KL expansion [58,119], principal component analysis [46] and singular value decomposition [184]. There are similarities and differences in these three techniques as discussed by Gerbrands [70]; however, in the context of statistical pattern recognition, all three can be used interchangeably. The KL expansion is based on the statistical properties of an image and has been used for data compression where the discrete variables are transformed into a set of uncorrelated coefficients, sometimes

referred to as the principal components [76]. Singular value decomposition has been considered a reliable method for computing the coefficients for a generalized least squares problem based on a matrix factorization [62,146]. It has been used to reduce the matrix dimensionality in the presence of redundancies, but this approach is deterministic in nature. The similarity between the singular value decomposition and the two stochastic approaches—KL expansion and principal component analysis—is based on the relationship between the singular values and the eigenvalues of a real symmetric matrix [62,70].

The KL expansion has been considered the optimal transform for signal representation based on a mean-squared-error criterion [70]. A complete knowledge of the probability structure for the input pattern is not required [12]. Although this transform was developed for a continuous process, the KL transform can be discretized for use in digital image processing [76] and it has been applied to BSPM [58,119,151,178,184]. There are several reasons why the approaches based on the KL expansion have been successful when applied to BSPM data. First, they are not based on the assumption of periodicity of the signal; the only requirement is that electrode placement should be consistent in order to make comparisons. Secondly, these methods are not sensitive to noise in the signal, in particular random noise that is often present in ECG signals. Lastly, the basis functions are derived from the data itself and are not predetermined as is the case with other transforms such as the Fourier transform.

Several studies have applied the KL theory to BSPM data — for both spatial and temporal reduction and diagnostic classification [9,46,58,78,105,151,185,188,189].

For example, dimensionality reduction reported was in the order of 16:1 and 12:1, with the entire set of temporal and spatial BSPM data being reconstructed from 216 coefficients and the corresponding basis functions [58,119]. Given that the original pattern space could be over 40,000 numbers, this was a substantial reduction. The low reported errors indicate that the salient features were maintained after reduction and classification procedures can be applied, based on these representative features [119]. The data-reduction procedures employed in this study were based on the KL-expansion theory.

Feature selection and classification

Ranking the eigenvalues in descending order of magnitude provides a set of principal features that best describe the total data set. Statistical procedures for classification can be then applied to the significantly reduced data. There are various approaches for defining a classification space, including those based on physiological considerations, those that are statistical in nature, and more recently neural-networks approach [178]. Only a few studies have addressed the diagnostic classification of VT applying statistical procedures to the principal features derived from the KL expansion of BSPM data [46,151,178]. One measure referred to as the nondipolar content, reflecting complexity in the BSPM patterns was extracted from the coefficients calculated for each KL feature based on the definition by Abildskov et al. [9]. The nondipolar content of a given map can be calculated [46] by computing the cumulative contribution of all eigenvectors beyond the third as a percentage of the total map content. This can be explained by the fact that the first three

eigenvectors are basically dipolar in nature (with only one maximum and one minimum), while the following ones contain more than two extrema and are said to be multipolar in nature. The set of coefficients y_i , which are characteristic for each subject from the KL transform, may be used to compute the contribution of the eigenvectors to the total map content. Several studies indicate that subjects who are vulnerable to ventricular arrhythmias have a multipolar, and thus more complex, QRST-integral distributions than normal subjects; this has been substantiated quantitatively by significant differences in nondipolar content [9,46,151]. Overlap between patient groups however suggests that this single measure may not provide sufficient separation [151] but should be further investigated.

For LQTS patients and normals, each feature coefficient has been compared separately by means of nonparametric methods [46]. Since the KL expansion orders the features based on their contribution, statistical methods for feature selection (such as discriminant analysis) could be applied directly to the feature coefficients. Investigators have applied discriminant analysis procedures to the KL features derived from BSPMs to differentiate patient groups such as coronary artery disease [78] and myocardial infarction [185] from normal control subjects with low classification errors. In the former study, 94% accuracy was reported for separating the normal subjects from coronary artery disease patients who displayed normal electrocardiograms [78]. Essentially the discriminant analysis attempts to find the best subset of features for differentiating between classes [110]. This can be achieved through forward, backward or stepwise procedures [93]. The latter method is independent of order and features are added and deleted by evaluating their discriminatory po-

tential, based on statistical criteria [93].

Methods based on the KL expansion itself have also been used for feature selection. Since the classification procedure depends to a large extent on the quality of the feature selection, the optimal feature selection procedure is of crucial importance. Kittler and Young [102] have discussed various techniques of diagnostic classification based on the KL expansion; they grouped these techniques into two broad categories: (1) those where feature ordering is made irrespective of the mean vectors of the individual classes, and (2) those where the utilization of information about the mean vectors is presumed to be non-optimal. Kittler and Young suggested a method of feature ordering that utilizes the discriminatory potential of both the class means and the class variances in the application of the KL transform [102]. The general theory for this approach is basically a two-stage KL decomposition, with the result being an optimal feature space for classification purposes. Feature selection is carried out by constructing the covariance matrix of the input vectors and by subtracting the mean vector for each class from the respective class vectors and normalizing this for the class variance. The resulting classification space is ordered—based on the differences between diagnostic groups—and incorporating *all* of the features in the analysis, rather than a small subset of features as in the discriminant analysis. Initial results based on the KnY approach illustrate its potential value for defining a classification space based on features derived from the BSPMs, of patients vulnerable to arrhythmia and those not vulnerable to arrhythmia [152]. The limitation of this result was that a very small sample size was used, thus the potential for overtraining existed.

Neural network algorithms have been explored for feature selection and classification. This approach was applied to classifying normal subjects, patients with ischemic heart disease, anterior myocardial infarctions and left bundle branch block [178]. While the classification results appear to be quite good, the author is cautious of the future applicability of the results because of the small sample size in each group and the problem of convergence which was not evaluated since there was no test set on which to validate the results. These issues are imperative to the future value of any classification space. In general, the less sophisticated approaches to feature selection and classification have apparent limitations in separating patients vulnerable to VT. The more sophisticated approaches, while seemingly superior, have not as yet been rigorously evaluated for their predictive value.

An examination of the literature illustrates that the number of features included in both the reduction and the classification space vary considerably [58,119,105,151] [184,178,185,189]. As mentioned previously, the important issue with respect to reconstruction is to ensure that adequate numbers of features are used to accurately represent the original pattern space [119]. In defining a classification space, a concern, particularly with small samples is to minimize the effect of tailoring the features to the training set from which they were derived. Kozmann et al. recently discussed this issue, suggesting that the number of features derived from body surface potential maps used in the classification space should be kept to a minimum to ensure that the space is statistically robust and efficient [106]. Incorporating large numbers of features into the classification space would reduce the general applicability of the space for classifying future observations [55]. In any case, results from a

training set alone are overly optimistic and are of limited value for predicting future classification [53,54,55]. Various methods for estimating the true error associated with a classification procedure include evaluation of the procedure on an independent test set, cross validation, jackknife and bootstrap [53,54,55]. The bootstrap and cross-validation have been shown to be effective estimates of the true error, in particular with small sample sizes [54]. Therefore, these methods provide an evaluation of the error bias in a given classification [27]. It is important to establish how well any set of features proposed reflect *a difference between diagnostic categories* rather than a difference between a specific group of patients.

2.3 Antiarrhythmic agents

In addition to studying distinct diagnostic classes, a further question addressed in this study related to assessing the myocardium that has a presumably altered arrhythmogenic state. Antiarrhythmic agents have facilitated the clinical study of arrhythmias, as they offer a controlled, easily altered treatment approach which has enhanced our understanding of arrhythmogenic mechanisms [30,98]. Many antiarrhythmic agents have been introduced [191,199]; they can be classified based on their predominant electrophysiological effects [172,197]. While modifications exist, the basic classifications are Class I, II, III, and IV, with a description of the differences and examples for each class presented in Table 2.1. The electrophysiological effects of the various drugs are not consistent across cells in the heart and Table 2.2 provides an overview of some of these effects for selected antiarrhythmic drugs [84,143,156,191,199], illustrating that functions of SA nodal, AV nodal, ventricular,

Table 2.1: Classification of antiarrhythmic agents

Class I	Class II	Class III	Class IV
Membrane stabilizers	Sympathetic blockers	Repolarization prolongation	Ca ⁺⁺ channel blockers
Procainamide	Propranolol	Amiodarone	Verapamil
Quinidine	Bevantolol	Sotalol	Tiapamil
Mexilentine	Atenolol	Bretylum	Nifedipine
Lidocaine	Timolol	Melperone	Gallopamil
Disopyramide	Oxprenolol	Sematilide	Bepriidil
Phenytoin	Alprenolol		
Tocainide	Nadolol		
Flecainide	Metoprolol		
Encainide	Labetolol		
Propafenone			

atrial and Purkinje cells may be altered differently with the same drug [98]. Also, drugs from the same class may have different effects on the same cardiac fiber and function, resulting in a large variation of effects on the total cardiac activation and repolarization process. These variations indicate that accurate assessment of the arrhythmogenic substrate would assist with evaluating the effectiveness of antiarrhythmic treatment. This is of particular interest since the proarrhythmic effects for class I antiarrhythmic agents, reported recently by investigators involved in the CAST trial [20,21,22] and the cessation of the use of flecainide and encainide in this trial [150], emphasize the need for accurate evaluation of therapy.

Are the antiarrhythmic agents actually altering the electrophysiological substrate for arrhythmias and can these alterations be accurately assessed? There are several difficulties with comparing the many efficacy studies and one has been the different operational definitions used to define efficacy of treatment [191]. The most common

Table 2.2: Electrophysiological effects of common antiarrhythmic agents

Agent	APD	v_{\max}	Automaticity	A-H	H-V	ERP-AVN	ERP-V
Quinidine	↑	↓	↓	↓, -, ↑	↑	↑, ↓	↑
Procainamide	↑	↓	↓	-, ↑	↑	-, ↑	↑
Propranolol	-, ↓	-, ↓	-, ↓	-, ↑	-	-, ↑	-
Sotalol	↑	-	-	↑	-	↑	↑
Amiodarone	↑	↓	↓	↑	↑	↑	↑

APD = action potential duration, v_{\max} = maximum velocity of upstroke, A-H = A-H interval, H-V = H-V interval, ERP-AVN = effective refractory period AV node, ERP-V = effective refractory period ventricle, ↑ = increase, ↓ = decrease, - = no change

methods for evaluating therapy are EPS and ambulatory monitoring; both methods have their limitations [22]. The association between suppression of ectopic activity and risk of VT has been recently questioned and while EPS has its drawbacks, its prognostic value for those that had their arrhythmia induced in a drug-free state and not induced in the drug state was relatively accurate [22]. More recently, analysis of late depolarization from signal-averaged ECGs [36] and assessment of BSPMs have been explored as method of evaluating effectiveness of antiarrhythmic therapy [132,131]. Initial results for both of these noninvasive methods indicate that they may be of value. Therefore, if noninvasive approaches are to be valuable they must be able to assess the electrophysiological effects of antiarrhythmic therapy by related changes in the surface potentials measured from ECG leads and detect a change (if one occurs) in the arrhythmogenic substrate. Since there was such a large variation in effects, even for agents within the same class, this study was limited to examining one agent, quinidine.

Quinidine is currently being used as a treatment for altering, in a relatively con-

trolled manner, the vulnerability state of individuals at risk for VT. Quinidine is a Class I drug; Class I drugs typically prolong action potential duration and are referred to as membrane-stabilizing drugs for reducing arrhythmias [96,124,197]. In-depth reviews of the pharmacokinetics, electrophysiological effects and clinical efficacy of quinidine as an antiarrhythmic agent have been presented elsewhere [84,190,191,199]. The ionic mechanisms of quinidine's action, which have been determined from single-cell and multicell studies [45,167], include inhibition of fast sodium current (I_{Na}), delayed rectifier current (I_x, I_K), pacemaker current (I_f, I_k), slow inward current (I_{si}), and steady-state "window sodium current." As indicated in Table 2.2, quinidine typically prolongs the action potential duration and increases the effective refractory period of the ventricular myocardium [51,84,143,167,191]. While there have been varied efficacies reported for its ability to reduce VT, there is evidence supporting its effectiveness for certain mechanisms and cellular environments [24,25,85,96,113,156,191]; in particular, it has been considered an effective drug for treating sustained ventricular arrhythmias, especially reentry rhythms [84,170,191]. In general, studies showed that quinidine therapy reduced the frequency of VT and fibrillation [24,25,42,96,170,130,200]. However, there is a considerable amount of evidence that it also has arrhythmogenic effects [45,160,161,162,170].

The effects of quinidine have been altered with changes in stimulation rates and in potassium (K^+) and magnesium (Mg^{++}) levels [45,143,161]. These alterations have been supported clinically with reported proarrhythmic effects of quinidine in the presence of hypokalemia and bradycardia, with the result often being a *torsades de pointes* rhythm [45,137,162]. The proarrhythmic effects reported in some studies

affected only a small percentage of patients [137], but electrolyte imbalance such as changes in potassium and magnesium concentrations have been shown to alter the effectiveness of this agent [45]. Therefore electrolyte imbalance is an important factor to assess in the clinical setting.

Studies of both the normal and abnormal myocardium demonstrate relatively consistent ECG changes with quinidine therapy. On the surface ECG, quinidine caused a dose-related response, increasing QRS and Q-T_c intervals [84,112,190]. From Table 2.2 the increase in QRS duration reflects the decrease in v_{\max} ; the increase in Q-T interval can be related to the increase in ventricular refractory period duration. The magnitude of these effects varies, based on several factors, including concentration levels, frequency of pacing, and time- and voltage-dependent factors [13,14,139]. The directions of the effects, however, appear to be relatively consistent, although there is evidence of a differential effect of quinidine on action potential duration in the endocardium and epicardium [13]. In addition to ECG alterations, differences have been noted in QRST-integral map variables between pretreatment and posttreatment maps of the patients who were treated with quinidine [131,132]. These differences were evaluated based on relatively simple quantitative measures, and no consistent changes were observed in map characteristics before and after treatment. Whether features from these maps can be quantified to assess objectively a change in arrhythmogenic state must be further explored.

In summary, the literature reviewed in this section provides the rationale for conducting this study. The study focusses on evaluating the QRST-integral BSPMs for diagnosis of an arrhythmogenic state. There is a sound theoretical basis for

pursuing this approach; however, there is limited empirical statistical evidence supporting the theory that the arrhythmogenic substrate (dispersion of repolarization) can be accurately quantified and used for diagnostic classification.

Chapter 3

Methodology

3.1 Subjects

Three sets of BSPM data were compiled: a training set, a test set and a treatment set. The training set was used to derive BSPM features suitable for diagnostic classification of patients vulnerable to ventricular arrhythmias. The applicability of the feature-selection and classification procedures was tested on an independent test set (in addition, the training set and test set were combined to evaluate the expected error for future diagnostic classification). The treatment set consisted of the posttreatment BSPM data of the training-set subjects who were vulnerable to ventricular arrhythmias before treatment; the latter group was used to explore the usefulness of training-set features in assessing effectiveness of antiarrhythmic drug therapy.

Training-set groups

The entire training set consisted of 153 subjects: 51 patients vulnerable to ventricular arrhythmias (VT_{train} group); 51 normal subjects (NC group); and 51 patients with myocardial infarction and no arrhythmias (MI_{train} group). Specific de-

mographic data and diagnoses for all training-set subjects are in Appendix A.

Subjects who comprised the VT_{train} group were selected from the patient population treated in the Cardiac Unit at the Foothills Hospital in Calgary, Alberta between January 1983 and January 1989. This population included males and females over the age of 15 years, who were diagnosed as suffering from VT. Patients were excluded from the study if there was a reversible cause of the VT, such as electrolyte imbalance, proarrhythmic drug therapy, or a recent MI (< 2 weeks). Each subject was informed of the procedures of the study, in accordance with the established ethical guidelines approved by the Conjoint Medical Ethics Committee of the Foothills Hospital and the University of Calgary. Patients were randomly assigned to different antiarrhythmic therapies. Those patients ($n = 74$) who were assigned to be treated with quinidine as their first antiarrhythmic drug were considered for the VT_{train} group, but only patients with pretreatment and posttreatment BSPM data of acceptable quality were selected. The final VT_{train} group consisted of 51 patients (i.e., 70% of the total quinidine group), 47 males and 4 females, of an age range 25–79 years and a mean age of 59.6 ± 12.2 years. All patients underwent thorough clinical examination, to establish functional angina class, dyspnea functional class and dominant-, secondary- and tertiary-heart-disease class; left ventricular ejection fraction (LVEF) was determined at rest by radionuclide ventriculography and the electrophysiological studies (EPS) were performed. All of the above procedures were part of the routine investigation.

Of importance to this study were the results of EPS, which were used to support the VT diagnosis and to determine the effectiveness of the antiarrhythmic therapy

(for the posttreatment evaluation). The programmed stimulation protocol used in EPS studies has been described in detail elsewhere [130]. Briefly, 3 extrastimuli at 3 pacing-cycle lengths of 600, 500 and 400 ms, at rates of 100, 120 and 150 beats per minute, were used. The end point of the programmed stimulation protocol used in EPS studies was an inducible monomorphic VT (5 consecutive VPDs at a rate > 120 beats/min), not necessarily sustained. VT was defined as sustained if it persisted for 30 s or more, or if it required termination because of hemodynamic collapse. All patients were free of any antiarrhythmic agent at the time of the initial EPS. Cycle lengths and durations of the induced arrhythmia were measured. According to the results for the duration of the VT induced by the EPS, 84% of the members of the VT_{train} group had a sustained VT, while the remaining 16% had a nonsustained VT. Patients were monitored by an ambulatory device for at least 24 hours during their drug-free state and the records were analyzed (if 18 hours of usable data were recorded) to determine the frequency and duration of abnormal sequences. The results of ambulatory monitoring were used to establish parameters associated with spontaneous ventricular arrhythmias, such as number of premature beats and runs of premature beats. The baseline BSPM data were acquired during normal sinus rhythm in a drug-free state. Detailed clinical characteristics for all patients of the VT_{train} group are presented in Appendix C.

The NC group and MI_{train} group were selected from a population that underwent BSPM recording at the Victoria General Hospital in Halifax. An attempt was made to match the VT_{train} group as closely as possible for age and gender. The main concern was that these subjects had no clinical evidence of arrhythmias and

that they had quality BSPM data recorded during sinus rhythm. Subjects who were selected for the NC group ($n = 51$; mean age = 45.9 ± 8.5 years), 47 males and 4 females, had no evidence of heart disease on history, 12-lead ECG, physical examination and echocardiographic examination. Patients in the MI_{train} group ($n = 51$; mean age = 57.2 ± 11.1), 45 males and 6 females, all had suffered an MI (with the majority > 2 weeks earlier) and were, based on clinical assessment, without arrhythmias. The diagnostic classification for each patient in the MI_{train} group is in Appendix A (Table A.3); in summary, 55% of patients had an anterior MI and 45% had an inferior MI.

Test-set groups

The test set consisted of 51 patients with recurrent ventricular tachycardia (VT_{test} group) and 51 patients with MI without arrhythmia (MI_{test} group). Specific demographic data and diagnoses for all test-set subjects are in Appendix B. Again an attempt was made to match patients based on their age and gender, but the main concern was that the VT_{test} group consisted of patients who were vulnerable to ventricular arrhythmias, based on clinical information, and the MI_{test} group consisted of patients who had no clinical arrhythmias.

The VT_{test} group ($n = 51$; mean age = 58.5 ± 14.9), 47 males and 4 females, was selected from the Cardiac Unit at the Foothills Hospital in Calgary, using the same inclusion criteria as for the VT_{train} group. The difference was that VT_{test} group was not restricted to one drug therapy, which was in this case irrelevant since no posttreatment evaluation was performed on BSPM data of these patients.

Diagnoses for all members of the VT_{test} group are in Appendix B (Table B.1). Briefly, of 51 patients in VT_{test} group, 57% had sustained VT induced by EPS; for the remaining 43%, VT diagnosis rested either on evidence of nonsustained VT (or SVT in 3 patients) induced by EPS, or on documented episodes of VT obtained during electrocardiographic evaluation.

The MI_{test} group ($n = 51$; mean age = 54.7 ± 8.9), 47 males and 4 females, was selected from the patients who underwent BSPM recording in Victoria General Hospital in Halifax, using the same criteria as for the patients of MI_{train} group. Diagnoses for all members of the MI_{test} group are in Appendix B (Table B.2); in summary, 27% of the patients had anterior MI, 59% had an inferior MI, 4% had both anterior and inferior MI, and the remaining 10% had an unspecified MI.

Posttreatment group

An antiarrhythmic agent, quinidine, was administered to the patients who belonged to the VT_{train} group—in the appropriate doses for the patient's age and body mass—and then the EPS studies were repeated. On the basis of the posttreatment EPS studies, the 51 patients of the VT_{train} group were divided into two subgroups. The PET subgroup ($n=14$) consisted of those patients for whom quinidine was the predicted effective therapy (since the VT could not be induced after treatment by programmed stimulation). The nPET subgroup ($n=37$) consisted of those patients who remained susceptible to ventricular arrhythmias (since the VT remained inducible by programmed stimulation even after treatment). The criterion for determining predicted effective therapy (PET) was that no more than 4 VPDs occur in

response to the programmed stimulation protocol. The posttreatment BSPM data were acquired within 24 to 48 hours of the EPS study; these recordings, like the pretreatment data, were collected during normal sinus rhythm.

Summary statistics for age, left ventricular ejection fraction, quinidine blood levels and VT cycle lengths induced in the drug-free state for each subgroup of the VT_{train} group are in Appendix C. Comparisons between groups on several of the above clinical characteristics were performed (the results are also in Appendix C). There were no statistically significant differences ($p \geq 0.05$) between groups for the quantitative measures. A chi square analysis revealed statistically significant differences ($p \leq 0.05$) between the PET and nPET groups for three qualitative assessments; the PETs had a lower percentage of patients with ischemic heart disease, near miss sudden cardiac death as the presenting symptom and sustained VT induced by programmed stimulation (pretreatment). The factor that differentiated between the two subgroups was their response to programmed stimulation following treatment, which reflected the predicted effectiveness of the quinidine therapy.

3.2 Body-surface potential mapping

Data acquisition and preprocessing

Body-surface potentials were recorded from 117 torso leads and 3 limb leads, using the procedures and instrumentation developed in this laboratory [87,122,171]. The electrode placement is illustrated in Figure 3.1. The electrical potential differences were measured with respect to a Wilson's Central Terminal. The data were collected for 15 s during normal sinus rhythm, with subjects in a supine position. The

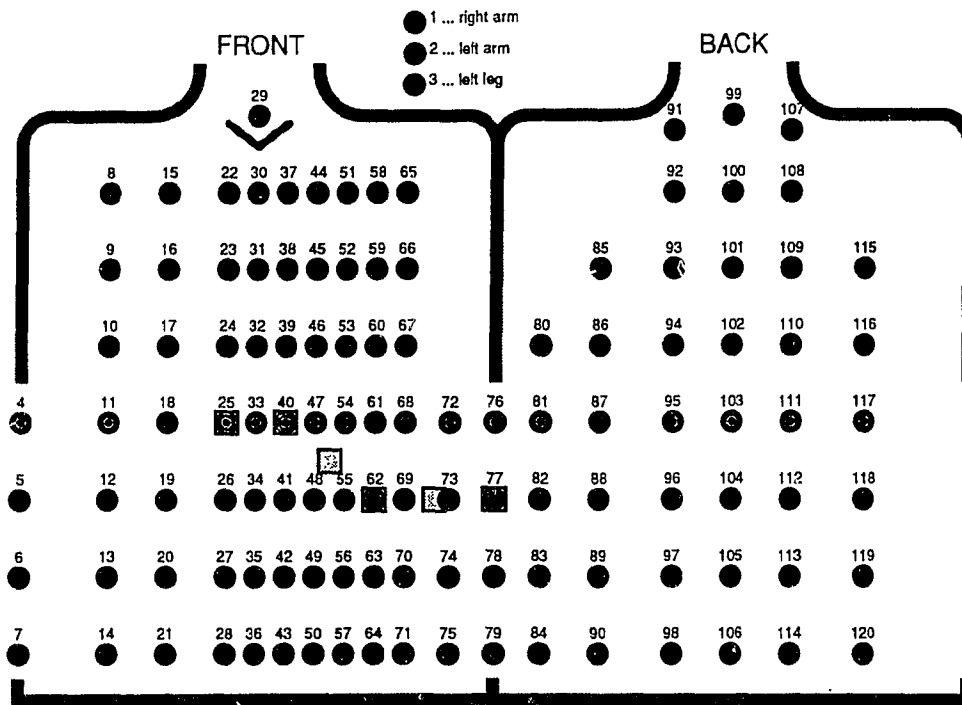


Figure 3.1: Electrode placement on the torso for the 120 body-surface leads. The right and left margins correspond to the right mid-axillary line and the middle corresponds to the left mid-axillary line; each \square corresponds to one of the six precordial leads.

analog signals were filtered (bandpass from 0.025 to 125 Hz), digitized at a sampling rate of 500 samples/s/channel, transferred to a PDP-11/24 computer, and stored on magnetic tape. Further data processing was performed on the VAX-11/780 computer (Digital Equipment Corp., Maynard, MA) and a Stellar GS1000 computer (Stardent Computer Inc, Concord, MA).

The raw-data plots were visually examined to determine the signal quality. The inspection was done by plotting 3 seconds of raw data. In addition, the entire 15-s recording was plotted for two leads. For randomly selected files, all 120 leads were plotted as a quality control. The raw data were then signal-averaged, using a T-P baseline; signal averaging was shown to be effective for reducing noise in ECG

signals [87]. The averaged data were plotted as scalar ECG plots for all 120 leads and those plots were visually inspected to identify bad leads and to verify the onsets and offsets for the QRS complex and T wave. The averaged data for the VT_{train} group (pretreatment data and posttreatment data), NC group, MI_{train} group, VT_{test} group and MI_{test} group were stored on a designated study tape (MT222).

In order to obtain the complete set of 117 body-surface potential values for each subject, including those with bad leads, three-dimensional interpolation of body-surface potentials was performed. A description of the interpolation procedure is in Appendix D. The interpolation was performed on the designated bad leads for all data files in this study, and the results were stored as 352 values for each time instant (corresponding to potential values at 352 nodes of the three-dimensional torso model [121]). This allowed retrieval of the complete set of 117 potentials for any subject and any time instant.

The QRST integrals were calculated for each subject, and for each of the 117 leads, by simple summation of sampled potentials:

$$\int QRST_i = \sum_{n=1}^{nsamp} V_i \delta t, \quad (3.1)$$

where $\int QRST_i$ is the QRST integral in μVs for lead i ; V_i is the potential measured in μV for lead i ; $nsamp$ is the number of discrete samples from R_{on} to T_{off} ; δt is the sampling interval in seconds ($\delta t = 0.002$ s) [89,135]. Isocontour maps for the QRST integrals (isointegral maps) were plotted and the set of 117 QRST-integral values per subject was used as the input for the data-reduction procedures.

Data reduction

The objective of the data-reduction procedures was to reduce the training-set pattern space to a feature space of smaller dimensionality, while maintaining the important diagnostic information in the measured data. Features that were the best discriminators for classification purposes were then selected by statistical methods from this reduced space [12]. The KL expansion has been considered the optimal transform for signal representation based on a mean-squared-error criterion [70], and since accurate representation of the original measured data was important, the approach adopted in this study was based on the KL expansion.

The KL transform was originally developed as the expansion of the stochastic process $\xi(t)$ in the time-domain, into a complete set of uncorrelated deterministic functions $\psi_i(t)$. (For a complete description of the transform refer to Gerbrands [70].) The KL transform can be discretized for use in digital image processing [76]; this discretized KL transform has been applied to BSPM data by several investigators [58,119,151,178,184].

In this study, the discretized KL transform was applied in the following manner to reduce the pattern space of the QRST-integral maps of the training set into a feature space. The processed BSPM data set consists of m channels and n discrete realizations of the random process. The number of body-surface ECG measurements at Dalhousie University and at the University of Calgary is 117 (i.e., $m = 117$). The vector \mathbf{x} was defined as the random vector \mathbf{x}_i , dimensioned 117×1 , representing the

potential distribution for subject i . Thus, we have n vectors \mathbf{x}_i ,

$$[X] = [\mathbf{x}_1, \mathbf{x}_2, \dots, \mathbf{x}_n], \quad (3.2)$$

where $[X]$ was a $117 \times n$ data matrix, and n was the number of subjects in the sample (since the QRST integral was used). Applying the KL expansion theory to determine the linear combination of orthonormal basis functions to minimize a mean square error criterion was as follows.

The unbiased estimate of the covariance matrix for both the KL expansion and principal component analysis is the sample covariance matrix $[S_c]$ of the columns of $[X]$ (see [70]).

$$\begin{aligned} [S_c] &= \frac{1}{n-1} \sum_{i=1}^n (\mathbf{x}_i - \mathbf{m}_x)(\mathbf{x}_i - \mathbf{m}_x)^t \\ \mathbf{m}_x &= \frac{1}{n} \sum_{i=1}^n \mathbf{x}_i \end{aligned} \quad (3.3)$$

or

$$[S_c] = \frac{1}{n-1} \{[X] - [\bar{X}]\} \{[X] - [\bar{X}]\}^t, \quad (3.4)$$

where $[S_c]$ is the sample covariance matrix, \mathbf{m}_x is a column vector of the means obtained from a vector summation of \mathbf{x}_i , and $[\bar{X}]$ is an $m \times n$ matrix in which the columns are equal to \mathbf{m}_x ; m is equal to 117 for the spatial reduction. Calculation of the sample covariance matrix $[S_c]$ for matrix $[X]$ from equation 3.4 was performed by the FORTRAN program **PCA.f**.

The KL transform of the vectors \mathbf{x}_i defined as,

$$\mathbf{y}_i = [T]^t \mathbf{x}_i \quad (3.5)$$

produces a vector of coefficients, \mathbf{y}_i , for each subject. The matrix $[T]$ was calculated from an eigenvalue and eigenvector analysis of $[S_c]$

$$[S_c] = [T][\Lambda][T]^t. \quad (3.6)$$

This was done by the FORTRAN program **EIGEN.f**, which incorporated the NAG library routine F02ABF (The Numerical Algorithms Group Ltd.) to calculate the eigenvalues and eigenvectors of a real symmetric matrix using Householder's reduction and the QL algorithm. $[\Lambda]$ is the diagonal matrix of eigenvalues, λ_i , ordered in descending order of magnitude to minimize the mean-squared error. $[T]$ is the matrix, dimension 117×117 , of orthonormal eigenvectors Φ_i . The expansion can be truncated to k terms, where $k < n$. The vector $\hat{\mathbf{x}}$ can be reconstructed using equation

$$\hat{\mathbf{x}}_i = [T_r]\mathbf{y}_{i(r)} \quad (3.7)$$

where $\hat{\mathbf{x}}_i$ is the reconstructed vector of body-surface potentials for subject i , $[T_r]$ is the reduced transform matrix of dimension $117 \times k$, and $\mathbf{y}_{i(r)}$ is the reduced coefficient vector of dimension k for subject i . If the number of basis vectors k is less than n , then data reduction is achieved. The required number of basis vectors k depends on the total information contained in them. An estimate of the error of truncation by k basis functions can be obtained from the average error e_k [58,119],

$$e_k = [(trace[S_c] - \sum_{i=1}^k \lambda_i)/117]^{1/2}. \quad (3.8)$$

This can be expressed as a percentage by considering the signal voltage associated

with the average error,

$$\%trace[S_c] = \left(\sum_{i=1}^k \lambda_i \right) \times \frac{100}{trace[S_c]}, \quad (3.9)$$

where $trace[S_c]$ is the trace of the sample covariance matrix; eigenvalues, λ_i , are in descending order of magnitude. The percent trace was used to determine the number of eigenvectors required for reconstruction of the BSPMs. The k eigenvectors representing the principal patterns were plotted as eigenmaps using the same display convention as that used for the measured BSPM data. The reduction and reconstruction were done by the FORTRAN program **RECON.f**.

The measured, reconstructed and difference maps ($\mathbf{x}_i - \hat{\mathbf{x}}_i$) for each subject were plotted and visually inspected for major discrepancies. The root-mean-squared error was calculated for each map as:

$$e_{rms} = \left(\frac{\sum_{i=1}^{117} |\mathbf{x}_i - \hat{\mathbf{x}}_i|^2}{117} \right)^{\frac{1}{2}}, \quad (3.10)$$

where e_{rms} is the root-mean-square error. The relative error was also calculated for each map by,

$$e_{rel} = \frac{\sum_{i=1}^{117} |\mathbf{x}_i - \hat{\mathbf{x}}_i|^2}{\sum_{i=1}^{117} \mathbf{x}_i^2} \times 100. \quad (3.11)$$

The peak error was defined as the maximum absolute difference between a measured and a reconstructed value at any lead for each map.

$$e_{peak} = \max |\mathbf{x}_i - \hat{\mathbf{x}}_i|. \quad (3.12)$$

Means and standard deviations were calculated for each of the error measures for the constituent groups of the training set, test set and posttreatment set. Worst-case errors were identified for each error measure for each group.

In summary, the KL expansion was used to reduce the training-set pattern space into a feature space. This feature space was assessed to determine whether the salient features were maintained from the measured data which would then justify applying stochastic methods to define a classification space based on these features.

Feature selection

The next step was to identify a subset of features that contain the necessary diagnostic information for classifying the constituent groups. Three approaches to feature selection from this reduced KL space were used. First, the *nondipolar content* of the QRST-integral maps was evaluated as a single measure reflecting the complexity in the BSPM patterns; this measure can be calculated as suggested by Abildskov et al. [9]. The nondipolar content of a given map can be calculated [46] by computing the cumulative contribution of all eigenvectors beyond the third as a percentage of the total map content. This definition is based on the fact that the first three eigenvectors are basically dipolar in nature (with only one maximum and one minimum), while the following ones contain more than two extrema and are said to be multipolar in nature. The set of coefficients y_i which are characteristic for each subject from the KL transform, may be used to compute the contribution of the eigenvectors to the total map content as

$$\%NDPC = \frac{\sum_{j=4}^k y_{ij}^2}{\sum_{j=1}^{117} x_{ij}^2} \times 100, \quad (3.13)$$

where $\%NDPC$ denotes the percentage non-dipolar content and $\sum_{j=1}^{117} x_{ij}^2$ denotes the total energy in the signal.

Thus, the 117 measured values were represented by only one feature of the map,

percent nondipolar content. Statistical tests were used to determine whether significant differences existed between the constituent groups for this variable; the significance level was 0.05. When more than two groups were being compared, an analysis of variance model was used and if a significant difference was found, multiple range pairwise comparisons were done. When only two groups were being compared, independent t-tests were calculated. For the pretreatment and posttreatment comparisons, dependent t-tests were performed. These tests were done using the SYSTAT statistical package [196]. (If statistically significant differences were found between the groups for this measure, a discriminant analysis using the SAS routine **DISCRIM** would be performed [93].)

The second approach utilized all k features derived from the eigenvector analysis. Since the KL expansion orders the features based on their contribution to the pattern space, they are not necessarily in the best order for the discriminant analysis. A step-wise discriminant analysis procedure, applied directly to the feature coefficients, was used to determine which features provided the best discrimination between the groups. This was done by using the SAS routine **STEPDISC** [93]. In this analysis, subjects were divided into groups based on their clinical diagnosis and the analysis was used to find the subset of features that best characterizes the differences between groups [93]. Features were entered into the model and removed, based on their discriminatory power as measured by Wilks lambda and the F approximation [93]. The KL feature coefficients were entered as input; even though they are not physiological variables themselves, they represent the BSPM patterns with an acceptable degree of accuracy.

Given that the sample size was 51 subjects per group, only a subset of three KL features was chosen. Thus, the ratio of number of features to number of subjects was relatively conservative (1:17), to minimize the possibility of tailoring the classification space to the training set. The three features were then used as the input for the discriminant analysis routine **DISCRIM**.

The final approach to feature selection was based on the application of the KL transform that uses an alternative method of feature ordering suggested by Kittler and Young [102]. This method utilizes the discriminatory potential of both the class means and the class variances. The general theory for this approach is a two-stage KL decomposition, which optimizes the feature space for classification purposes. Feature selection is carried out by constructing the covariance matrix of the input vectors by subtracting the mean vector for each class from the respective class vectors and performing a series of KL decompositions.

The Kittler and Young (KnY) transform procedure was applied to the k weighting-coefficient vectors \mathbf{y} , derived from the eigenvector analysis for each subject. It was in essence a two-stage KL decomposition of the k -dimensional vector $\mathbf{y}_{i(r)}$, denoting values of KL weighting coefficients for each subject's QRST-integral map. Each vector may belong to any one of the 3 (or 2) possible diagnostic classes ω , which were predetermined from clinical evaluation of subjects. Each class was centralized by subtracting the mean of the coefficient vectors \mathbf{m}_ω for that class. The sample covariance matrix for each class, $[S_{c\omega}]$, was constructed as

$$[S_{c\omega}] = E\{(\mathbf{y}_i - \mathbf{m}_\omega)(\mathbf{y}_i - \mathbf{m}_\omega)^t\}. \quad (3.14)$$

For the n classes of equal size, the sample covariance matrix $[C_{K_n Y}]$ may be expressed as

$$[C_{K_n Y}] = \sum_{\omega=1}^n \frac{1}{n} [S_{c\omega}], \quad (3.15)$$

where the probability of occurrence of each class is $1/n$. The eigenvalues λ and matrix of eigenvectors $[R]$, arranged in decreasing order of eigenvalue magnitude, were computed for the covariance matrix $[C_{K_n Y}]$. The eigenvalues Λ of $[C_{K_n Y}]$ represent only the transformed class variances, as the class means have been removed. The feature vector \mathbf{c} was constructed using

$$\mathbf{c}^t = \mathbf{y}^t [R]. \quad (3.16)$$

The second part of the transform normalized the variances by doing a simple linear transformation of the feature vector \mathbf{c} into a new feature vector \mathbf{g} by

$$\mathbf{g}^t = \mathbf{y}^t [R] [Q], \quad (3.17)$$

where $[Q]$ is a diagonal matrix, with the elements of the diagonal given as

$$q_{kk} = \frac{1}{\text{sqrt}(\lambda_k)} \quad (3.18)$$

i.e., this transformation weights each feature in inverse proportion to its standard deviation. The mean vector of each class was now defined as

$$\mathbf{k}_i^t = \mathbf{m}_i^t [R] [Q]. \quad (3.19)$$

and the covariance matrix $[S_{c\omega}]$ defined as

$$[S_{c\omega}] = E\{(\mathbf{g}_i - \mathbf{k}_i)(\mathbf{g}_i - \mathbf{k}_i)^t\}. \quad (3.20)$$

is the identity matrix. Applying the KL expansion to the transformed vectors \mathbf{g} resulted in a new basis set $[\mathbf{B}]$. The transformation of the vector \mathbf{g} by the eigenvectors $[\mathbf{B}]$ yields a set of uncorrelated coordinate coefficients \mathbf{f} , such that

$$\begin{aligned}\mathbf{f}^t &= \mathbf{y}^t[\mathbf{R}][\mathbf{Q}][\mathbf{B}] \\ &= \mathbf{y}^t[\mathbf{P}],\end{aligned}\tag{3.21}$$

where $[\mathbf{P}] = [\mathbf{R}][\mathbf{Q}][\mathbf{B}]$, and $[\mathbf{B}]$ was the system of eigenvectors of the covariance matrix of \mathbf{g} arranged in the decreasing order of eigenvalue magnitude. The matrix $[\mathbf{C}_g]$ is defined as;

$$[\mathbf{C}_g] = \sum_{\omega=1}^n 1/n E\{\mathbf{g}\mathbf{g}^t\}.\tag{3.22}$$

The FORTRAN program **KnY.f** was used to calculate the covariance matrices and perform the eigenvalue and eigenvector analysis described above for the KnY transformation. Kittler and Young showed that the final feature vector \mathbf{f} is ordered with respect to the discriminatory potential assumed to be optimal with respect to the class means and the class variance set to unity by the normalization process. Thus, the selection of ℓ features according to the descending order of their total variances will provide a ℓ -component feature vector where the first ℓ ($\ell < k$) feature coefficients have good classification potential. Kittler and Young showed that once the features were ordered using this two-stage KL expansion, a discriminant function analysis was the better method of classification compared to the nearest neighbour and nearest mean approaches [102]. The SAS routine **STEPPDISC** [93] was used to determine which features, from this KnY feature space, provided the best discrimination between the groups. Again, this analysis was limited to three features (to maintain a conservative ratio of features to the number of subjects), and these were

then used as input to the discriminant analysis routine **DISCRIM**.

3.3 Classification based on discriminant analysis

After the features were selected that discriminated best between groups, a set of linear discriminant functions was calculated that minimized the squared differences between groups [110]. These functions were evaluated for classification purposes, with the assumption that the initial classification was correct. The SAS routine **DISCRIM** [93] evaluated the general linear equation,

$$df_{i\omega} = a_{0\omega} + a_{1\omega} \cdot z_{1i} + a_{2\omega} \cdot z_{2i} + \dots, \quad (3.23)$$

where $df_{i\omega}$ is the discriminant function for subject i , evaluated for each class ω ; a_0 is the constant for class ω ; $a_1, a_2 \dots$ are the discriminant coefficients for the features chosen from the **STEPPDISC** analysis for class ω ; $z_{1i}, z_{2i} \dots$ are the weighting coefficient from either the KL expansion ($y_{1i}, y_{2i} \dots$) or the KnY transform ($f_{1i}, f_{2i} \dots$) for subject i , for features 1, 2, ... from the **STEPPDISC** analysis. This equation would have only one term for the nondipolar content. The rule for classifying subject i was based on the value of their linear discriminant function for each group. Subjects were classified into the group corresponding to the largest $df_{i\omega}$.

Three variables were calculated to assess the classification results: sensitivity (SE), predictive value (PV) and diagnostic performance (DP). Sensitivity was defined as

$$SE = \frac{n_{ca/\omega}}{n_{a/\omega}} \times 100, \quad (3.24)$$

where SE is sensitivity in percent; $n_{ca/\omega}$ is the number of subjects classified into

group ω that were from group ω ; $n_{a/\omega}$ is the number of subjects actually in group ω . Sensitivity expressed the number of correct classifications for each group. The predictive value (PV) quantified the ability to classify only those subjects that truly belong to a group into that group and was expressed as

$$PV = \frac{n_{ca/\omega}}{n_{c/\omega}} \times 100, \quad (3.25)$$

where PV is predictive value in percent; $n_{c/\omega}$ is the total number of subjects classified into group ω . Diagnostic performance was a single measure based on sensitivities for all constituent groups, defined as

$$DP = \frac{1}{g} \sum_{i=1}^g SE_i, \quad (3.26)$$

where DP is the diagnostic performance for the classification that involves g groups and SE_i is sensitivity for group i . The above three measures were only applied to the classification results for the training set and the independent test set. The results pertaining to the treatment group were only evaluated to determine whether the posttreatment classification differed from the pretreatment classification.

Error estimation

The question of how well the discriminant functions will perform for classifying future observations has to be addressed, in order to assess the value of the selected features and discriminant functions [110]. The apparent error from the training set (defined as $e_{\text{app}} = 100\% - DP$) provides an overly optimistic estimate of the true error for future classification [54,55]. Four methods for estimating the expected or true error (defined as $e_{\text{true}} = e_{\text{app}} + e_{\text{bias}}$) associated with the classification spaces were employed.

First, the classification space derived from the training set was applied to classify an independent test set and the difference between the training set and test set provided one estimate of the error bias [55]. In addition to the estimated errors calculated from the test sets, three other error estimates were calculated by methods that did not require an independent test set, but instead utilized all available data [54,53,55]. The bootstrap without replacement (random half sampling) [53], randomized bootstrap with replacement [54] and cross-validation [54] were employed.

In order to employ these stochastic techniques to estimate the true errors, the entire data set (training set + test set) was combined. The classification space for the KL feature space and KnY feature space were defined and evaluated for the entire set of data. The stepwise discriminant analysis procedure defined the features and their order in the subsets.

The bootstrap method without replacement randomly assigned patient maps to a training set ($n = 102$) and the remaining 102 maps constituted the test set. The discriminant functions derived from a training set were applied to the corresponding test set for each randomization and the classification was based on the linear discriminant functions applied to the new test set. Using the same rules as in section 3.3, this was repeated 1000 times. The average classification performance and variance estimates were calculated for the 1000 trials.

The bootstrap method with replacement randomly assigned maps to training sets comprised of 204 maps [54]. The average number of maps in the designated bootstrap test sets were approximately 37% of the entire sample. Again, 1000 randomizations were performed and average performance and variance estimates

for classifying the bootstrap training and test sets were calculated from the data.

Lastly, a method of cross-validation was employed as described by Efron [54,53,55]. All maps but one were designated as the training set from which the discriminant functions were derived and the classification space was applied to the remaining test map. This procedure was repeated in a systematic fashion until all maps were excluded once. The variance estimates for this data were calculated using a binomial distribution.

The error estimates calculated as described above provided estimates of the true error of the classification space derived in this study. This approach was also used to evaluate the appropriateness of the number of KL features included in the stepwise discriminant analysis and the KnY transformation. The three error estimates were employed to calculate the expected classification errors associated with the classification space—which was derived from k features in either the discriminant analysis of the KL feature space or in defining the KnY feature space. This analysis was aimed at evaluating the effects of increased numbers of features on tailoring the discriminant functions to the training set. If the error bias between the training set and the test set was very large, or the training-set error decreased while the test-set error increased, this would provide evidence of overtraining or tailoring.

Because of the large number of repetitions involved in these analyses, it was too cumbersome to call the SAS routine **DISCRIM**. Therefore, FORTRAN routines were written to perform the sampling procedures for each method of estimating the true error; they also calculated the linear discriminant functions for classification purposes.

Chapter 4

Classification of the three-group training set

This chapter deals with three-group classification of the training set consisting of 51 patients with recurrent ventricular tachycardia (VT_{train} group), 51 normal subjects (NC group), and 51 patients with myocardial infarction but no history of clinical arrhythmias (MI_{train} group). These groups are described in detail in section 3.1 and in Appendix A. This chapter is developed in an order consistent with the objectives stated in chapter 1.

Firstly, the pattern space comprised of the ECG measurements of all members of the training set was reduced to a much smaller feature space and the errors associated with this data reduction were assessed. The measurements consisted of 117 values of the QRST integral, obtained for each subject from 117 ECG leads, which were recorded simultaneously by a digital acquisition system. The QRST integral was chosen because it is known to reflect the primary repolarization properties of the ventricle, as established in chapter 2. A data reduction was accomplished by an eigenvector analysis of the sample covariance matrix, based on the KL expansion theory (see section 3.2). The ability of the feature space derived from this analysis

to represent accurately the original pattern space was evaluated by an error analysis of the reconstructed QRST-integral values for each map.

Secondly, in the feature space, three different approaches were used to determine whether there were statistically significant differences among the constituent groups that could be exploited in diagnostic classification. The first approach used an analysis of variance (ANOVA) to determine whether there were significant differences in *nondipolar content* among the three groups. The second approach used 16 KL features derived from all members of the training set in a stepwise discriminant analysis. The third approach required a transformation of the 16 feature coefficients by KnY transformation, to optimize the discriminating content before the discriminant analysis.

4.1 Eigenvector analysis of QRST-integral maps

The pattern space for the three-group training set was represented by a matrix $[X]$, dimensioned 117×153 , which contained 117 QRST-integral values for each member of the training set. The sample covariance matrix $[S_c]$ and its eigenvalues and eigenvectors were then calculated for $[X]$. The percent trace was calculated to estimate the error of reconstruction; for the 16 highest eigenvalues it was 99% (Fig. 4.1). The 16 corresponding eigenvectors were plotted as eigenmaps (Fig. 4.2). The percent contribution of eigenvectors beyond 9 was very small; however, 16 eigenvectors were chosen to ensure that complex features that may contain diagnostic information were included.

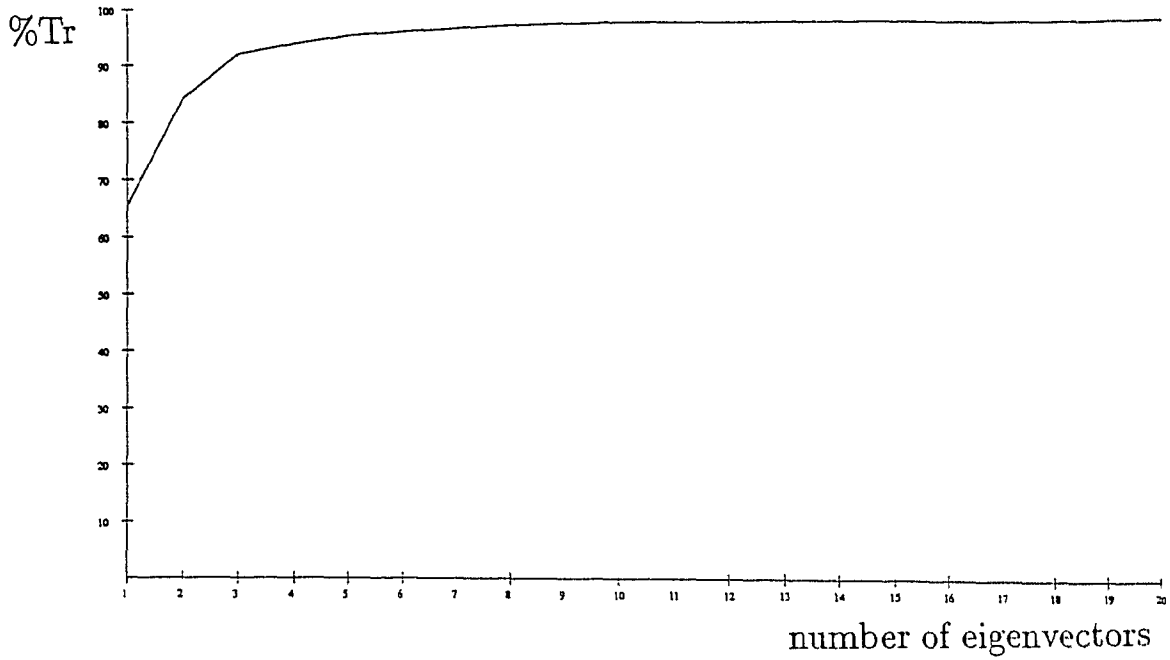


Figure 4.1: Percent trace vs. eigenvectors derived from the three-group training set

Table 4.1: Reconstruction errors for the three-group training set

		Training set ($n=153$)	VT_{train} ($n=51$)	NC ($n=51$)	MI_{train} ($n=51$)
rms error [μVs]	mean	3.25	3.42	3.01	3.31
	SD	0.93	0.90	0.87	0.99
relative error [%]	mean	2.47	4.16	0.57	2.67
	SD	4.64	5.71	0.48	5.10
peak error [μVs]	mean	11.42	10.96	10.78	12.51
	SD	4.87	3.78	5.81	4.71

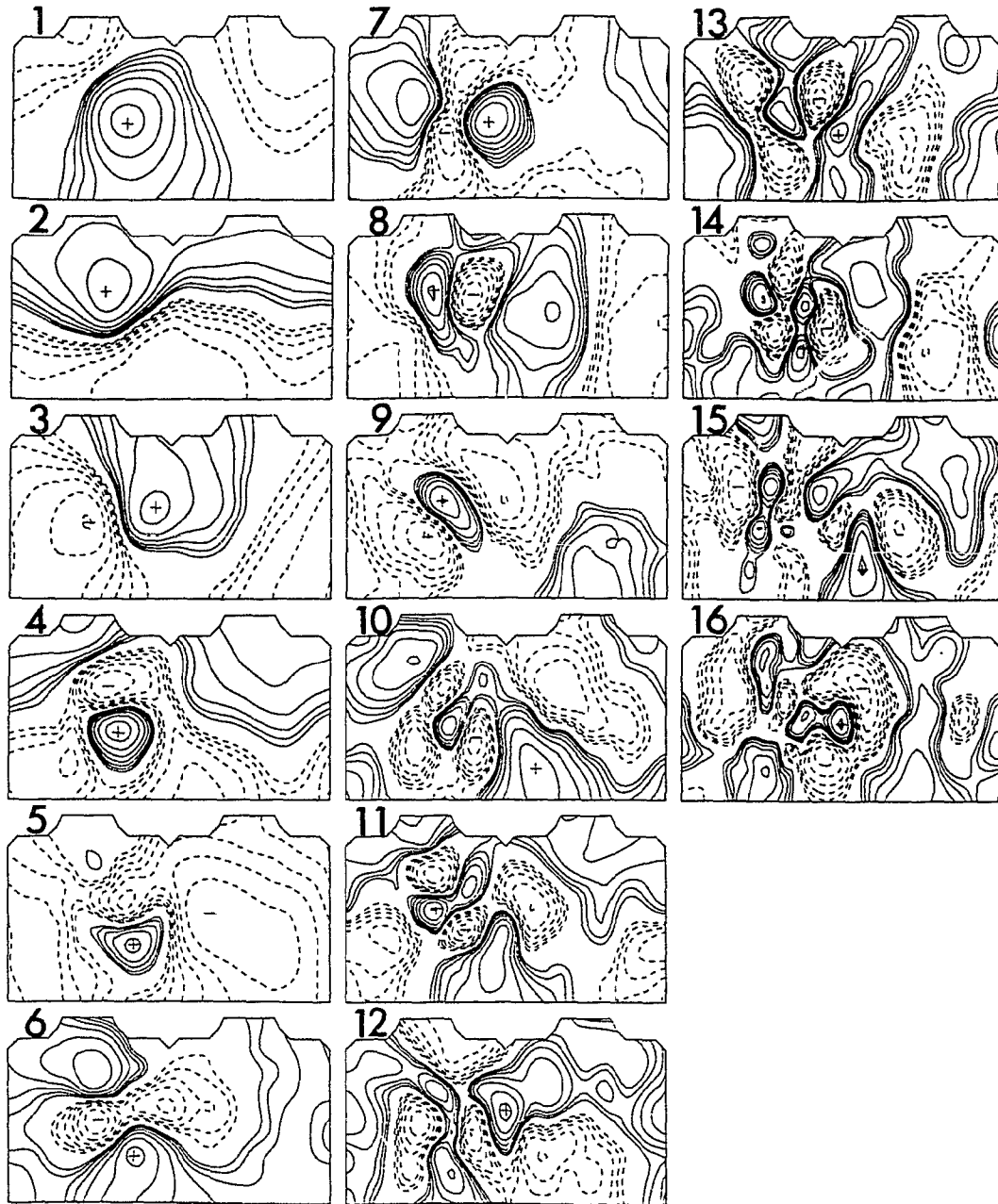


Figure 4.2: Eigenvectors derived from the three-group training set. Eigenvectors are plotted as spatial maps on the torso and arranged in descending order of the magnitude of their contribution. The plotting convention is the same as for the measured maps, i.e., the map's left and right margins correspond to the right mid-axillary line, with the left side of the map corresponding to the anterior torso and the right side to the posterior torso.

The weighting coefficients y_i were then calculated for each of the 16 eigenvectors and for each subject, so as to account for the measured QRST-integral values. The 16 weighting coefficients for each subject and the eigenvectors derived from the entire training set were then used to reconstruct the QRST-integral maps for each subject. These reconstructed maps were qualitatively examined, to detect possible differences in spatial patterns as compared to the measured maps, and three error measures were calculated to quantify differences between the measured and reconstructed maps: a root-mean-squared error (rms error), relative error and peak error. A summary of the errors for the total three-group training set and for each of the three constituent groups is in Table 4.1.

The worst-case rms error was $6.6 \mu\text{Vs}$, the worst-case relative error was 34.4%, and the worst-case peak error was $41.2 \mu\text{Vs}$. The measured and reconstructed maps for the worst cases are in Fig. 4.3. While the rms error and the peak error were consistent across the three groups, the relative error was *much smaller* for the NC group than for both MI_{train} and VT_{train} groups, and was the largest for the VT_{train} group.

4.2 Nondipolar content of QRST-integral maps

The QRST-integral maps were qualitatively different in VT_{train} , NC and MI_{train} groups; this is evident in Fig. 4.4. The QRST-integral maps of subjects who belonged to NC group had a consistently smooth spatial pattern with one maximum and one minimum, whereas patients belonging to both VT_{train} and MI_{train} groups showed more variability in their distributions and had multiple extrema. The first at-

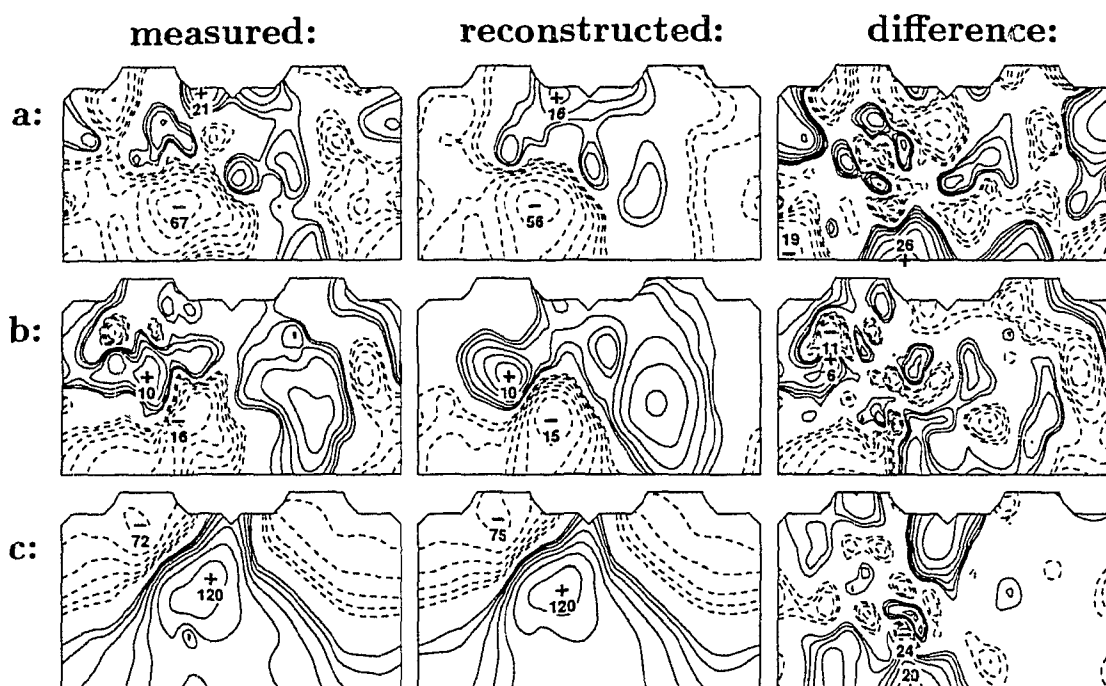


Figure 4.3: Worst-case reconstruction errors for the three-group training set. The reconstruction was based on 16 weighting coefficients and corresponding eigenvectors. In the left column are measured maps, middle column are the reconstructed maps and right column the difference maps. a) Worst-case rms error ($e_{\text{rms}} = 6.6 \mu\text{Vs}$, $e_{\text{rel}} = 11.0\%$, $e_{\text{peak}} = 24.7 \mu\text{Vs}$). b) Worst-case relative error ($e_{\text{rms}} = 3.3 \mu\text{Vs}$, $e_{\text{rel}} = 34.4\%$, $e_{\text{peak}} = 13.7 \mu\text{Vs}$). c) Worst-case peak error ($e_{\text{rms}} = 5.6 \mu\text{Vs}$, $e_{\text{rel}} = 1.2\%$, $e_{\text{peak}} = 41.2 \mu\text{Vs}$). The plotting convention is similar to that used in Fig. 4.2.

tempt to quantify the difference in spatial patterns employed the nondipolar-content measure as the feature representing the map. The nondipolar content was calculated for each subject in the training set. A one-way ANOVA on this data revealed a significant difference at the $p \leq 0.05$ level, and Duncan multiple-range test showed that the mean (\pm SD) nondipolar content of the NC group (6.31 ± 5.61) differed significantly ($p \leq 0.05$) from those of the VT_{train} group (13.10 ± 9.57) and the MI_{train} group (12.83 ± 10.37). However, there was no significant difference between the VT_{train} and MI_{train} groups, and, because of the high degree of overlap between these two groups (Fig. 4.5), a classification procedure based on the nondipolar-content measure was not attempted.

4.3 Discriminant analysis employing KL features

To identify features that would separate the three constituent groups of the training set, a stepwise discriminant analysis was performed. The discriminant analysis described in this section used as input data the 16 weighting coefficients associated with the 16 eigenvectors of the KL expansion. Three coefficients (y_1, y_2 and y_4) were identified by the stepwise analysis as having the best discriminating abilities in separating the three groups of the training set. The spatial KL patterns corresponding to these weighting coefficients are depicted as maps 1, 2 and 4 in Fig. 4.2; two of these three spatial patterns are dipolar by definition. Results of the classification that employed the discriminant functions derived for the three KL features y_1, y_2 and y_4 , are summarized in Table 4.2. These results can be better judged from Table 4.3; 84% of subjects in the NC group were correctly classified, while only

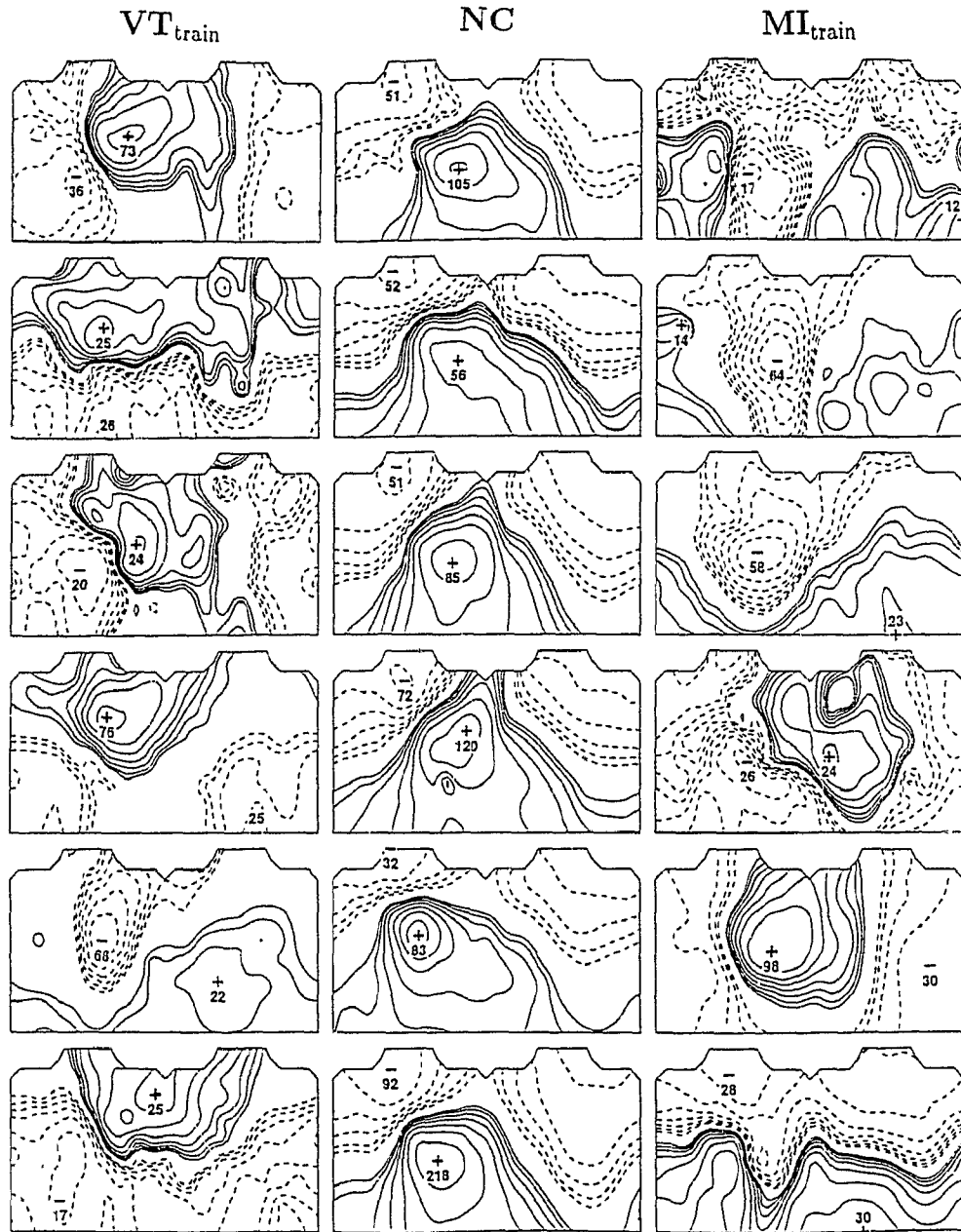


Figure 4.4: Examples of QRST-integral maps for the three-group training set. Randomly selected examples of QRST-integral maps for individuals in each of the three constituent groups (VT_{train} , NC and MI_{train}). The plotting convention is the same as in Fig. 4.2.

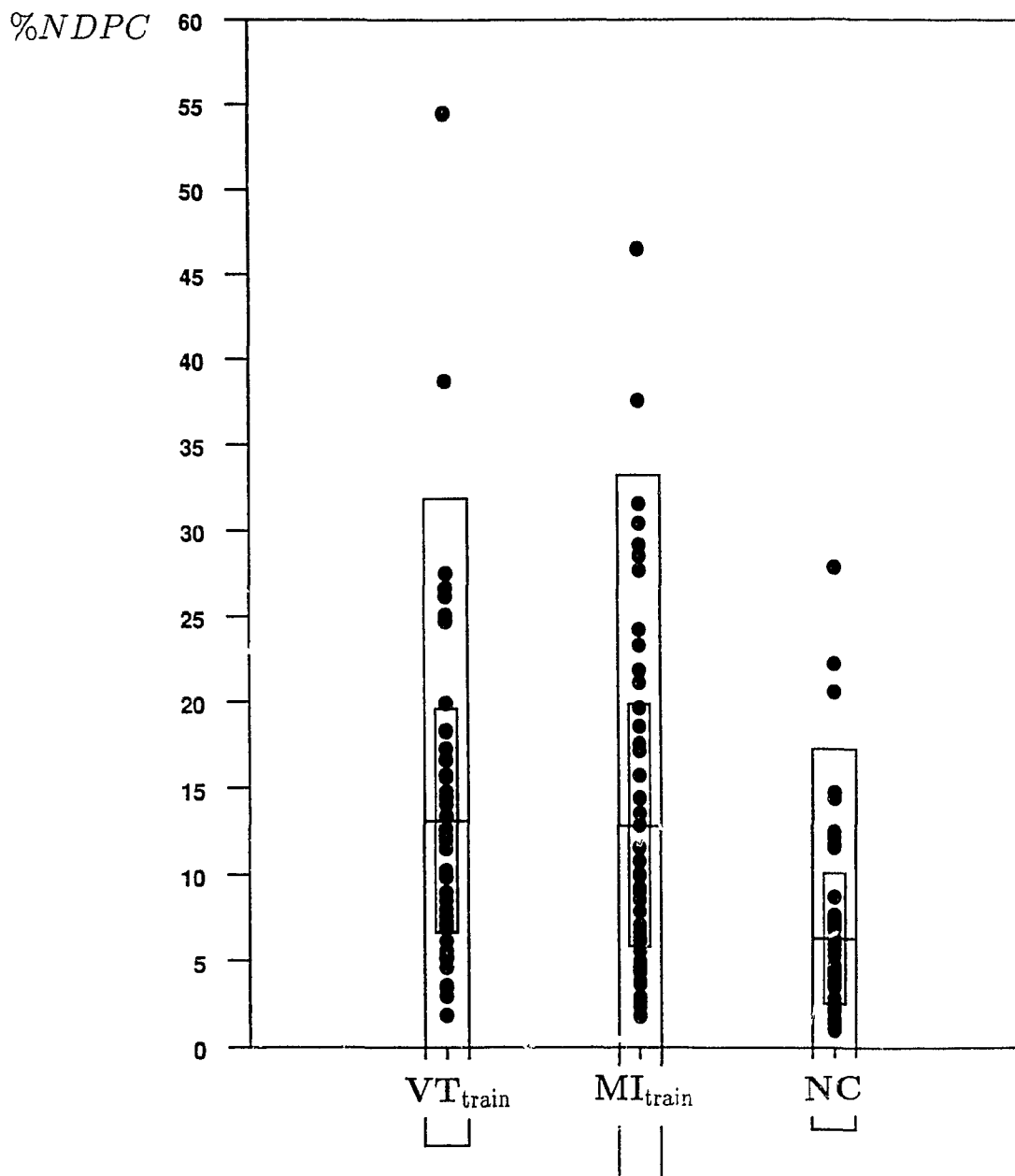


Figure 4.5: Nondipolar content for the three-group training set. The inner box corresponds to the 50% confidence limits and the outer box to the 95% confidence limits. Mean for each group is indicated by the horizontal line.

Table 4.2: Classification of the three-group training set: discriminant analysis based on KL features y_1, y_2 and y_4 derived from this set

Group	Category		
	VT	NC	MI
VT _{train} ($n=51$)	36	0	15
NC ($n=51$)	0	43	8
MI _{train} ($n=51$)	18	7	26
Total ($n=153$)	54	50	49
Priors	.333	.333	.333

Table 4.3: Sensitivity, predictive value and diagnostic performance of classification based on KL features y_1, y_2 and y_4 derived from the three-group training set

Group	Sensitivity [%]	Predictive Value [%]
VT _{train} ($n=51$)	71	67
NC ($n=51$)	84	86
MI _{train} ($n=51$)	51	53
$DP = 69\%; \kappa = .53$		

51% of patients in the MI_{train} group were correctly classified. The overall diagnostic performance for this classification was 69%; i.e., this approach allowed correct classification of 69% of subjects who belonged to the training set. As in the analysis based on the nondipolar content (section 4.2), the most difficult task proved to be separating the VT_{train} and MI_{train} groups.

4.4 Discriminant analysis employing KnY features

In an attempt to pack more diagnostic information into fewer features, the KnY transformation was performed on the 16 weighting coefficients associated with the

Table 4.4: Classification of the three-group training set: discriminant analysis based on KnY features f_1 and f_2 derived from this set

Group	Category		
	VT	NC	MI
VT _{train} ($n=51$)	44	0	7
NC ($n=51$)	2	42	7
MI _{train} ($n=51$)	10	5	36
Total ($n=153$)	56	47	50
Priors	.333	.333	.333

16 KL features derived from the three-group training set. This transformation yielded 16 new features (KnY features), each of which was a linear combination of the 16 weighting coefficients y_i from the KL space. It followed from the stepwise discriminant analysis of this transformed data that the bulk of the discriminating information was contained in only two KnY coefficients, f_1 and f_2 . The results of classification of the 153-subject training set, based on this analysis, are in Table 4.4. Sensitivities were 86%, 82%, and 71% for the VT_{train}, NC and MI_{train} groups, respectively, as shown in Table 4.5; thus, the sensitivity for the VT_{train} and MI_{train} groups was improved compared to the one achieved in the KL feature space (Section 4.3). The two KnY coefficients for each subject were plotted in two-dimensional space as shown in Fig. 4.6, illustrating the improved separation of the three groups in this feature space. Overall diagnostic performance achieved by this approach was 80%, as shown in Table 4.5; i.e., 80% of all subjects in the training set were correctly classified.

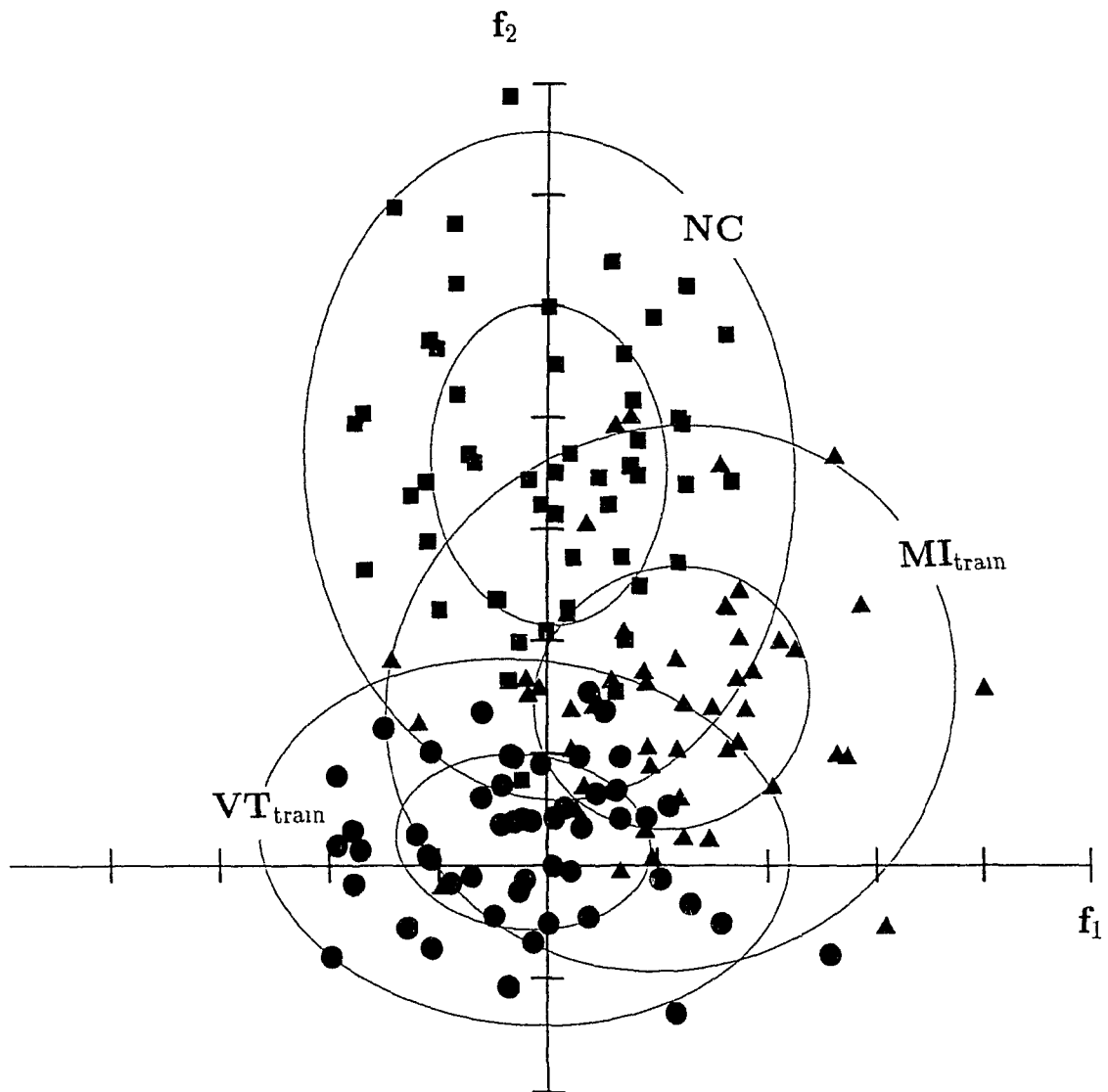


Figure 4.6· Kny coefficients f_1 and f_2 derived from the three-group training set. Coefficient f_1 is on the abscissa and f_2 on the ordinate; the inner ellipses correspond to the 50% confidence intervals and the outer ellipses to the 95% confidence intervals; ● represents one VT_{train} patient; ■ represents one NC subject; ▲ represents one MI_{train} patient.

Table 4.5: Sensitivity, predictive value and diagnostic performance of classification based on KnY features f_1 and f_2 derived from the three-group training set

Group	Sensitivity [%]	Predictive Value [%]
VT _{train} ($n=51$)	86	79
NC ($n=51$)	82	89
MI _{train} ($n=51$)	71	72
$DP = 80\%; \kappa = .70$		

4.5 Summary and discussion

The results presented in this chapter demonstrate that reduction of the pattern space, consisting of electrocardiographic QRST-integral measurements, into 16 KL features can be achieved with relatively low average reconstruction errors. This was shown for the training set of 153 subjects. Even when the reconstruction errors were high, qualitative assessment of the maps showed that the overall patterns were maintained on reconstruction. The statistical analysis based on nondipolar content (quantitatively evaluated as a signal energy of all KL coefficients beyond y_4 , relative to the total signal energy) demonstrated that this measure offered little discriminating value for separating the VT_{train} and MI_{train} groups, although it separated both of these groups well from the NC group. The discriminant analysis based on the three KL features y_1, y_2 and y_4 , selected out of 16 KL features derived from the three-group training set, was again most effective in identifying the NC subjects, while the VT_{train} and MI_{train} groups were not easily separated. The KnY transform of the 16 KL weighting coefficients derived from the training set yielded two new features, f_1 and f_2 , which represented the majority of the diagnostic information.

Analysis based on these new KnY features improved overall diagnostic performance of classification from 69% to 80%. The highest sensitivity (86%) was achieved for the VT_{train} group, while the NC group still retained the highest predictive value (89%). It is worth noting that no subjects from the VT_{train} group, and only 5 subjects from the MI_{train} group, were classified as NC subjects; this was reflected in the high predictive value for the NC group. Therefore, the KnY transform—applied to the weighting coefficients derived from the eigenvector analysis of the sample covariance matrix based on the QRST-integral measurements from the body surface—was the most effective approach for discriminating among training-set groups.

The results presented in this chapter show that the major classification errors were associated with separating the VT_{train} and MI_{train} groups from each other, not in separating the VT_{train} and MI_{train} groups from NC group.

Chapter 5

Classification of the two-group training set

It follows from the results of the previous chapter that inclusion of the NC group produced a discriminant function that distinguished well between normal individuals and patients but that separated VT and MI patients poorly. Therefore, the strategy adopted in the analysis presented in this chapter was to derive the set of 16 KL features solely from the sample of VT and MI patients. The two-group training set consisted of 51 patients with recurrent ventricular tachycardia (VT_{train} group) and 51 patients with myocardial infarction but no history of clinical arrhythmias (MI_{train} group). These groups are described in detail in section 3.1 and in Appendix A. The objectives of this new classification strategy were identical to those stated for the three-group analysis, and the results are presented in the same order.

5.1 Eigenvector analysis of QRST-integral maps

The pattern space for the two-group training set was a matrix $[X]$, dimensioned 117×102 , which contained 117 QRST-integral values for the 102 patients. The sample covariance matrix $[S_c]$ and its eigenvalues and eigenvectors were then calculated

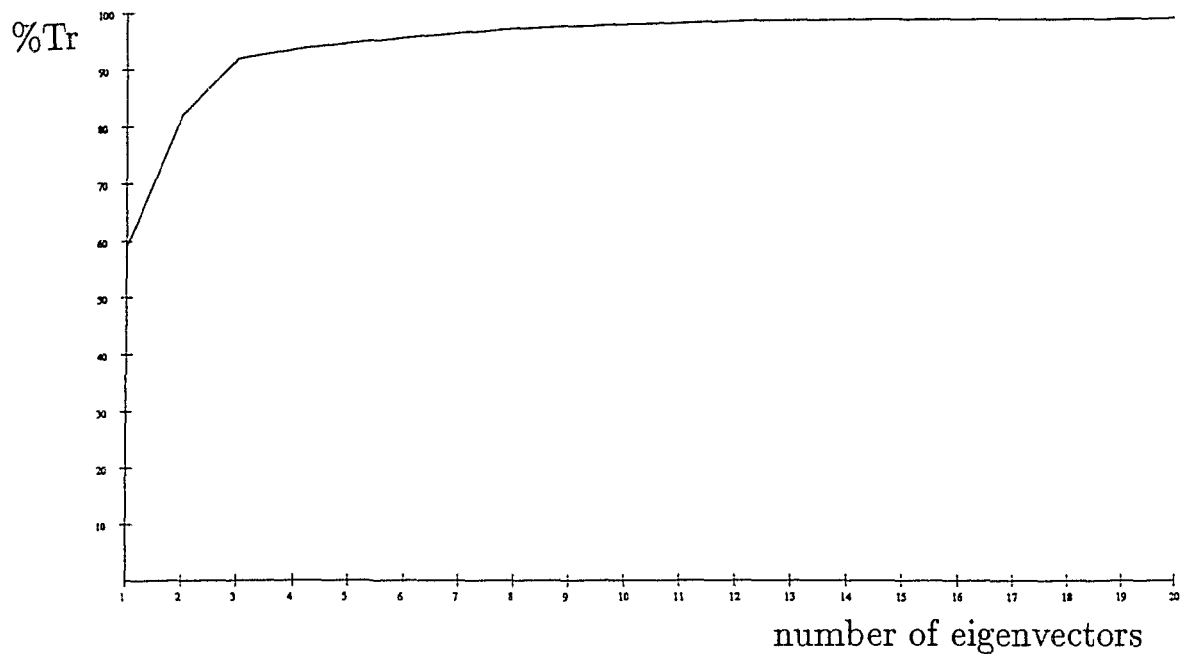


Figure 5.1: Percent trace vs. eigenvectors derived from the two-group training set for $[X]$. The percent trace for the 16 eigenvalues in descending order was 99%, as illustrated in Fig. 5.1. The corresponding eigenvectors were plotted as spatial maps (Fig. 5.2).

The 16 eigenvectors and the measured QRST-integral values from the 102 files were used to calculate 16 weighting coefficients y_i for each subject. The 16 weighting coefficients and 16 eigenvectors were then used to reconstruct QRST-integral maps for each subject. The mean and standard deviation for the three error measures associated with this reconstruction are presented in Table 5.1. The mean rms error and the mean peak error were similar in both constituent groups, while the VT_{train} group had a slightly higher relative error compared to the MI_{train} group. The mean and standard deviation for all three error measures were lower for this reconstruc-

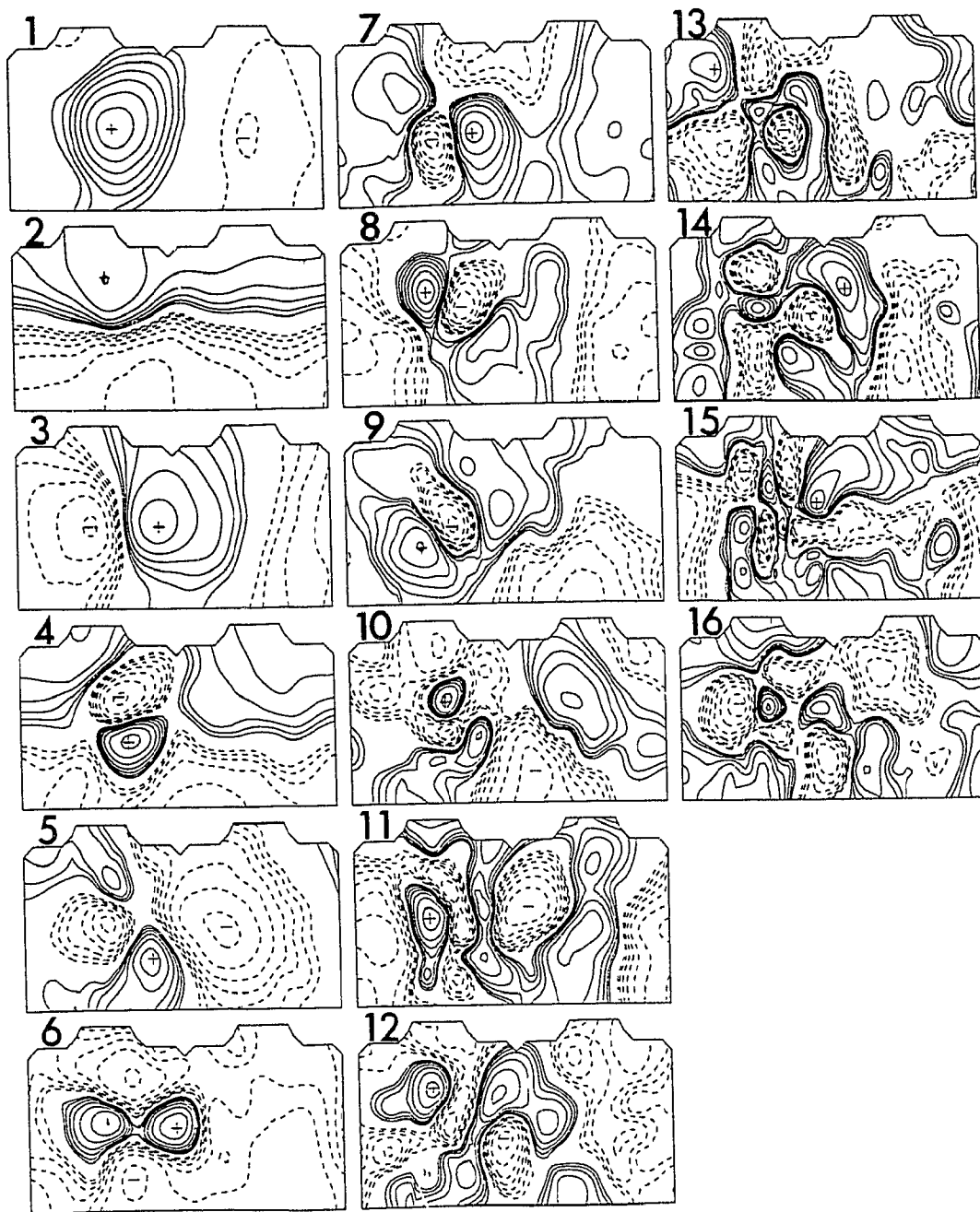


Figure 5.2: Eigenvectors derived from the two-group training set. Eigenvectors are plotted as spatial maps on the torso; the maps are arranged in descending order of the magnitude of their contribution; the plotting convention is the same as in Fig. 4.2.

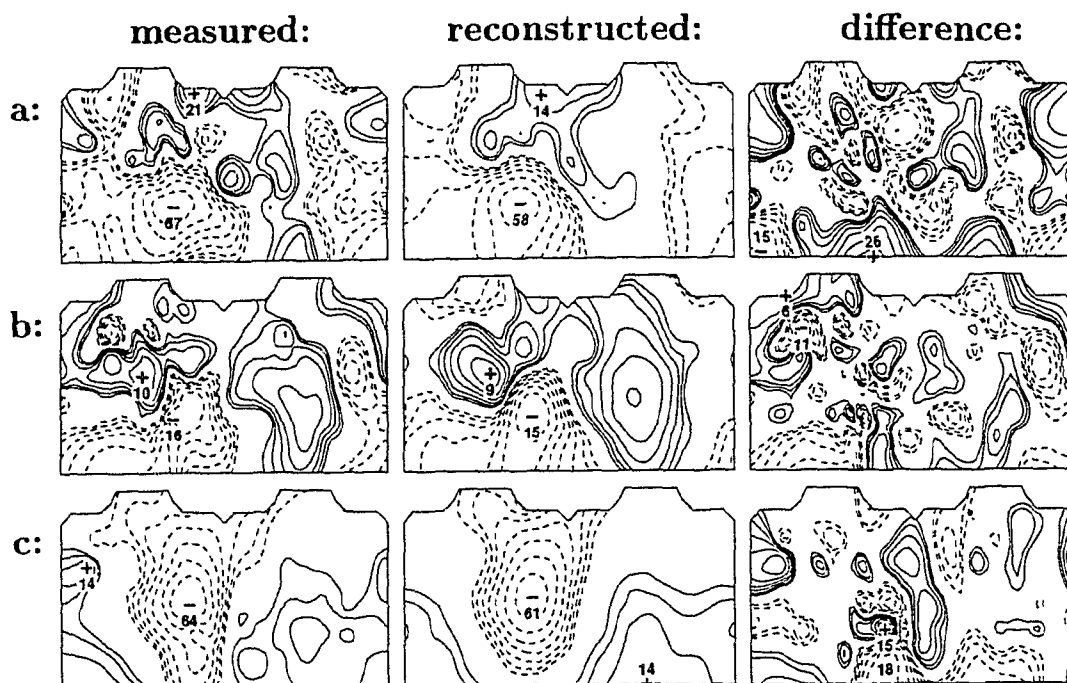


Figure 5.3: Worst-case reconstruction errors for the two-group training set. The reconstruction is based on 16 weighting coefficients and corresponding eigenvectors. In the left column are measured maps, the middle column are reconstructed maps and the right column are difference maps. a) Worst-case rms error ($e_{\text{rms}} = 6.5 \mu\text{Vs}$, $e_{\text{rel}} = 10.6\%$, $e_{\text{peak}} = 21.3 \mu\text{Vs}$). b) Worst-case relative error ($e_{\text{rms}} = 3.2 \mu\text{Vs}$, $e_{\text{rel}} = 33.4\%$, $e_{\text{peak}} = 13.8 \mu\text{Vs}$). c) Worst-case peak error ($e_{\text{rms}} = 4.2 \mu\text{Vs}$, $e_{\text{rel}} = 5.1\%$, $e_{\text{peak}} = 22.6 \mu\text{Vs}$).

Table 5.1: Reconstruction errors for the two-group training set

		Training set ($n=102$)	VT_{train} ($n=51$)	MI_{train} ($n=51$)
rms error [μVs]	mean	3.20	3.22	3.17
	SD	0.80	0.70	0.89
relative error [%]	mean	3.26	3.95	2.57
	SD	5.29	5.56	4.97
peak error [μVs]	mean	10.70	10.21	11.18
	SD	3.77	3.23	4.22

tion than were the errors that arose for the VT_{train} and MI_{train} groups when the eigenvectors were derived from the three-group training set (see Table 4.1). The measured and reconstructed QRST-integral maps for the worst cases are shown in Fig. 5.3. Even in these maps representing the worst cases, the main patterns are preserved.

5.2 Nondipolar content of QRST-integral maps

The mean (\pm SD) nondipolar content of the VT_{train} group was 13.13 (\pm 9.69) %, and that of the MI_{train} group was 12.92 (\pm 10.19) %. An independent t-test revealed no significant difference between the nondipolar content of the VT_{train} and MI_{train} groups at the $p \leq 0.05$ level (Fig. 5.4); thus, there was no improvement compared to the result achieved for the three-group training set. Because of the high degree of overlap in nondipolar content, no discriminant analysis was attempted on this data.

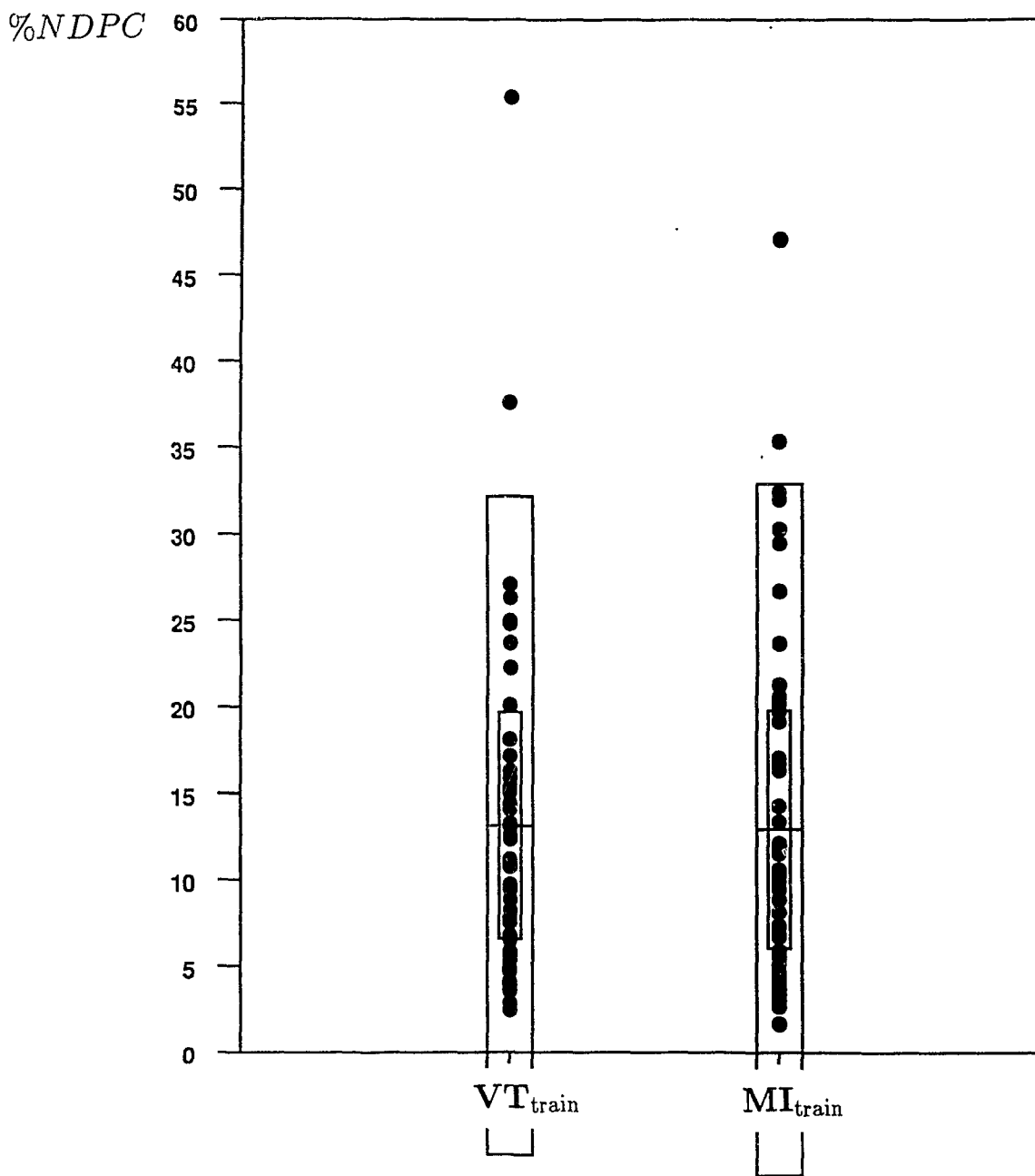


Figure 5.4: Nondipolar content for the two-group training set. The inner box corresponds to the 50% confidence interval and the outer box to the 95% confidence interval; the mean for each group is indicated by the horizontal line.

Table 5.2: Classification of the two-group training set: discriminant analysis based on KL features y_6, y_2 and y_4 derived from this set

Group	Category	
	VT	MI
VT _{train} ($n=51$)	45	6
MI _{train} ($n=51$)	16	35
Total ($n=102$)	61	41
Priors	.50	.50

Table 5.3: Sensitivity, predictive value and diagnostic performance of classification based on KL features y_6, y_2 and y_4 derived from the two-group training set

	Sensitivity [%]	Predictive Value [%]
VT _{train} ($n=51$)	88	74
MI _{train} ($n=51$)	69	85
$DP = 78\%; \kappa = .57$		

5.3 Discriminant analysis employing KL features

The stepwise discriminant analysis based on the 16 weighting coefficients for the two-group training set revealed that the three KL features with greatest discriminating capabilities between the VT_{train} and MI_{train} groups corresponded to—in order of their discriminating power—the sixth, the second and the fourth eigenvector (y_6, y_2 and y_4) displayed in Fig. 5.2. Thus, two of these features were by definition *nondipolar*. Table 5.2 summarizes the results of the classification based on the discriminant functions which employed features y_6, y_2 and y_4 ; Table 5.3 shows that 88% of the VT patients and 69% of the MI patients were correctly classified, which resulted in the diagnostic performance of 78%. Thus, 78% of all patients were correctly classified

by this method based on three KL coefficients derived from the two-group training set. These performance figures represent a marked improvement over corresponding figures achieved by the same approach based on features y_1, y_2 and y_4 of the three-group classification.

5.4 Discriminant analysis employing KnY features

The KnY transform was applied to the 16 weighting coefficients associated with the 16 KL patterns derived from the two-group training set. This produced 16 KnY features that were each a linear combination of the 16 KL weighting coefficients. The stepwise discriminant analysis revealed that virtually all diagnostic information discriminating between the VT_{train} and MI_{train} groups was contained in one KnY feature associated with coefficient f_1 . Results of the classification of the 102-patient training set, by discriminant analysis based on one KnY coefficient, are presented in Tables 5.4 and 5.5: 92% of the VT patients and 86% of the MI patients were correctly classified. The diagnostic performance of this analysis was 89%. The KnY coefficient for each subject of both VT_{train} and MI_{train} groups is plotted in Fig. 5.5, with group means and confidence intervals. Overall this approach led to correct classification of 89% of patients from the entire two-group training set.

5.5 Summary and discussion

The errors associated with the reconstruction of the QRST-integral maps from the 16 eigenvectors derived from the two-group training set, were lower than corresponding

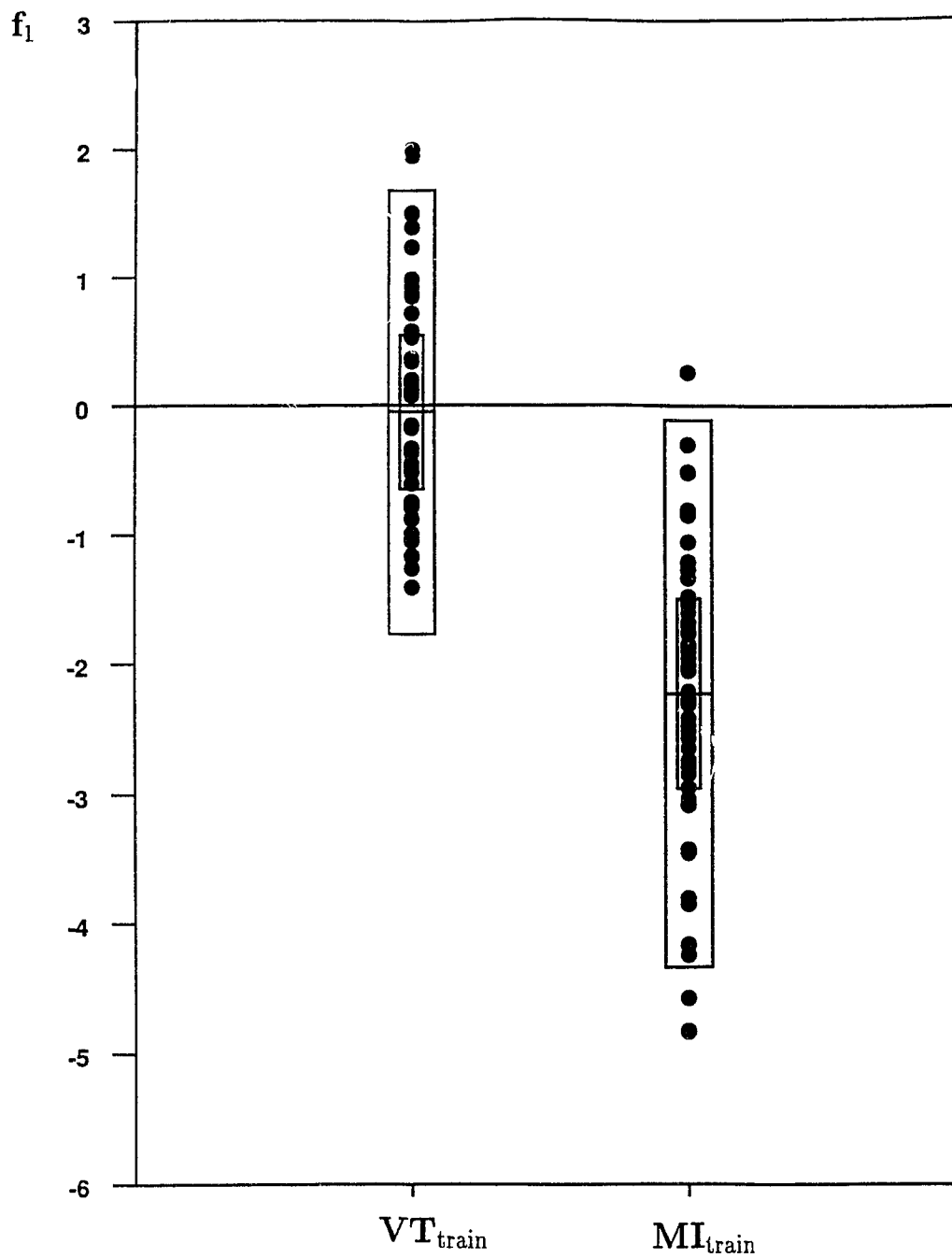


Figure 5.5: KnY coefficient f_1 derived from the two-group training set. The inner box corresponds to the 50% confidence interval and the outer box to the 95% confidence interval. The mean is indicated by the horizontal bar.

Table 5.4: Classification of the two-group training set: discriminant analysis based on KnY feature f_1 derived from this set

	Category	
Group	VT	MI
VT _{train} ($n=51$)	47	4
MI _{train} ($n=51$)	7	44
Total ($n=102$)	54	48
Priors	.50	.50

Table 5.5: Sensitivity, predictive value and diagnostic performance of classification based on one KnY feature f_1 derived from the two-group training set

	Sensitivity [%]	Predictive Value [%]
VT _{train} ($n=51$)	92	87
MI _{train} ($n=51$)	86	92
$DP = 89\%; \kappa = .78$		

errors for the VT_{train} and MI_{train} groups in the reconstruction from the 16 eigenvectors derived from the three-group training set. Thus, excluding the NC group and using the two-group eigenvectors appears to have reduced the variability in the data set. The results of the nondipolar-content analysis were disappointing—showing that this measure was not capable of separating VT_{train} and MI_{train} groups.

Discriminant analysis of the 16 weighting coefficients, derived from the two-group training set, resulted in the classification that identified 78% of all patients correctly, compared to 61% for the classification based on the eigenvectors from the three-group training set. It is interesting to note that the order of the KL features with the greatest discriminating abilities *differed* between the three-group and two-group classification. In the latter case, a more complex spatial pattern (feature 6)

contains the largest amount of diagnostic information, followed by features 2 and 4. This contrasts with the three-group analysis, in which features 1, 2 and 4 were selected, in that order, as the best discriminators.

The KnY transform of the 16 weighting coefficients produced a single feature, which contained most of the diagnostic information discriminating between the VT_{train} and MI_{train} groups. The discriminant analysis in the KnY feature space provided the best results—with 89% of all patients being correctly classified (only 4 VT patients and 7 MI patients were classified incorrectly). These results were a substantial improvement over the same analysis applied to the three-group training set, in which only 78% of the patients were correctly classified (7 VT patients and 15 MI patients were classified incorrectly). The high diagnostic performance achieved by this analysis provides clear evidence that important diagnostic information can be derived from the electrocardiographic QRST-integral distribution, noninvasively measurable on the body surface. At the same time, it is obvious—from the comparison with the results of the simple nondipolar-content analysis—that this valuable diagnostic information has to be extracted by the reduction of feature space and by the careful selection of features.

Chapter 6

Classification of an independent test set

The next issue, addressed in this chapter, was the ability of the features derived from the training set to classify an independent group of test-set subjects. The test set was analyzed by using the features and discriminant functions derived from both the three-group and the two-group training sets. The test set comprised independent sets of 51 patients with recurrent ventricular tachycardia (VT_{test} group) and 51 patients with myocardial infarction but with no history of arrhythmias (MI_{test} group); these groups were described in detail in section 3.1. Since the nondipolar content results obtained for the training set showed that this measure had limited potential for differentiating between the VT_{train} and MI_{train} groups, nondipolar content was not analyzed for the test set. Therefore, the results consist only of (1) a reconstruction-error assessment, (2) the discriminant analysis in the KL feature space, and (3) the discriminant analysis in the KnY feature space.

Before the discriminant analysis of the test-set data was performed, plots of the QRST-integral maps were examined; examples of these maps from each of the two constituent groups of the test set are plotted in Fig. 6.1. This figure illustrates the

Table 6.1: Reconstruction errors for the test set: based on eigenvectors from the three-group training set

		Test set ($n=102$)	VT_{test} ($n=51$)	MI_{test} ($n=51$)
rms error [μVs]	mean	3.50	3.34	3.66
	SD	1.31	1.30	1.30
relative error [%]	mean	2.41	3.03	1.79
	SD	2.44	2.58	2.14
peak error [μVs]	mean	12.33	12.14	12.53
	SD	5.50	5.64	5.41

complexity of the maps from the VT_{test} and MI_{test} groups, which was also evident from the maps of the VT_{train} and MI_{train} groups of the training set (see Fig. 4.4).

6.1 Analysis based on features from the three-group training set

The 117 measured QRST-integral values for each patient of the test set, and the 16 eigenvectors from the three-group training set (see section 4.1) were used to calculate the weighting coefficients y_i for each eigenvector and for each test-set subject. The 16 weighting coefficients for each test-set subject and the eigenvectors from the three-group training set were then used to reconstruct the QRST-integral maps for each test-set subject. These reconstructed maps were visually examined to detect possible differences in patterns compared to the measured values. A summary of the three error measures for the total test set and the two constituent groups is in Table 6.1. The errors for the VT_{test} and MI_{test} groups were comparable to the results obtained for the three-group training set (Table 4.1). The worst-case rms error was $8.5 \mu\text{Vs}$, the worst-case relative error was 11.2%, and the worst-case peak

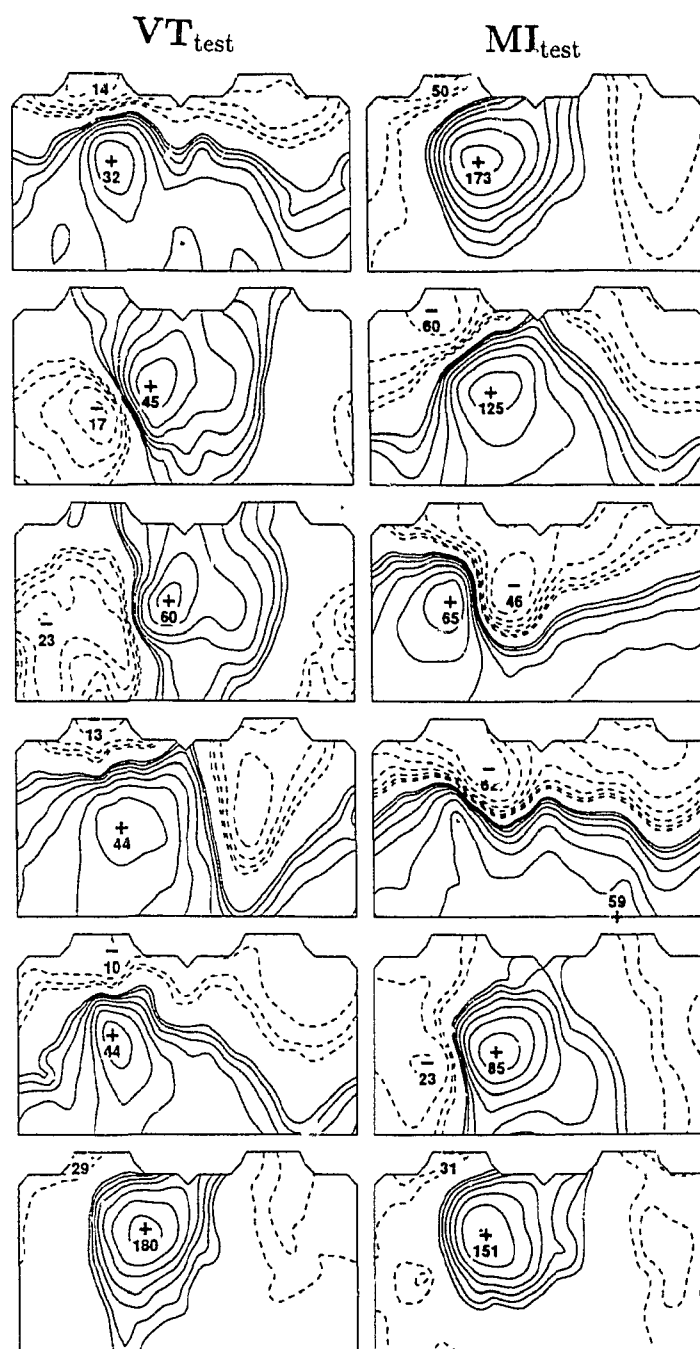


Figure 6.1: Examples of QRST-integral maps for the two-group test set. The display convention is the same as in Fig. 4.2.

error was $31.7 \mu\text{Vs}$. The measured and reconstructed maps for the worst cases are shown in Fig. 6.2. In general, the reconstructed maps were qualitatively similar to the measured maps.

Discriminant analysis employing KL features

The discriminant functions derived for the three-group training set—which were based on the three KL features y_1 , y_2 and y_4 corresponding to spatial patterns shown as maps 1, 2 and 4 in Fig. 4.2—were applied to the corresponding three weighting coefficients evaluated for each subject of the test set. The results of this classification are summarized in Tables 6.2 and 6.3. Only 42% of the patients in the test set were classified correctly. Many patients (41%) who belonged to MI_{test} group were classified as NC subjects, but on the other hand, only 4% of patients who belonged to VT_{test} group were classified as NC subjects. The poor result of this classification was not unexpected, since the classifier for the three-group training set only identified 61% of the VT and MI patients correctly (cf. results in section 4.3). What was surprising was the amount of drop in diagnostic performance, which was reflected in the large error bias (19%) between the training and test set. These results indicate a poor ability of this classifier, based on the three KL features and discriminant functions derived from the three-group training set, to perform satisfactorily on an independent patient population.

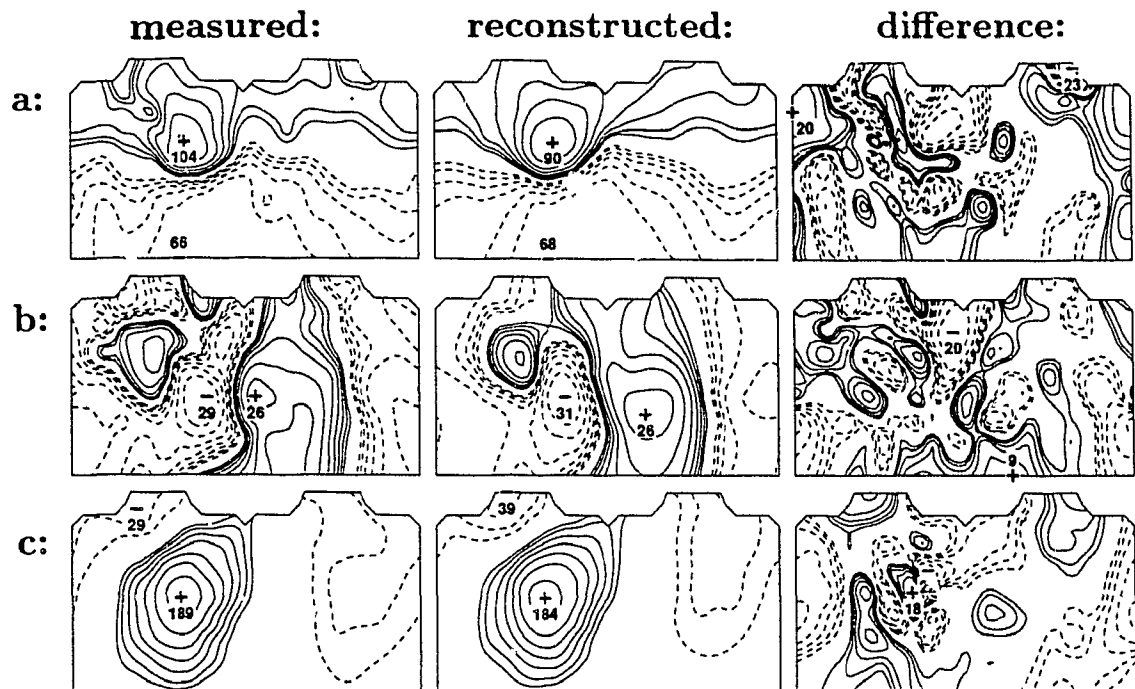


Figure 6.2: Worst-case reconstruction errors for the two-group test set: based on eigenvectors derived from the three-group training set.

Measured, reconstructed and difference maps are arranged in three columns; rows contain maps for: a) Worst-case rms error ($e_{\text{rms}} = 8.5 \mu\text{Vs}$, $e_{\text{rel}} = 4.7\%$, $e_{\text{peak}} = 27.7 \mu\text{Vs}$). b) Worst-case relative error ($e_{\text{rms}} = 4.3 \mu\text{Vs}$, $e_{\text{rel}} = 11.2\%$, $e_{\text{peak}} = 12.5 \mu\text{Vs}$). c) Worst-case peak error ($e_{\text{rms}} = 6.5 \mu\text{Vs}$, $e_{\text{rel}} = 1.2\%$, $e_{\text{peak}} = 31.7 \mu\text{Vs}$).

Table 6.2: Classification of the test set: discriminant analysis based on KL features y_1 , y_2 and y_4 derived from the three-group training set

Group	Category		
	VT	NC	MI
VT _{test} ($n=51$)	26	2	23
MI _{test} ($n=51$)	13	21	17
Total ($n=102$)	39	23	40
Priors	.33	.33	.33

Table 6.3: Sensitivity, predictive value and diagnostic performance of the test-set classification based on KL features y_1 , y_2 and y_4 derived from the three-group training set

	Sensitivity [%]	Predictive Value [%]
VT _{test} ($n=51$)	51	67
MI _{test} ($n=51$)	33	43
$DP = 42\%$		

Discriminant analysis employing KnY features

The discriminant analysis of the KnY coefficients derived from the three-group training set produced two features f_1 and f_2 which contained most of the discriminating information for separating the training-set groups. Therefore, the 16 coefficients y_i from the test set were first transformed, using the KnY feature space derived from the three-group training set, and then the discriminant functions based on KnY features f_1 and f_2 were applied to this transformed data. The results of the classification based on this analysis show that (see Tables 6.4 and 6.5) only 63% of the patients from the test set were classified correctly, compared to 78% of the patients from the training set. A 15% error bias between the training and test sets indicates that the KnY features derived for the three-group training set did not contain enough discriminating diagnostic information that could be extrapolated to independent groups. Fig. 6.3 is a plot of the two KnY coefficients for each subject in the test set; the ellipses from the three-group training set (Fig. 4.6) are redrawn in this figure. These results demonstrate that the discriminant analysis based on the KnY feature space, while improved from the one in the KL feature space, still provided poor sensitivity and PV for the MI_{test} group.

Since the results of classification for the test set based on the features derived from the three-group training set were so poor, no further analysis of these data was performed. These features did not seem to contain diagnostic information that would be capable of separating a test set of patients vulnerable to arrhythmia from

Table 6.4: Classification of the test set: discriminant analysis based on KnY features f_1 and f_2 derived from the three-group training set

Group	Category		
	VT	NC	MI
VT _{test} ($n=51$)	39	2	10
MI _{test} ($n=51$)	6	20	25
Total ($n=102$)	45	22	35
Priors	.33	.33	.33

Table 6.5: Sensitivity, predictive value and diagnostic performance of the test-set classification based on KnY features f_1 and f_2 derived from the three-group training set

	Sensitivity [%]	Predictive Value [%]
VT _{test} ($n=51$)	76	87
MI _{test} ($n=51$)	49	71
$DP = 63\%$		

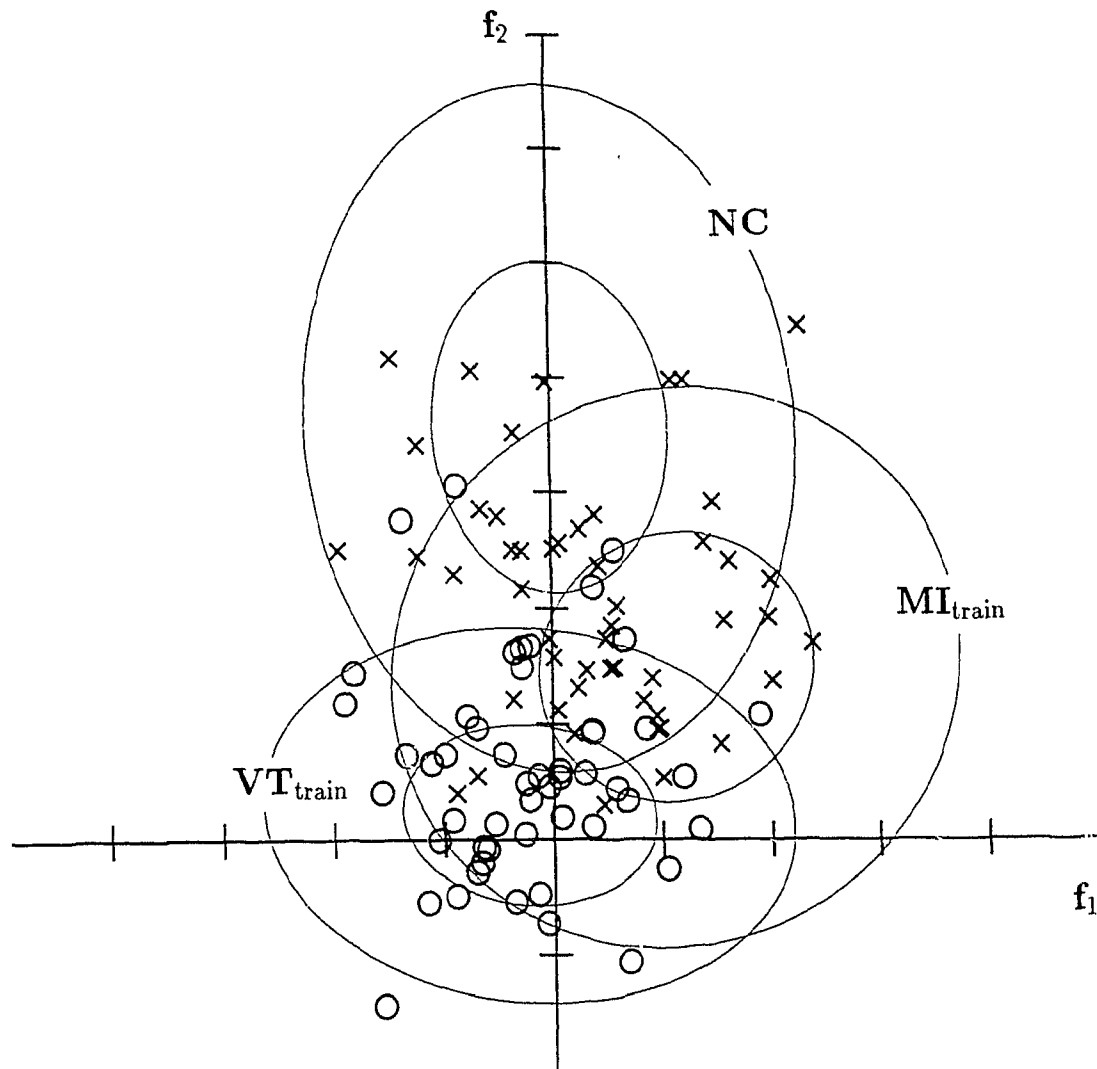


Figure 6.3: Two-group test set in feature space of KnY coefficients f_1 and f_2 derived from the three-group training set.

The inner ellipses correspond to the 50% confidence intervals and the outer ellipses correspond to the 95% confidence intervals; \circ represents patient who belongs to VT_{test} group; \times represents patient who belongs to MI_{test} group.

Table 6.6: Reconstruction errors for the test set: based on 16 eigenvectors derived from the two-group training set

		Test set ($n=102$)	VT_{test} ($n=51$)	MI_{test} ($n=51$)
rms error [μVs]	mean	3.65	3.44	3.86
	SD	1.36	1.33	1.36
relative error [%]	mean	2.54	3.15	1.93
	SD	2.44	2.54	2.20
peak error [μVs]	mean	12.38	12.10	12.67
	SD	5.36	5.38	5.39

those who are not vulnerable to arrhythmia. Therefore, these features would have little value in classifying future observations.

6.2 Analysis based on features from the two-group training set

The 16 eigenvectors calculated for the two-group training set (section 5.1) were used to calculate weighting coefficients y_i for each subject in the test set. The reconstruction errors for the QRST-integral maps of the test set are summarized in Table 6.6. The mean errors are slightly higher than the errors for the two-group training set (cf. Table 5.1) and for the corresponding reconstruction for the test set based on the eigenvectors derived from the three-group training set (cf. Table 6.1). Fig. 6.4 shows the worst-case differences between the measured maps and the reconstructed maps. As in previous observations, the main patterns were preserved after reconstruction based on 16 features.

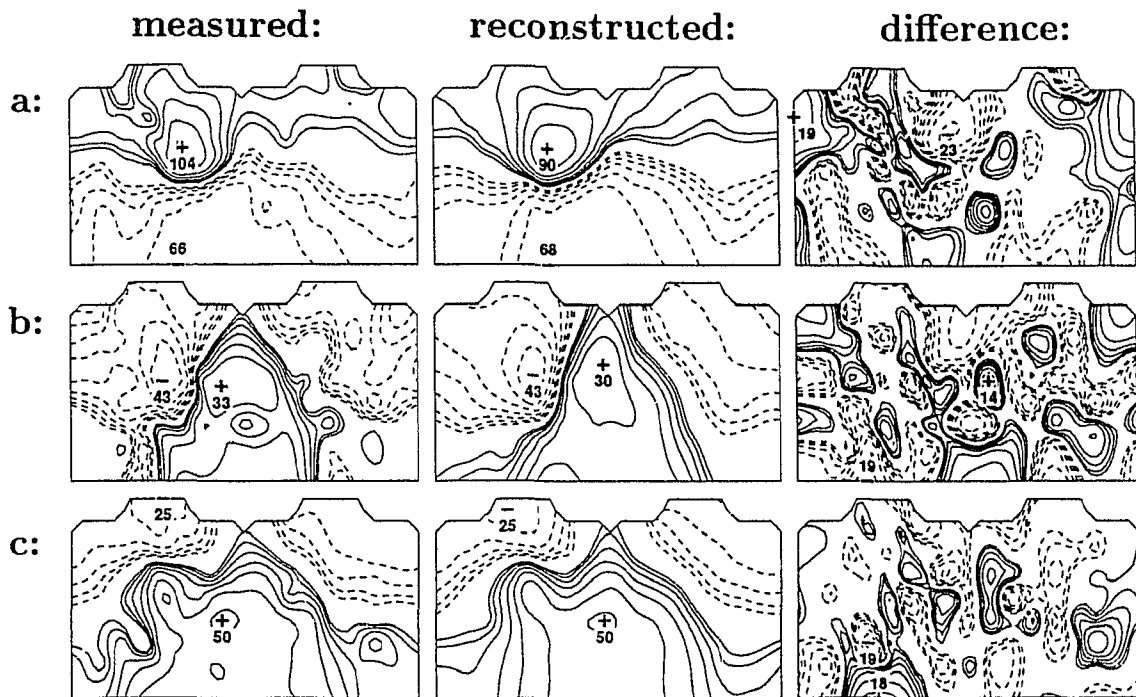


Figure 6.4: Worst-case reconstruction errors for the two-group test set: based on eigenvectors derived from the two-group training set.

Measured, reconstructed and difference maps are arranged in three columns; rows contain maps for: a) Worst-case rms error ($e_{\text{rms}} = 8.5 \mu\text{Vs}$, $e_{\text{rel}} = 4.7\%$, $e_{\text{peak}} = 28.1 \mu\text{Vs}$) b) Worst-case relative error ($e_{\text{rms}} = 5.7 \mu\text{Vs}$, $e_{\text{rel}} = 10.5\%$, $e_{\text{peak}} = 17.5 \mu\text{Vs}$) and c) Worst-case peak error ($e_{\text{rms}} = 4.8 \mu\text{Vs}$, $e_{\text{rel}} = 3.9\%$, $e_{\text{peak}} = 26.8 \mu\text{Vs}$).

Table 6.7: Classification of the test set: discriminant analysis based on KL features y_6 , y_2 and y_4 derived from the two-group training set

	Category	
Group	VT	MI
VT _{test} ($n=51$)	40	11
MI _{test} ($n=51$)	14	37
Total ($n=102$)	54	48
Priors	.50	.50

Discriminant analysis employing KL features

The three features from the two-group training set with the best discriminating capabilities correspond to maps 6, 2 and 4 in Fig. 5.2; the linear discriminant functions derived from these features were applied to the test set. The results of classification for the test set are in Tables 6.7 and 6.8. Overall, 75% of the patients from the test set were correctly classified, compared to 78% from the training set; in both cases, the same three KL features were used (Section 5.3). This represents a 3% error bias between the apparent error of classification from the training set and the error from the test set. Of interest is the fact that while, as expected, the sensitivity for the VT_{test} group dropped in comparison with the VT_{train} group, the sensitivity of the MI_{test} group actually improved in comparison with the MI_{train} group (from 69% to 73%).

Table 6.8: Sensitivity, predictive value and diagnostic performance of the test-set classification based on KL features y_6 , y_2 and y_4 derived from the two-group training set

	Sensitivity [%]	Predictive Value [%]
$VT_{test} (n=51)$	78	74
$MI_{test} (n=51)$	73	77
$DP = 75\%; \kappa = .51$		

Discriminant analysis employing KnY features

The KnY features derived from the two-group training set were applied to the 16 weighting coefficients y_i of the test set, as derived from the KL features from the two-group training set. The discriminant functions derived for the one KnY feature f_1 from the two-group training set were then applied to the test set. The results of the classification based on the linear discriminant analysis are presented in Tables 6.9 and 6.10. There were 87 subjects (85%) in the test set who were classified correctly, compared to 89% classified correctly for the training set by using the same approach (cf. Section 5.4); this is a 4% error bias. The KnY coefficients for the two training-set groups and the two test-set groups are plotted in Fig. 6.5. These results demonstrate that the diagnostic performance achieved in separating the VT_{train} and MI_{train} groups was well maintained for the VT_{test} and MI_{test} groups. While the VT_{test} sensitivity decreased as expected in comparison with sensitivity achieved for the VT_{train} group, the MI_{test} sensitivity remained the same as the MI_{train} sensitivity. The sensitivity and PV were similar for both VT_{test} and MI_{test} groups.

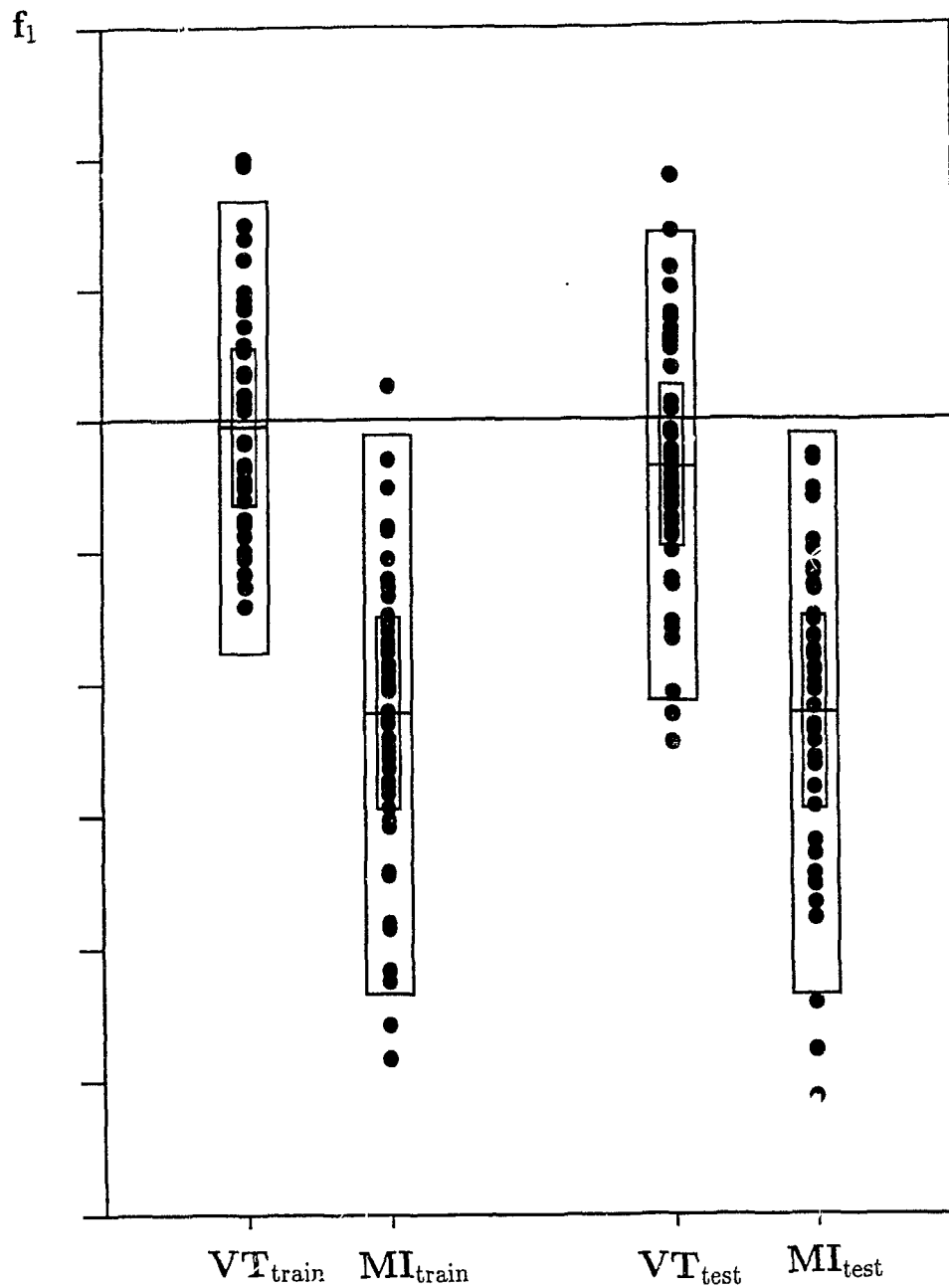


Figure 6.5: Two-group test set and two-group training set in feature space of Kny coefficient f_1 derived from the two-group training set.

The inner box corresponds to the 50% confidence interval and the outer box to the 95% confidence interval; the mean is indicated by the horizontal bar.

Table 6.9: Classification of the test set: discriminant analysis based on KnY feature f_1 derived from the two-group training set

Group	Category	
	VT	MI
VT _{test} ($n=51$)	43	8
MI _{test} ($n=51$)	7	44
Total ($n=102$)	50	52
Priors	.50	.50

Table 6.10: Sensitivity, predictive value and diagnostic performance of the test-set classification based on KnY feature f_1 derived from the two-group training set

	Sensitivity [%]	Predictive Value [%]
VT _{test} ($n=51$)	84	86
MI _{test} ($n=51$)	86	85
$DP = 85\%; \kappa = .71$		

6.3 Summary and discussion

In summary, the errors for reconstructing the QRST-integral maps for the independent test set, by means of the eigenvectors derived from both the three-group and two-group training sets were comparable to the reconstruction errors for the training sets. The main patterns were maintained upon reconstruction. The classification results for the test set, based on the eigenvectors derived from the three-group training set, were poor. Both the discriminant analysis based on the three KL features and the discriminant analysis based on the two KnY features derived from the three-group training set, yielded low diagnostic performance in classifying the VT_{test} and MI_{test} groups. In contrast, the diagnostic performance of the test-set classification

based on the features derived from the two-group training set was maintained in comparison with that for the training set. The best result was achieved for the discriminant analysis based on the KnY feature space. The test-set result of 85% correctly classified patients was comparable to the training-set result of 89% of patients classified correctly. These results provide evidence that important diagnostic information for discriminating patients vulnerable to ventricular arrhythmias from those not vulnerable was contained in their QRST-integral maps. Features derived from a training set were capable of classifying independent groups of patients with a low error associated with the classification. The diagnostic performance achieved in classifying test-set patients provides one assessment of the expected error in performance for classifying future observations based on the features derived from the training set.

Chapter 7

Classification of the posttreatment VT group

The next issue addressed was whether the features derived from the training set were sensitive to *changes* in arrhythmogenic state resulting from antiarrhythmic treatment. This chapter focussed on evaluating whether the differences in posttreatment QRST-integral maps corroborated the results of programmed stimulation in the clinical assessment of the arrhythmogenic state. The features derived from the three-group and two-group training sets were applied in the analysis of the posttreatment QRST-integral maps of patients with recurrent ventricular tachycardia who were included in the training set (VT_{train} group). These 51 VT patients, whose clinical characteristics are described in section 3.1 and in Appendices A and C, were divided into a predicted effective therapy (PET) subgroup and a non-predicted effective therapy (nPET) subgroup, depending on the results of posttreatment EPS. The objective of this analysis was to explore the applicability of the features derived from the three-group and two-group training sets in assessing the outcome of treatment (see objectives in chapter 1). The specific aim was to examine whether the classification of posttreatment QRST-integral maps would differ from their pretreat-

Table 7.1: Reconstruction errors for the posttreatment VT group: based on eigenvectors derived from the three-group training set

		PET+nPET ($n=51$)	PET ($n=14$)	nPET ($n=37$)
rms error [μ Vs]	mean	4.34	4.53	4.27
	SD	1.89	2.05	1.86
relative error [%]	mean	7.93	6.91	8.32
	SD	8.10	6.59	8.65
peak error [μ Vs]	mean	14.31	16.42	13.51
	SD	7.61	11.05	5.82

ment classification, and if it did, which maps would remain classified as belonging to VT category and which would move to non-VT category (NC or MI).

The first step of this analysis was to reconstruct the posttreatment QRST-integral maps in the feature space derived from the three-group and two-group training sets and to evaluate the errors associated with each of these reconstructions. Subsequently, the capability of each feature space to serve as a basis for diagnostic classification was evaluated. The results are presented in the same order as in the previous chapters.

7.1 Analysis based on features from the three-group training set

The 16 eigenvectors derived from the three-group training set and the QRST-integral maps of the posttreatment VT group were used to calculate the 16 weighting coefficients y_i for each subject. The posttreatment maps were reconstructed by using these weighting coefficients and the errors between the original and reconstructed maps were quantified. The root-mean-squared errors, relative errors and peak errors

are summarized in Table 7.1. The mean rms error and peak error for the nPET subgroup were smaller than for the PET subgroup, whereas the relative error for the PET subgroup was smaller than for the nPET subgroup. The errors for the entire posttreatment group were, as expected, larger than the corresponding errors for the pretreatment data of patients belonging to VT_{train} group (cf. Table 4.1). Fig. 7.1 shows the worst cases (in terms of quantitative error measures) for the reconstruction of posttreatment group's QRST-integral maps from the three-group-training-set eigenvectors. In general, the main spatial patterns were maintained following reconstruction, but the reconstructed maps were smoother as a result of truncation of KL expansion.

Nondipolar content of QRST-integral maps

There were notable qualitative differences between the pretreatment and posttreatment QRST-integral maps for some of the patients belonging to VT_{train} group. Fig. 7.2 shows the pretreatment and posttreatment maps for six randomly selected cases. (The larger reconstruction errors presented in the previous section are indicative of this difference as well.) A preliminary report showed that there were no differences in the number of extrema between the PET and nPET subgroups before treatment, indicating similar multipolarity indices between these two subgroups [131]. In the nPET subgroup, a significant difference ($p \leq 0.05$) was found between the number of extrema before and after treatment (with the posttreatment number being higher [131]). In the PET subgroup, there was no significant difference between the number of extrema before and after treatment.

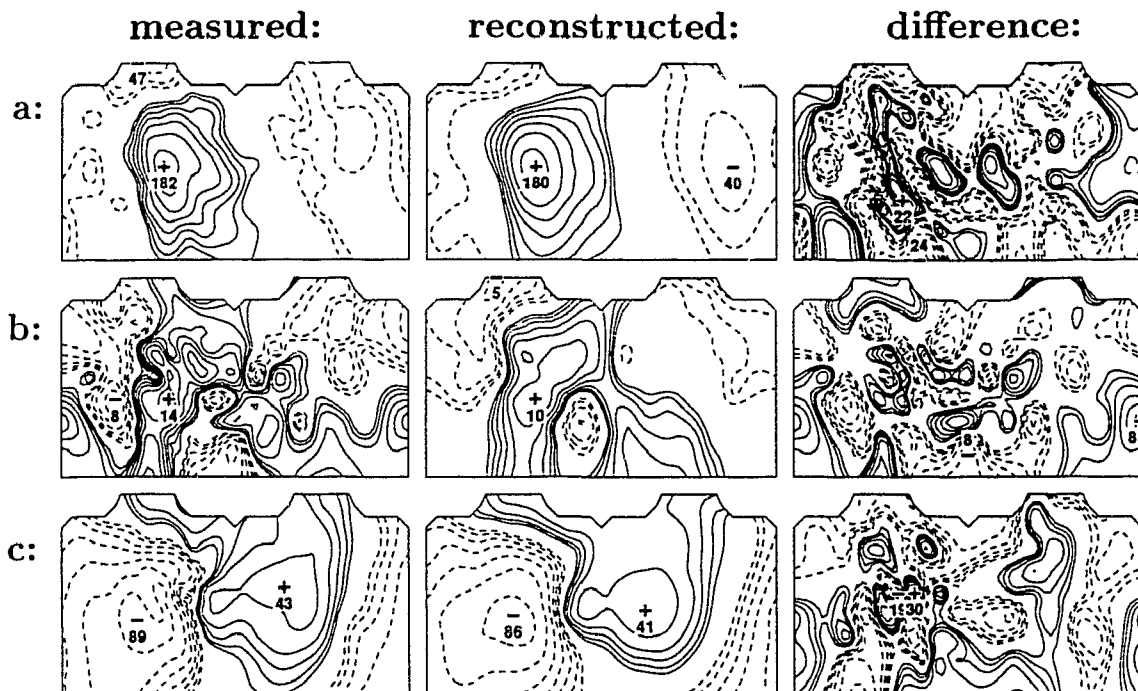


Figure 7.1: Worst-case reconstruction errors for the posttreatment VT group. 16 weighting coefficients and 16 eigenvectors derived from the three-group training set were used in reconstruction. In the left column are measured maps, in the middle column are reconstructed maps and the right column are difference maps. a) Worst-case rms error ($e_{\text{rms}} = 12.3 \mu\text{Vs}$, $e_{\text{rel}} = 4.4\%$, $e_{\text{peak}} = 36.0 \mu\text{Vs}$). b) Worst-case relative error ($e_{\text{rms}} = 3.5 \mu\text{Vs}$, $e_{\text{rel}} = 47.8\%$, $e_{\text{peak}} = 10.3 \mu\text{Vs}$). c) Worst-case peak error ($e_{\text{rms}} = 9.4 \mu\text{Vs}$, $e_{\text{rel}} = 6.2\%$, $e_{\text{peak}} = 51.0 \mu\text{Vs}$).

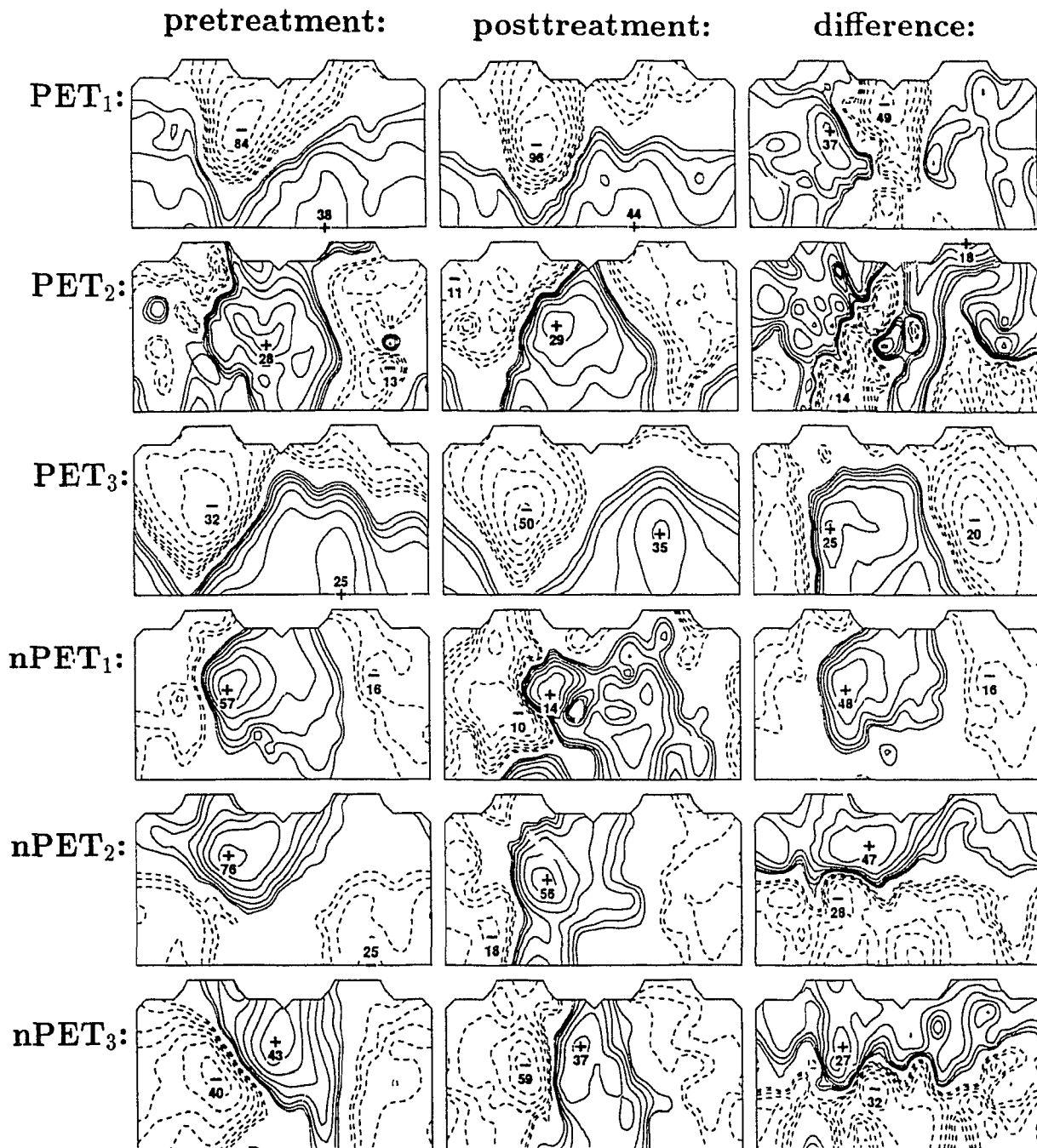


Figure 7.2: Examples of pretreatment and posttreatment QRST-integral maps for the VT group.

The upper three rows are from the PET subgroup and the lower three rows are from the nPET subgroup. In the left column are the pretreatment maps, in the middle column are the posttreatment maps and in the right column are the difference maps. The same display convention as in Fig. 4.2 is used.

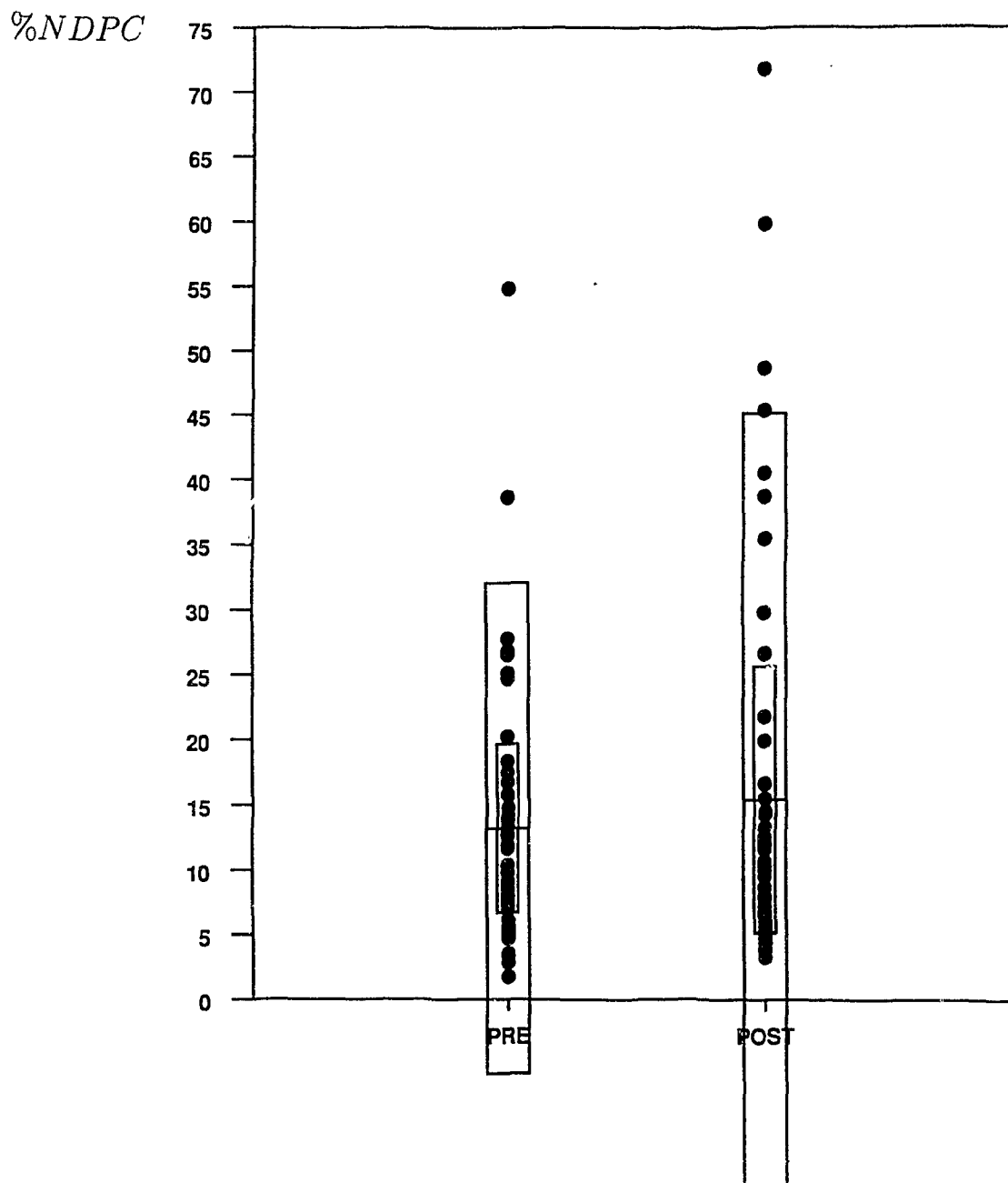


Figure 7.3: Nondipolar content of pretreatment and posttreatment QRST-integral maps for the VT_{train} group.

Based on eigenvectors derived from three-group training set. The inner box corresponds to the 50% confidence limits and the outer box to the 95% confidence limits; mean for each group is indicated by the horizontal line; PRE = pretreatment values; POST = posttreatment values.

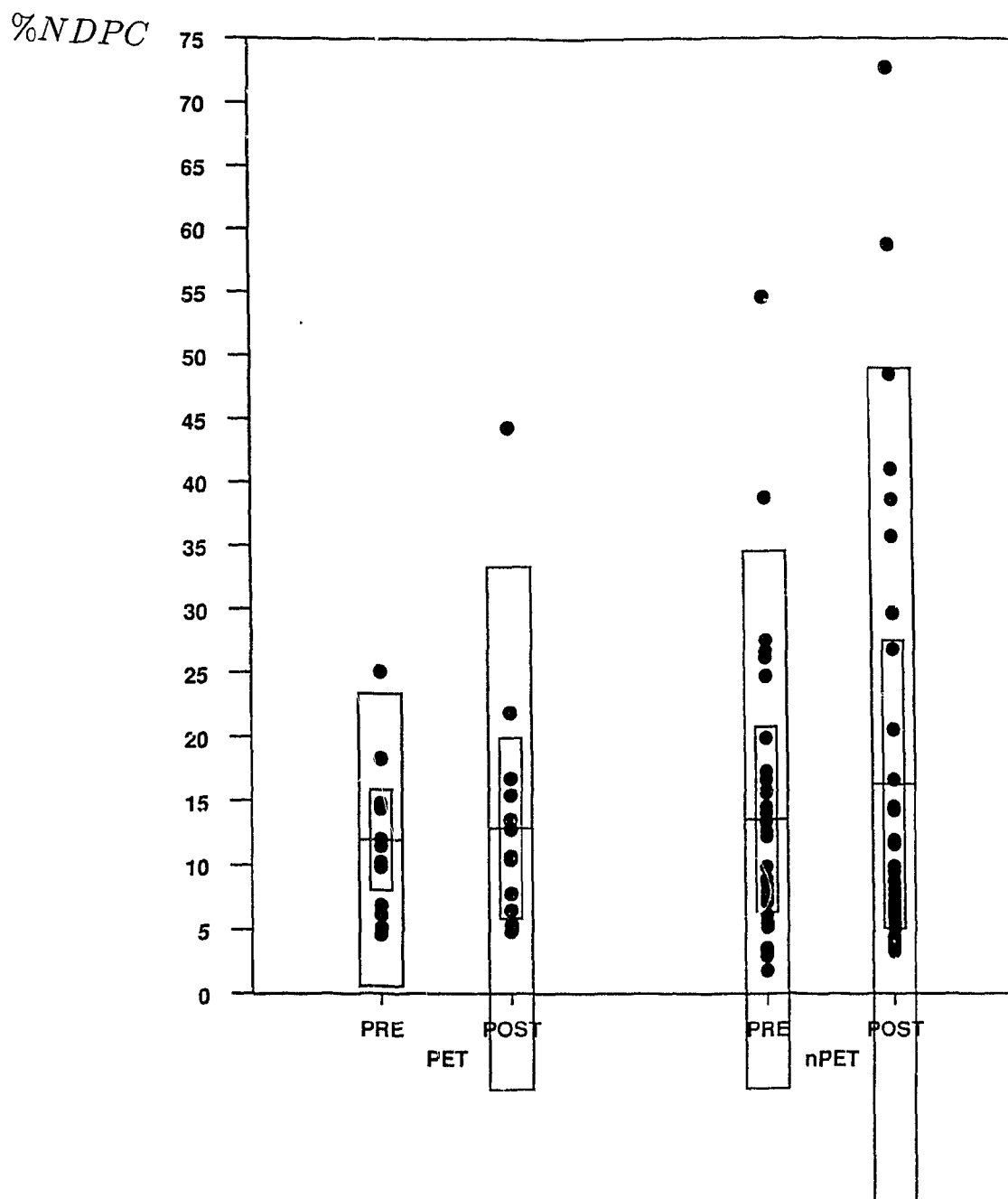


Figure 7.4: Nondipolar content of pretreatment and posttreatment QRST-integral maps for PET and nPET subgroups. Based on eigenvectors from three-group training set. Box-plot convention is the same as in Fig. 7.3.

Quantification of these differences was attempted by applying features derived from the training-set to the posttreatment maps, to determine if differences existed in maps recorded before and after treatment, or between posttreatment maps for the PET and nPET subgroups. The mean (\pm SD) nondipolar content for the total posttreatment group and for its subgroups was calculated. Box plots of the pretreatment and posttreatment states for the VT_{train} group, and the pretreatment and posttreatment states for the PET and nPET subgroups are in Figures 7.3 and 7.4. While the total posttreatment mean (15.36 ± 15.16 %) and the posttreatment mean for the nPET subgroup (16.31 ± 16.63 %) were higher than the mean for the PET subgroup (12.84 ± 10.39 %), an independent t-test showed no statistically significant ($p \geq 0.05$) differences between the PET and nPET subgroups for this measure. Dependent t-tests on the differences between the pretreatment and the posttreatment values for the total group, the PET subgroup and the nPET subgroup showed no statistically significant differences at the 0.05 level of significance.

Discriminant analysis employing KL features

The discriminant functions based on the three KL features from the three-group training set were applied to the posttreatment coefficients y_i of the PET and nPET subgroups. The results of this analysis are summarized in Table 7.2. These results were evaluated based on whether subjects were classified into a group vulnerable to arrhythmia (VT) or a group nonvulnerable to arrhythmia (NC or MI). It was found that 71% of the PET and 73% of the nPET patients were classified into the VT group. Of the entire posttreatment group, 73% remained classified as vulnerable to

Table 7.2: Classification for the posttreatment VT group: discriminant analysis based on KL features y_1, y_2 and y_4 derived from the three-group training set

		Category		
Group		VT	NC	MI
PET ($n=14$)	cases	10	0	4
	%	71	0	29
nPET ($n=37$)	cases	27	1	9
	%	73	3	24
Total ($n=51$)	cases	37	1	13
	%	73	2	25
Priors		.33	.33	.33

VT; therefore, 27% of the entire posttreatment group were classified as nonvulnerable to VT. This result was similar to the classification of this group before treatment (VT_{train} group), when 71% of patients were correctly classified into VT category (cf. Table 4.3).

Discriminant analysis employing KnY features

The discriminant functions based on the two KnY features f_1 and f_2 from the three-group training set were applied to the coefficients derived for the QRST-integral maps of the posttreatment VT group. Two patients in the PET subgroup were classified in the MI group and six patients in the nPET subgroup were classified in the MI group. Fig. 7.5 demonstrates the overlap between PET and nPET subgroups; it shows that a large proportion of the posttreatment values lies within the 95% confidence interval of the pretreatment values of the VT_{train} group.

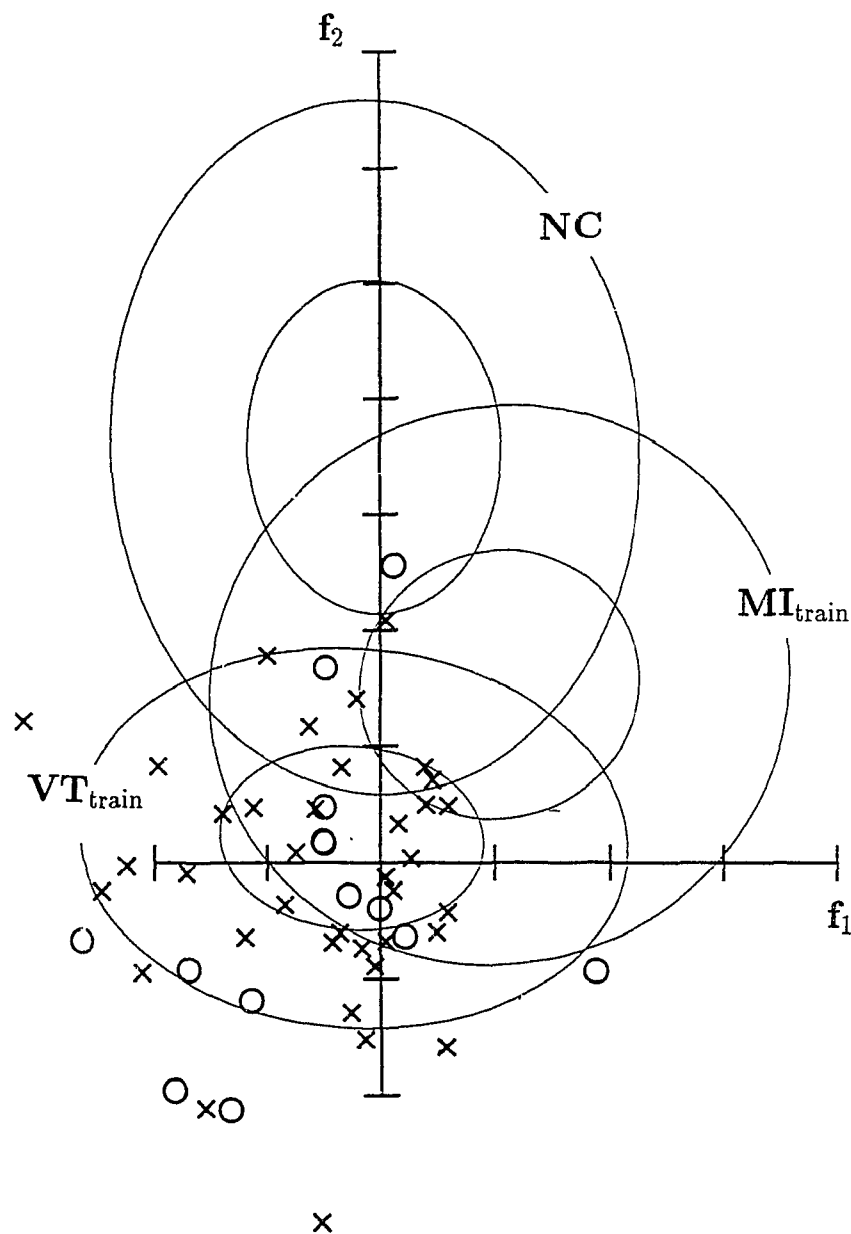


Figure 7.5: Posttreatment VT group in feature space of KnY coefficients f_1 and f_2 derived from the three-group training set.

Coefficient f_1 is on the abscissa and f_2 on the ordinate; the inner ellipses correspond to the 50% confidence intervals and the outer ellipses to the 95% confidence intervals (cf. Fig. 4.6); \odot represents patient who belongs to PET subgroup; \times represents patient who belongs to nPET subgroup.

Table 7.3: Reconstruction errors for the posttreatment VT group: based on eigenvectors derived from the two-group training set

		PET+nPET ($n=51$)	PET ($n=14$)	nPET ($n=37$)
rms error [μ Vs]	mean	4.37	4.54	4.31
	SD	1.83	2.00	1.79
relative error [%]	mean	7.97	6.86	8.39
	SD	8.05	6.41	8.64
peak error [μ Vs]	mean	14.22	16.09	13.52
	SD	7.68	10.86	6.13

7.2 Analysis based on features from the two-group training set

The QRST-integral maps for the posttreatment group and the 16 eigenvectors derived from the two-group training set were used to calculate weighting coefficients y_i for each subject in the PET and nPET posttreatment subgroups. These weighting coefficients for each subject in the posttreatment VT group, and the 16 eigenvectors from the training-set analysis, were used to reconstruct the QRST-integral maps. Summary statistics for three error measures of this reconstruction are in Table 7.3. The mean rms error, relative error and peak error were all higher than the errors for the VT_{train} group (cf. Table 5.1). The rms error and relative error were slightly higher for this reconstruction than for the reconstruction of the same maps in the feature space derived from the three-group training set (cf. Table 7.1). The peak error was slightly lower for the two-group eigenvector reconstruction than for the three-group reconstruction. The worst cases, in terms of reconstruction errors, are shown in Fig. 7.6.

Nondipolar content of QRST-integral maps

The mean (\pm SD) nondipolar content was calculated, based on eigenvectors derived from the two-group training set, for the entire posttreatment VT group (15.16 ± 15.64 %) and for the PET (12.35 ± 10.63 %) and nPET (16.23 ± 17.17 %) subgroups. An independent t-test revealed no significant ($p \geq 0.05$) difference for this variable between the PET and nPET subgroups. As well, dependent t-tests between pretreatment and posttreatment measures did not show significant differences, at the 0.05 level of significance, for the entire VT_{train} group or the PET and nPET subgroups. The overlap between subgroups for the nondipolar-content measure is apparent in the box plots for the pretreatment and posttreatment maps of the entire VT_{train} group (Fig. 7.7) and the PET and nPET subgroups (Fig. 7.8).

Discriminant analysis employing KL features

The discriminant functions for the three features y_6 , y_2 and y_4 derived from the two-group training set, were applied to the coefficients y_i from the QRST-integral maps of the posttreatment VT group. The results of the discriminant analysis of weighting coefficients for the posttreatment VT group are in Table 7.4. These results show that 84% of all QRST-integral maps for posttreatment VT group were classified into the VT category; this is a similar result to the one obtained for the classification of pretreatment maps for the VT_{train} group (cf. Table 5.4).

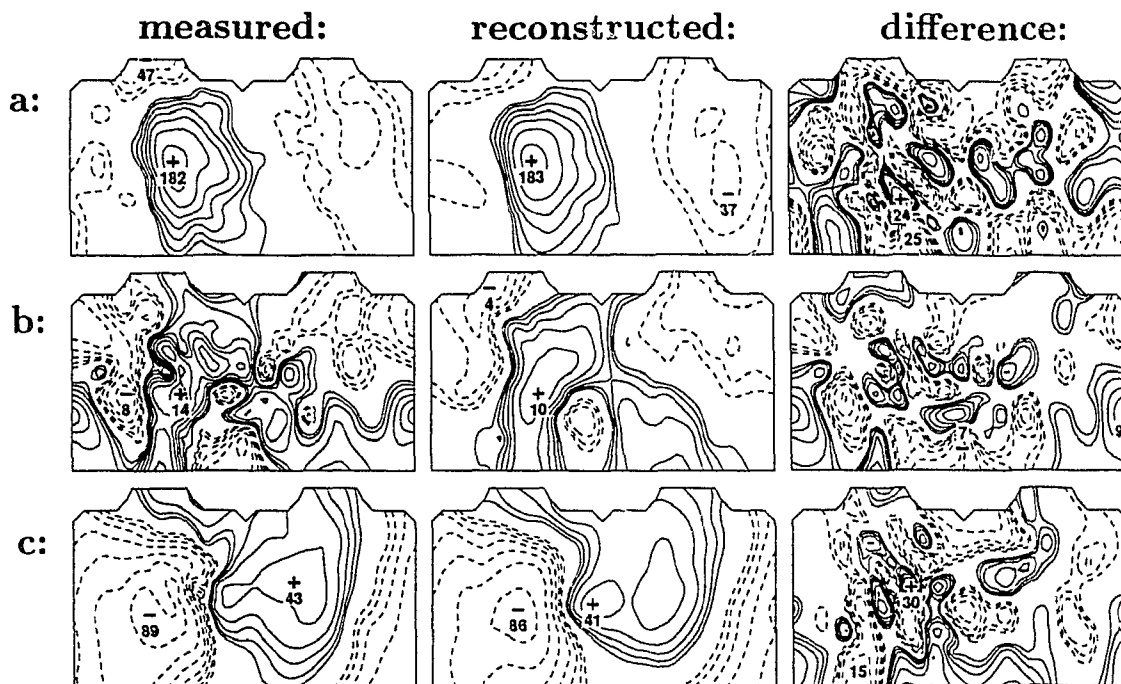


Figure 7.6: Worst-case reconstruction errors for the posttreatment VT group. Based on 16 weighting coefficients and 16 eigenvectors derived from the two-group training set. In the left column are measured maps, in the middle column are reconstructed and the right column are difference maps. a) Worst-case rms error ($e_{\text{rms}} = 11.7 \mu\text{Vs}$, $e_{\text{rel}} = 4.0\%$, $e_{\text{peak}} = 37.9 \mu\text{Vs}$); b) Worst-case relative error ($e_{\text{rms}} = 3.6 \mu\text{Vs}$, $e_{\text{rel}} = 49.1\%$, $e_{\text{peak}} = 11.2 \mu\text{Vs}$); c) Worst-case peak error ($e_{\text{rms}} = 9.4 \mu\text{Vs}$, $e_{\text{rel}} = 6.2\%$, $e_{\text{peak}} = 51.2 \mu\text{Vs}$).

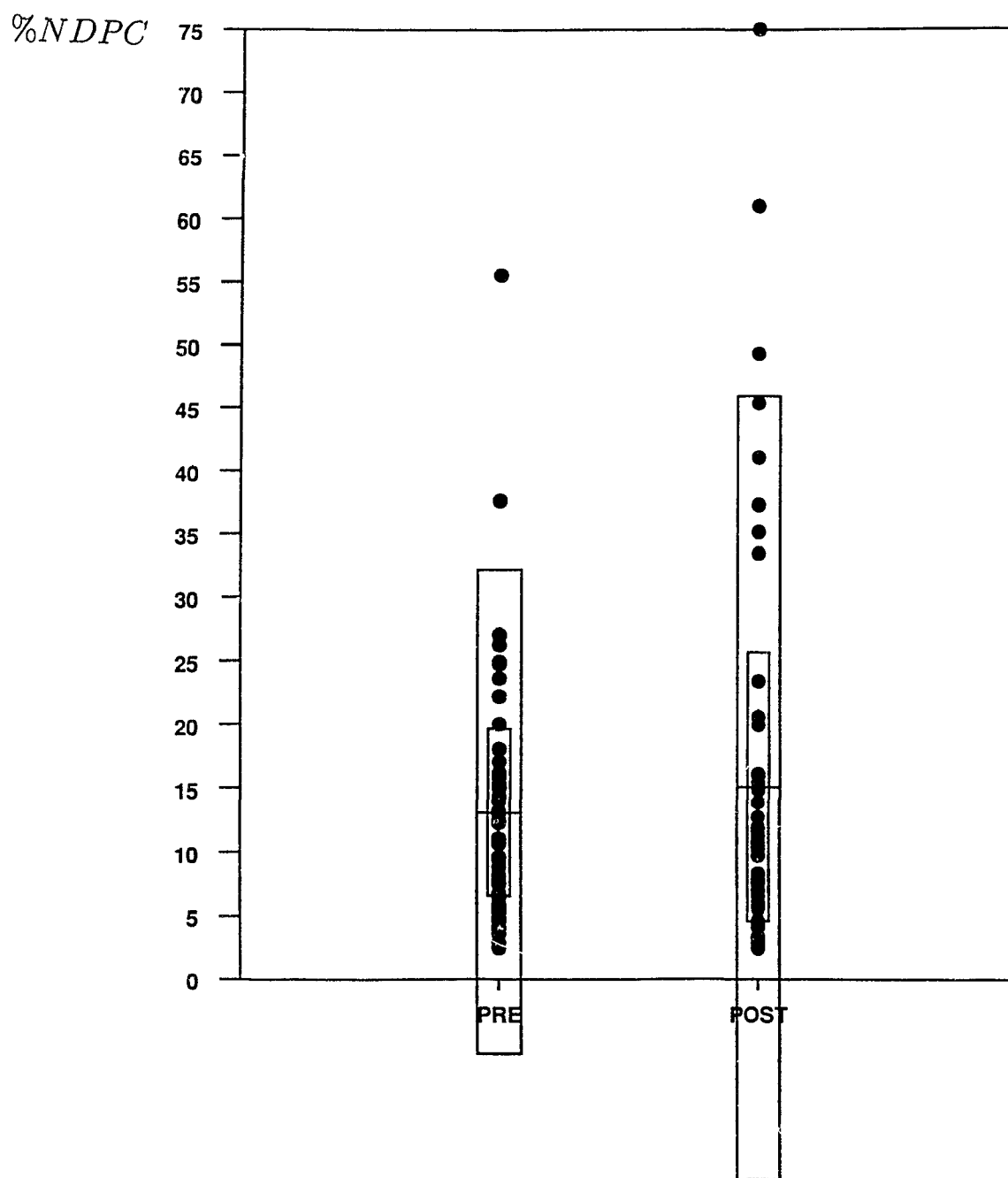


Figure 7.7: Nondipolar content for pretreatment and posttreatment VT group. Based on eigenvectors derived from the two-group training set. Box-plot convention is the same as in Fig. 7.3.

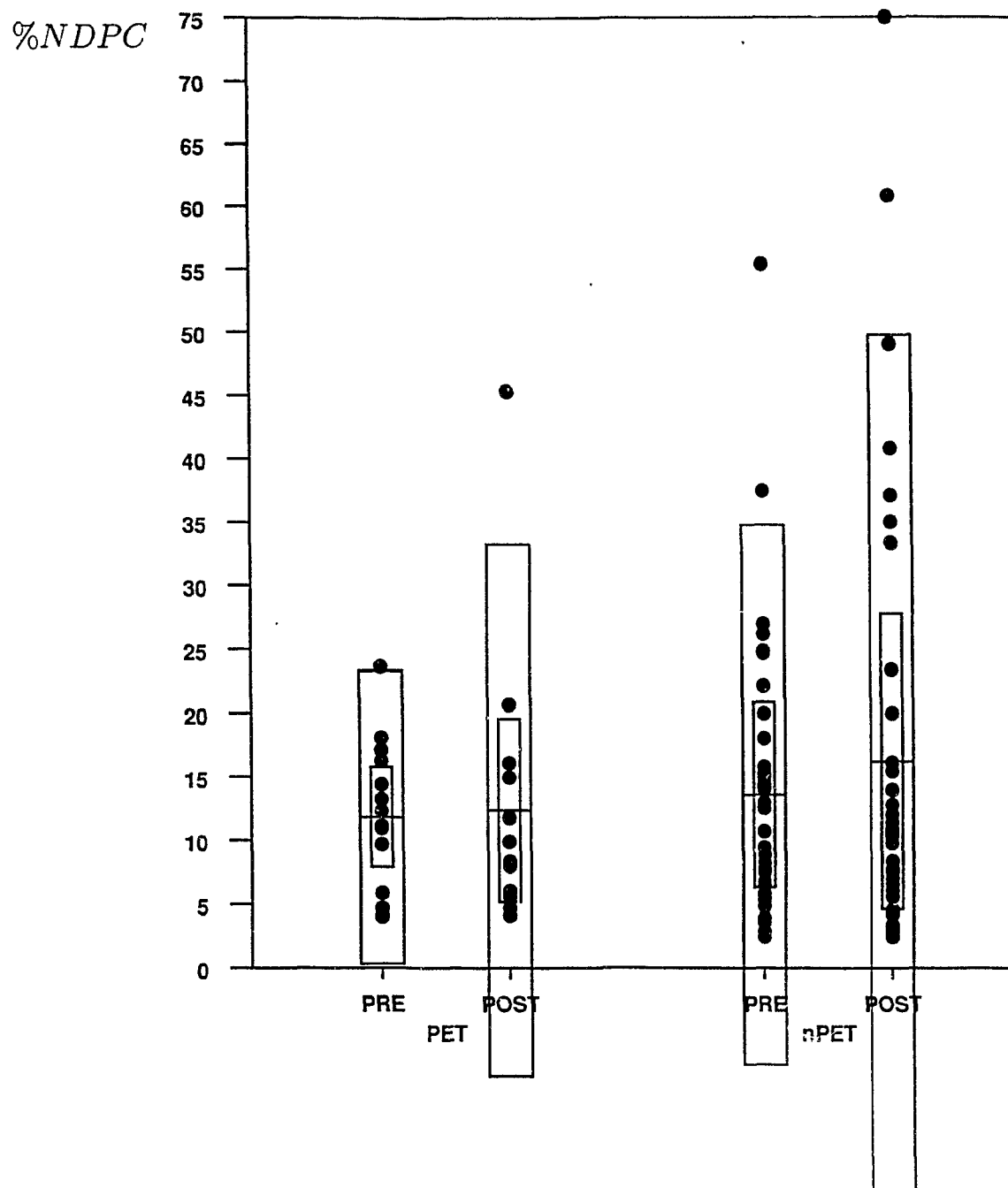


Figure 7.8: Nondipolar content for pretreatment and posttreatment PET and nPET subgroups.

Based on eigenvectors derived from the two-group training set. Box-plot convention is the same as in Fig. 7.3.

Table 7.4: Classification of the posttreatment VT group: discriminant analysis based on KL features y_6 , y_2 and y_4 derived from the two-group training set

		Category	
Group		VT	MI
PET ($n=14$)	cases	11	3
	%	79	21
nPET ($n=37$)	cases	32	5
	%	86	14
Total ($n=51$)	cases	43	8
	%	84	16
Priors		.50	.50

Discriminant analysis employing KnY features

The discriminant functions derived for the KnY feature f_1 derived from the two-group training set were applied to the coefficients of the posttreatment VT group. The results of classification are summarized in Table 7.5; 9 of 14 PET patients and 32 of 37 nPET patients were classified into the VT category. Therefore, 80% of the posttreatment maps were classified as belonging to the VT category. The percentage of PET patients classified as vulnerable to VT was lower than the percentage of nPET patients: 64% versus 86%. Plots of the KnY coefficient f_1 for the PET and nPET subgroups are in Fig. 7.9. The mean of both posttreatment groups was slightly lower than the pretreatment mean for the VT_{train} group. Examination of the direction of change in the KnY coefficient (posttreatment state relative to pretreatment state) showed that 71% ($n=10$) of the PET coefficients moved toward the MI group, whereas 29% ($n=4$) went in the opposite direction. This difference in percentages was not statistically significant ($p = 0.11$). Fifty nine percent ($n=20$)

Table 7.5: Classification of the posttreatment VT group: discriminant analysis based on KnY feature f_1 derived from the two-group training set

		Category	
Group		VT	MI
PET	cases	9	5
	%	64	36
nPET	cases	32	5
	%	86	14
Total	cases	41	10
	%	80	20
Priors		.50	.50

of the nPET subgroup had a change in their KnY coefficients toward the MI group and 41% ($n=17$) moved in the opposite direction. The probability for this latter result was $p = 0.25$, and thus this difference was also not significant. Fig. 7.10 shows the direction of change between pretreatment and posttreatment KnY coefficients for the PET and nPET subgroups.

7.3 Summary and discussion

The reconstruction errors for the posttreatment maps were higher in comparison with errors for the pretreatment maps of the same patients; this was the case for both the reconstruction based on eigenvectors from the three-group and two-group training sets. The nondipolar-content measure could not differentiate between the PET and nPET posttreatment data — although there was a trend for higher nondipolar content in the nPET posttreatment subgroup. There was a large variability associated with the nondipolar content for the posttreatment data. The results of the

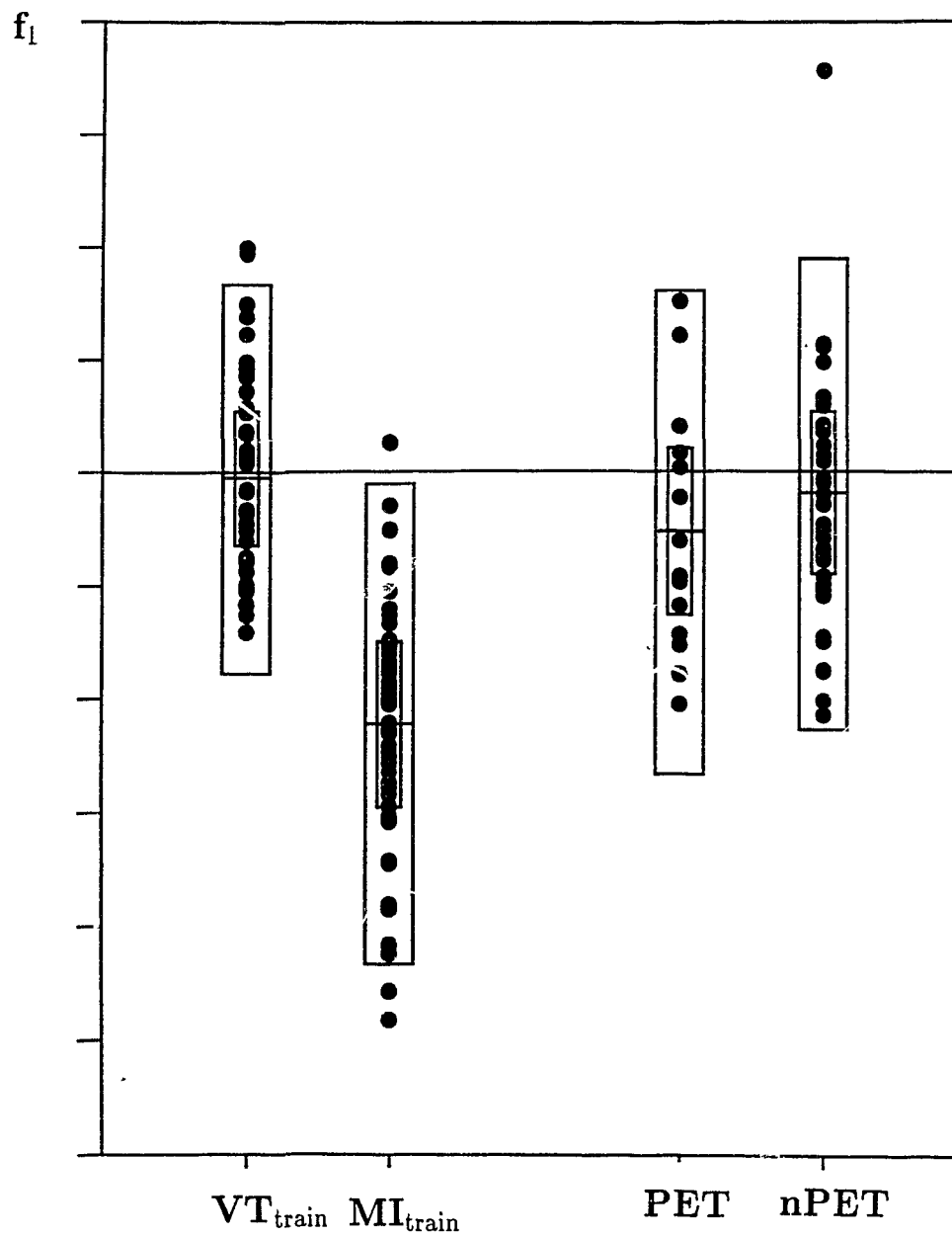


Figure 7.9: Posttreatment PET and nPET subgroups in terms of KnY coefficient f_1 derived from the two-group training set. Box-plot convention is similar to that used in Fig. 7.3.

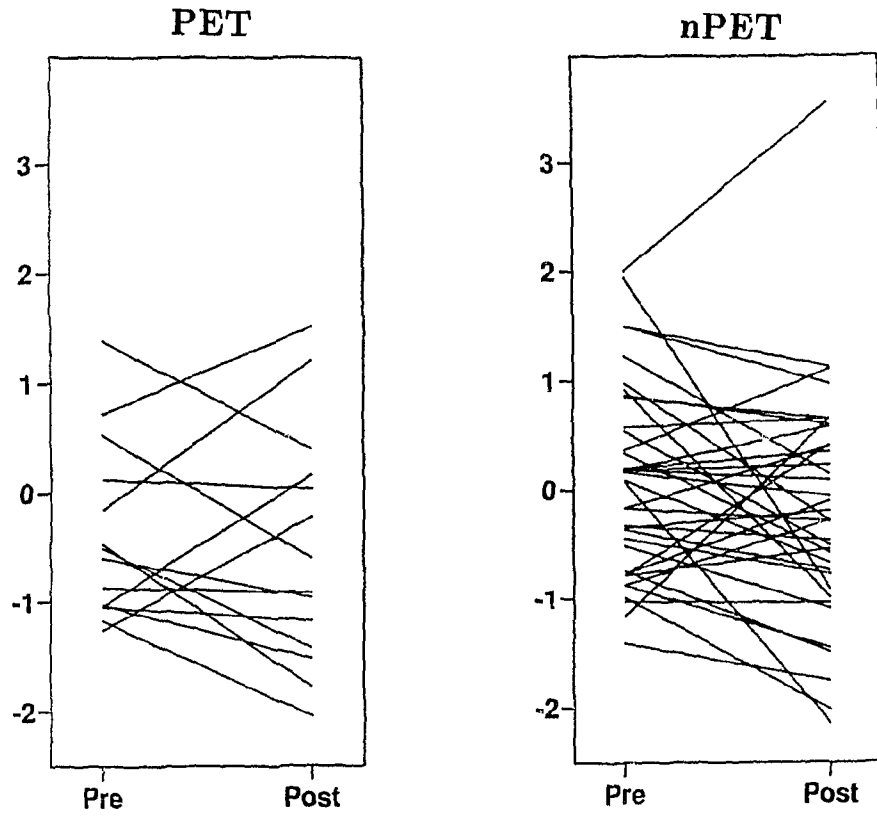


Figure 7.10: Pretreatment and posttreatment PET and nPET subgroups in terms of KnY coefficient f_1 derived from the two-group training set. PRE = baseline, POST = after treatment.

discriminant analysis, employing the three KL coefficients and the two KnY coefficients from the three-group training set, did not indicate any discernible changes in electrocardiographic measurements as a result of treatment. The discriminant analysis of the posttreatment VT data, based on the three KL coefficients derived from the two-group training set, showed only a slight improvement over the three-group results. The KnY features derived from the two-group training set provided the best results — in terms of differences between pretreatment and posttreatment data of the VT_{train} group; however, the results do not corroborate the assessment provided by EPS studies. The small sample size (in particular for the PET subgroup) and to some extent the uncertainty associated with the prediction of effective therapy, provide some explanation as to why it is so difficult to differentiate between PET and nPET subgroups.

Chapter 8

Error estimates for classification procedures

The issue of diagnostic performance of the classification procedures has been partially addressed in chapter 6. As expected, the diagnostic performance for the test set was lower than that for the training set. The best diagnostic performance for the test set was achieved by the discriminant analysis based on the features derived from the two-group training set. These results illustrate that the features derived from the QRST-integral maps of the two-group training set contain information that could be used to classify independent observations. In contrast, the test-set results based on the features derived from the three-group training set were poor, indicating that these features have limited diagnostic value. This chapter focuses on evaluating, for the diagnostic features identified in chapter 5, classification errors and confidence limits associated with the classification procedures for discriminating between the two patient groups.

In the discriminant analysis, the error bias is the difference between the apparent classification error for the training set and the true error of classification. The difference between classification errors for the original training set and for the test

set provides one estimate of the error bias; this estimate has been obtained for every error measure in chapter 6. The stochastic methods used in this study for evaluating the true error require that all of the data be allocated to training and test sets according to the different schemes, which are specific for each method. Therefore, the entire patient population was combined into the *total patient set* and used to identify the features that contained the best diagnostic information for classifying the two patient groups. The features derived from the total patient set were also applied to the posttreatment VT_{train} group to evaluate whether their sensitivity to electrophysiological changes resulting from drug therapy was improved with a new stable set of features.

This chapter presents the error estimates calculated for the classification procedures that employed the KL features derived from the total patient set ($n=204$). Three different methods were used to evaluate the true error from the total patient set: the bootstrap method without replacement; bootstrap method with replacement [54]; and cross validation method [55]. These approaches (described in chapter 3) are particularly useful for estimating true error in relatively small data sets.

8.1 Eigenvector analysis of QRST-integral maps

As for the previous data sets, the first task was to reduce the pattern space for the total patient set (consisting of all patients, i.e., $VT_{\text{train}} + VT_{\text{test}} = 102$ and $MI_{\text{train}} + MI_{\text{test}} = 102$), and the next task was to find an optimal classification procedure in this reduced feature space. The pattern space for the total patient set was a matrix $[X]$, dimensioned 117×204 , for the QRST-integral maps of 204

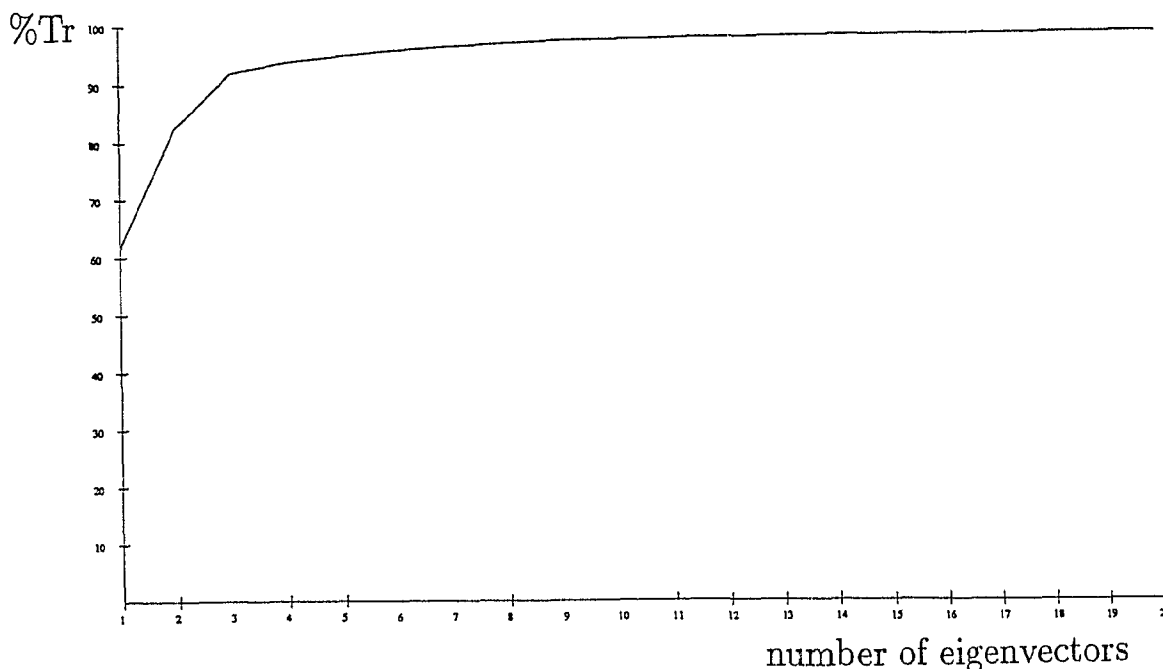


Figure 8.1: Percent trace vs. number of eigenvectors for the total patient set patients. The sample covariance matrix $[S_c]$ and its eigenvalues and eigenvectors were calculated for $[X]$. The percent trace for the 16 highest eigenvalues was 99% (Fig. 8.1); the 16 corresponding eigenvectors were plotted as eigenmaps (Fig. 8.2).

The measured QRST-integral values and the 16 eigenvectors derived from the total patient set were used to calculate the weighting coefficients y_i for each eigenvector and for each patient. The 16 weighting coefficients for each patient and the corresponding eigenvectors were then used to reconstruct the QRST-integral maps for each patient. These reconstructed maps were qualitatively examined to detect differences in patterns compared with the measured maps. Three measures of error were calculated to quantify differences between the measured and reconstructed maps: a root-mean-squared error (e_{rms}), relative error (e_{rel}) and peak error (e_{peak}).

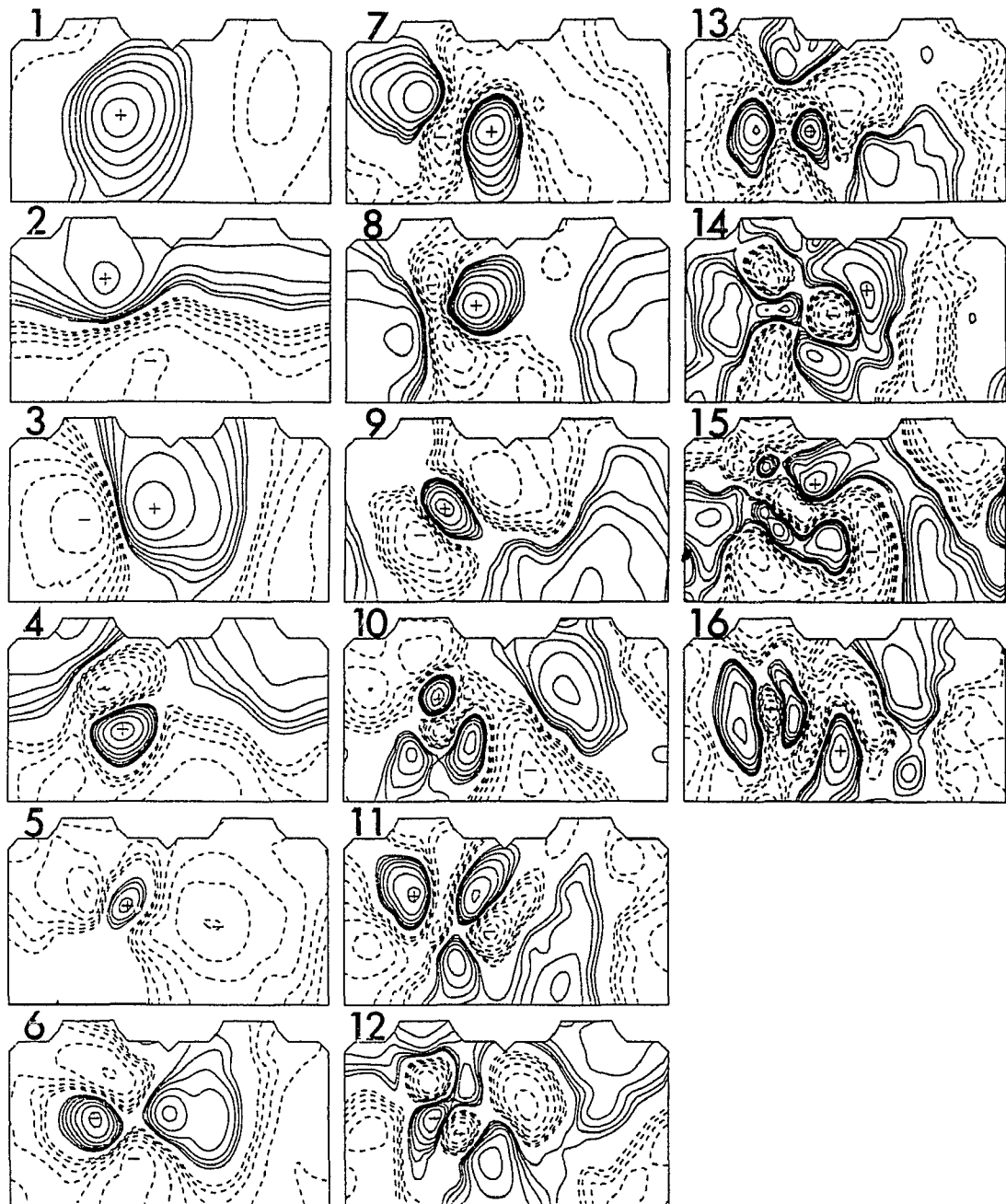


Figure 8.2: Eigenvectors for the total patient set. Eigenvectors are plotted as spatial maps on the torso, in descending order of the magnitude of their contribution; the plotting convention is the same as in Fig. 4.2.

Table 8.1: Reconstruction errors for the total patient set

		Total ($n=204$)	VT_{total} ($n=102$)	MI_{total} ($n=102$)
rms error [μ Vs]	mean	3.18	3.15	3.21
	SD	1.00	0.99	1.02
relative error [%]	mean	2.67	3.28	2.06
	SD	4.10	4.30	3.81
peak error [μ Vs]	mean	11.24	10.88	11.60
	SD	4.47	4.18	4.74

Table 8.1 summarizes the errors for the total patient set and for the two constituent groups. The rms error and peak error were similar between the two patient groups, with the VT_{total} group having a slightly higher relative error compared to the MI_{total} group. These errors were similar to the errors that were associated with the reconstruction for the two-group training set and for the test set, both based on the features derived from the two-group training set. The measured and reconstructed QRST-integral maps for the worst cases, in terms of errors, are shown in Fig. 8.3.

8.2 Discriminant analysis employing KL features

The stepwise discriminant analysis of the 16 weighting coefficients for the total patient set revealed that the three features with the greatest discriminating capabilities between the two constituent groups of patients (VT_{total} and MI_{total}) corresponded to maps 6, 4 and 13 from Fig. 8.2; thus, *all three* KL features that were selected were nondipolar by definition. The results of diagnostic classification based on the discriminant analysis which employed the KL features y_6, y_4 and y_{13} are in Table

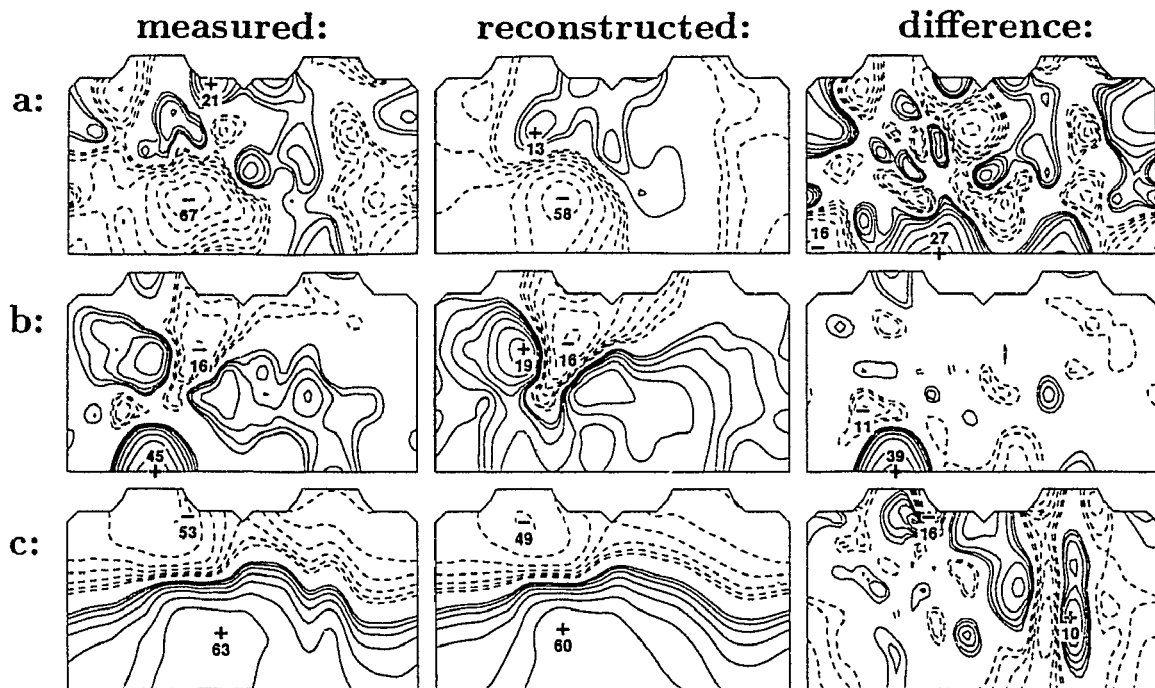


Figure 8.3: Worst-case reconstruction errors for the total patient set. Reconstruction was based on 16 weighting coefficients and corresponding eigenvectors. In the left column are measured maps, middle column are reconstructed maps and right column are difference maps. a) Worst-case rms error ($e_{\text{rms}} = 6.8 \mu\text{Vs}$, $e_{\text{rel}} = 11.8\%$, $e_{\text{peak}} = 21.8 \mu\text{Vs}$). b) Worst-case relative error ($e_{\text{rms}} = 4.5 \mu\text{Vs}$, $e_{\text{rel}} = 29.5\%$, $e_{\text{peak}} = 15.4 \mu\text{Vs}$). c) Worst-case peak error ($e_{\text{rms}} = 4.6 \mu\text{Vs}$, $e_{\text{rel}} = 1.9\%$, $e_{\text{peak}} = 24.1 \mu\text{Vs}$).

Table 8.2: Classification of the total patient set: stepwise discriminant analysis based on KL features y_6, y_4 and y_{13} derived from this set

Group	Category	
	VT	MI
VT _{total} ($n=102$)	84	18
MI _{total} ($n=102$)	25	77
Total ($n=204$)	109	95
Priors	.50	.50

Table 8.3: Sensitivity, predictive value and diagnostic performance of total-patient-set classification based on KL features y_6, y_4 and y_{13} derived from this data set

	Sensitivity [%]	Predictive Value [%]
VT _{total} ($n=102$)	82	77
MI _{total} ($n=102$)	76	81
$DP = 79\%; \kappa = .58$		

8.2. Summary of overall diagnostic performance is in Table 8.3.

The percentage of patients correctly classified (79%) for the total patient set was the same as the number for the two-group training set (cf. section 5.3). However, the results of classification for the constituent groups VT_{total} and MI_{total} of the total patient set were different from those obtained for the original training set groups VT_{train} and MI_{train}; the sensitivities appeared to be more balanced, with the sensitivity for the VT category being 6% lower and the sensitivity for the MI category being 7% higher.

8.3 Discriminant analysis employing KnY features

The KnY transform was performed on the 16 KL features derived from the total patient set. The stepwise discriminant analysis of the KnY feature space identified one coefficient, f_1 , that contained nearly all of the information discriminating between the two constituent groups of patients. This one feature was used for classification in a linear discriminant analysis. The results of diagnostic classification for the total patient set, consisting of 204 patients, are in Tables 8.4 and 8.5. Overall, 89% of the patients belonging to the total patient set were correctly classified; this is the same percentage as for the original two-group training set in chapter 5. The percentage of patients who were classified correctly for each of the two constituent groups was similar to that obtained for the original training set (cf. Table 5.4). The mean and confidence intervals for the one KnY feature, characterizing constituent groups VT_{total} and MI_{total} of the total patient set, are depicted in Fig. 8.4. The variability for the KnY feature was lower for the VT_{total} group than for the MI_{total} group. These results demonstrate that the diagnostic information contained in the QRST-integral maps can be represented with a high degree of sensitivity by a single KnY feature. The ability of one single feature to characterize an arrhythmogenic state is striking, as evidenced by the VT sensitivity of 92%.

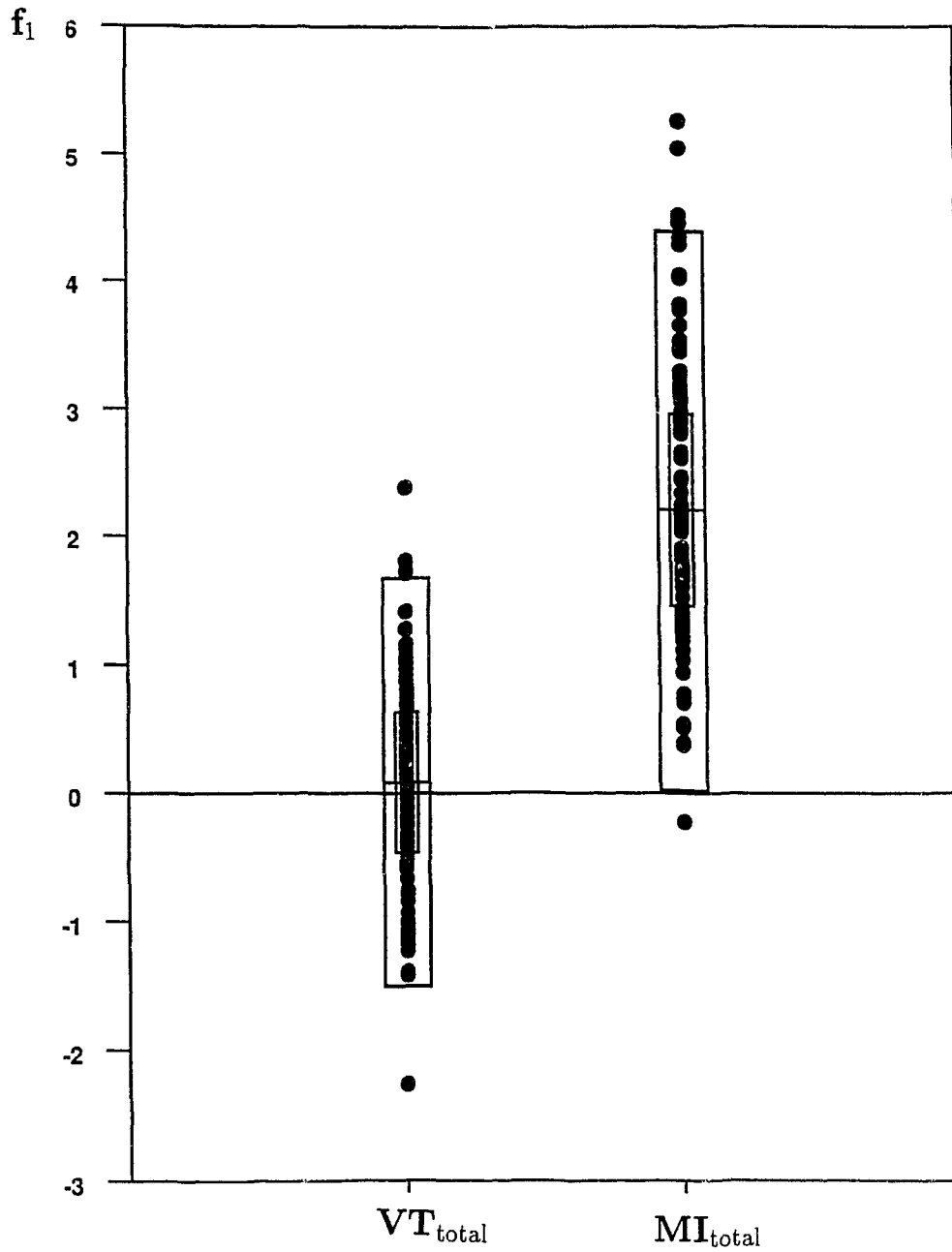


Figure 8.4: KnY coefficient f_1 for the total patient set. The inner box corresponds to the 50% confidence interval and the outer box to the 95% confidence interval; the mean is indicated by the horizontal bar.

Table 8.4: Classification of the total patient set: discriminant analysis based on KnY feature f_1 derived from this data set

	Category	
Group	VT	MI
VT _{total} ($n=102$)	94	8
MI _{total} ($n=102$)	14	88
Total ($n=204$)	108	96
Priors	.50	.50

Table 8.5: Sensitivity, predictive value and diagnostic performance of total-patient-set classification based on KnY feature f_1 derived from this data set

	Sensitivity [%]	Predictive Value [%]
VT _{total} ($n=102$)	92	87
MI _{total} ($n=102$)	86	92
$DP = 89\%; \kappa = .78$		

8.4 Classification of the posttreatment VT group

The 16 eigenvectors derived from the total patient set were applied to the measured QRST-integral maps for the posttreatment VT_{train} group. The weighting coefficients y_i for each eigenvector and for each patient were calculated, and the QRST-integral maps were reconstructed and compared with the measured maps. The errors for this reconstruction are in Table 8.6. The reconstruction errors were higher and more variable than the errors for the total patient set, the original training set or the test set. They were, however, similar to the errors found for the reconstruction of post-treatment data in sections 7.1 and 7.2. The worst cases, in terms of reconstruction errors, are plotted in Fig. 8.5.

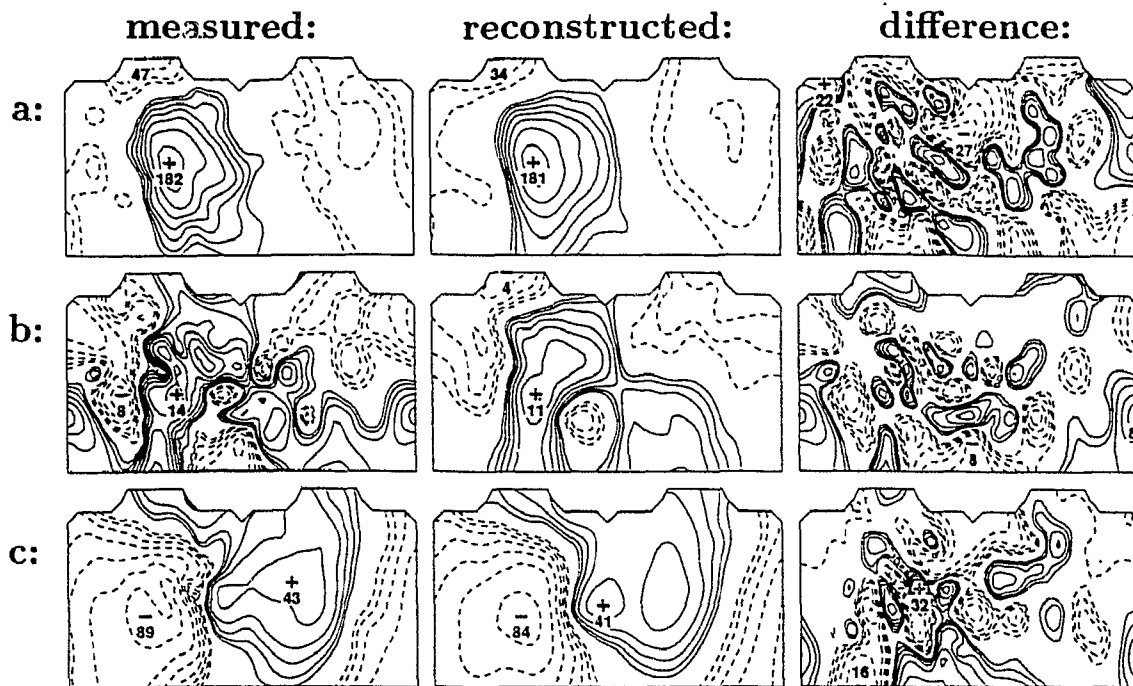


Figure 8.5: Worst-case reconstruction errors for the posttreatment VT group. Reconstruction was based on 16 KL coefficients derived from the total patient set. In the left column are measured maps, the middle column are reconstructed maps and the right column are difference maps. a) Worst-case rms error ($e_{\text{rms}} = 11.3 \mu\text{Vs}$, $e_{\text{rel}} = 3.7\%$, $e_{\text{peak}} = 35.9 \mu\text{Vs}$). b) Worst-case relative error ($e_{\text{rms}} = 3.5 \mu\text{Vs}$, $e_{\text{rel}} = 48.5\%$, $e_{\text{peak}} = 10.9 \mu\text{Vs}$). c) Worst-case peak error ($e_{\text{rms}} = 9.3 \mu\text{Vs}$, $e_{\text{rel}} = 6.0\%$, $e_{\text{peak}} = 53.1 \mu\text{Vs}$).

Table 8.6: Reconstruction errors for the posttreatment VT group: based on features derived from the total patient set

		PET+nPET ($n=51$)	PET ($n=14$)	nPET ($n=37$)
rms error [μ Vs]	mean	4.21	4.37	4.14
	SD	1.83	2.06	1.76
relative error [%]	mean	7.58	6.50	7.99
	SD	8.01	6.36	8.60
peak error [μ Vs]	mean	13.95	16.08	13.15
	SD	7.90	11.74	5.87

Table 8.7: Classification of the posttreatment VT group: discriminant analysis based on KL features y_6, y_4 and y_{13} derived from the total patient set

		Category	
Group		VT	MI
PET ($n=14$)	cases	13	1
	%	93	7
nPET ($n=37$)	cases	31	6
	%	84	16
Total ($n=51$)	cases	44	7
	%	86	14
Priors		.50	.50
$\kappa = .054$			

The classification results for the posttreatment maps, based on the discriminant functions employing KL features y_6, y_4 and y_{13} from the total patient set, are summarized in Table 8.7. These results show that 86% of the QRST-integral maps were classified as belonging to the VT category.

The results of classification for the posttreatment VT maps, based on the single KnY feature derived from the total patient set, are summarized in Table 8.8; 86%

Table 8.8: Classification of the posttreatment VT group: discriminant analysis based on KnY feature f_1 derived from the total patient set

		Category	
Group		VT	MI
PET ($n=14$)	cases	12	2
	%	86	14
nPET ($n=37$)	cases	32	5
	%	86	14
Total ($n=51$)	cases	44	7
	%	86	14
Priors		.50	.50
$\kappa = .005$			

of the QRST-integral maps remained classified in the VT category. The PET and nPET subgroups had a similar ratio of patients who were classified to the VT and MI categories. These results differed from those obtained for the posttreatment-VT-group classification, based on the one KnY feature derived from the two-group training set (section 7.2). The KnY coefficient for both the PET and nPET subgroups is plotted in Fig. 8.6. As is evident from this figure, there was a large overlap between the two posttreatment subgroups (PET and nPET) and the VT_{total} group.

It follows from these results that—in terms of features that were best able to classify the VT from the MI categories—there is apparently no significant change in the posttreatment QRST-integral maps as a result of treatment.

8.5 Error estimates

The diagnostic performance of classification based on the one KnY feature was consistently better than that based on the three KL features, for both training

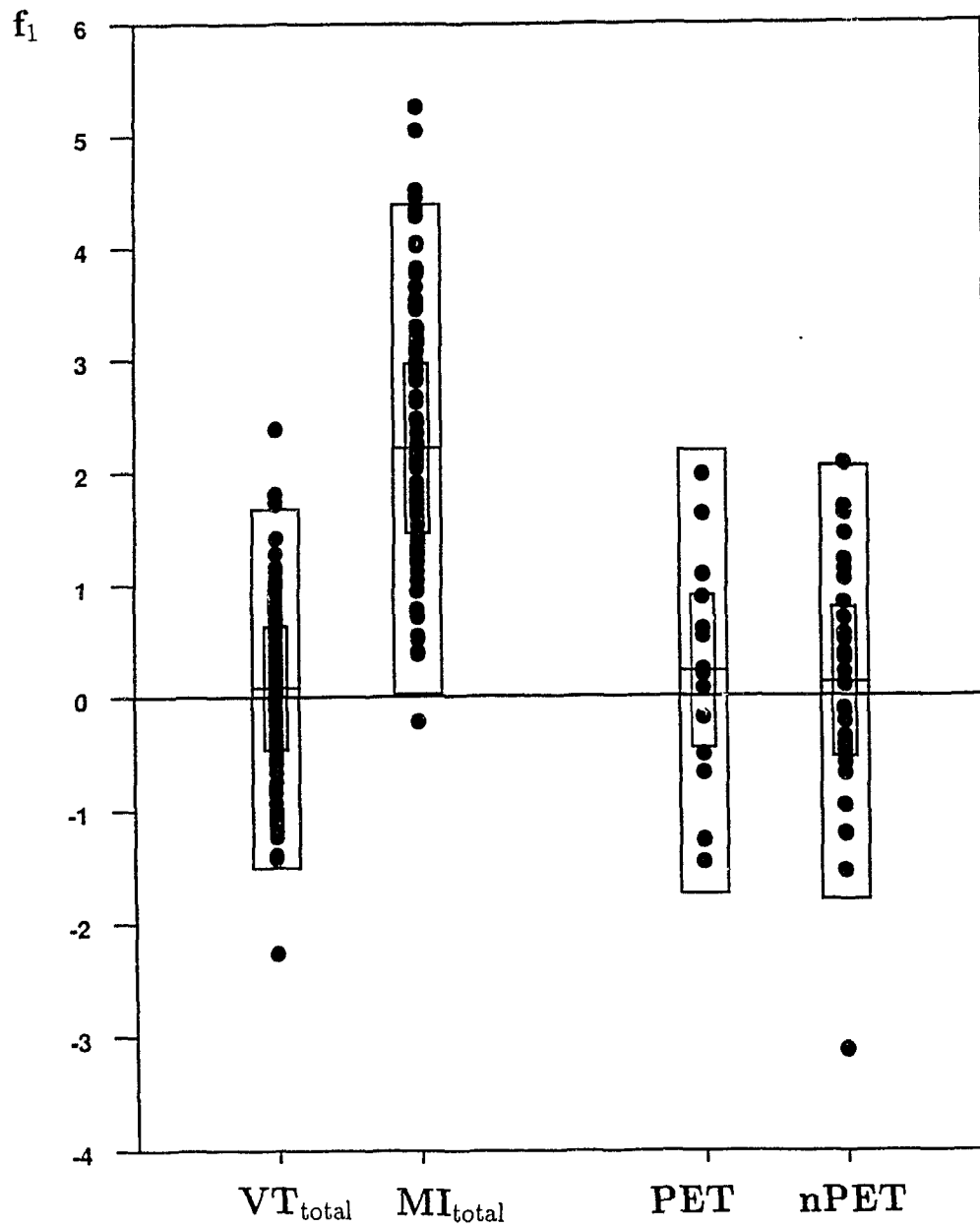


Figure 8.6: Posttreatment VT group in terms of KnY coefficient f_1 from the total patient set.

The inner box corresponds to the 50% confidence interval and the outer box to the 95% confidence interval; the mean is indicated by the horizontal bar.

Table 8.9: Error and variance estimates of correct classifications for KL and KnY feature spaces obtained by bootstrap method without replacement

Group	KL (features y_6, y_4 and y_{13})	KnY (feature f_1)
	mean (± 1.96 SD)	mean (± 1.96 SD)
Training set ($n=102$)	79 (6) DP	89 (5) DP
VT ($n=51$)	82 (7) SE_{VT}	93 (6) SE_{VT}
MI ($n=51$)	77 (7) SE_{MI}	85 (7) SE_{MI}
Test set ($n=102$)	78 (6) DP	82 (7) DP
TVT ($n=51$)	81 (10) SE_{VT}	87 (8) SE_{VT}
TMI ($n=51$)	75 (12) SE_{MI}	77 (13) SE_{MI}

Total number of 1000 classifications were used. Training set = sets of data randomly designated as the training set; VT = the training-set group vulnerable to ventricular arrhythmia; MI = the training-set group with myocardial infarction; Test set = sets of data randomly designated as the test set; TVT = the test-set group vulnerable to ventricular arrhythmia; TMI = the test-set group with myocardial infarction; mean = mean of 1000 randomizations; \pm = 95% confidence interval (± 1.96 SD).

and test sets. The analysis described in this section provides an evaluation of the error associated with the classification procedures, based on both the KL and KnY feature space, and provides an estimate of the classifier's ability to extrapolate, i.e., to classify independent observations. The error and variance estimates obtained by a bootstrap method and cross-validation method for the classification features are presented in Tables 8.9–8.11.

The results obtained by the bootstrap method without replacement are in Table 8.9; these error and variance estimates were generated from 1000 randomizations of the total patient set into equal training and test sets. The 95% confidence limits were calculated from the results of these 1000 replications.

The error and variance estimates obtained by the bootstrap method with re-

Table 8.10: Error and variance estimates of correct classifications for KL and KnY feature spaces obtained by bootstrap method with replacement

Group	KL (features y_6, y_4 and y_{13})	KnY (feature f_1)
	mean (± 1.96 SD)	mean (± 1.96 SD)
Training set ($n=204$)	80 (6) DP	89 (5) DP
VT ($n=102$)	82 (8) SE_{VT}	93 (6) SE_{VT}
MI ($n=102$)	77 (8) SE_{MI}	84 (7) SE_{MI}
Test set ($\bar{n}=75$)	78 (8) DP	82 (8) DP
TVT ($\bar{n}=37.5$)	80 (13) SE_{VT}	87 (12) SE_{VT}
TMI ($\bar{n}=37.5$)	75 (14) SE_{MI}	77 (15) SE_{MI}

Total number of 1000 classifications were used. Training set = sets of data randomly designated as the training set; VT = the training-set group vulnerable to ventricular arrhythmia; MI = the training-set group with myocardial infarction; Test set = sets of data randomly designated as the test set; TVT = the test-set group vulnerable to ventricular arrhythmia; TMI = the test-set group with myocardial infarction.

placement are in Table 8.10. These results are based on 1000 randomizations of the total patient set into training set and test set by means of a sampling with replacement procedure. The training set was made up of data for 204 patients (some with repetitions) and the test set comprised data for 75 patients who were not selected by the sampling procedure.

Table 8.11 summarizes the results produced by the cross-validation method, which consists of systematically removing one case from the total patient set of 204 cases. The training set was made up of the data for 203 patients and the test set consisted of data for just one patient. The results were derived from 204 classifications. The 95% confidence limits were calculated assuming a binomial distribution.

Table 8.11: Error and variance estimates of correct classifications for KL and KnY feature spaces obtained by cross-validation method

Group	KL (features y_6, y_4, y_{13})	KnY (feature f_1)
	mean (± 1.96 SD)	mean (± 1.96 SD)
Training set	79 (6) DP	90 (4) DP
VT	82 (7) SE_{VT}	93 (5) SE_{VT}
MI	76 (8) SE_{MI}	86 (7) SE_{MI}
Test set	78 (6) DP	84 (5) DP
TVT	79 (8) SE_{VT}	88 (6) SE_{VT}
TMI	76 (8) SE_{MI}	80 (8) SE_{MI}

Total number of 204 classifications were used. Training set = set designated as training set (204 sets of 203 maps); VT = the training-set group vulnerable to ventricular arrhythmia; MI = the training-set group with myocardial infarction; Test set = data designated as test set (204 sets of 1 map); TVT = the test-set group vulnerable to ventricular arrhythmia; TMI = the test-set group with myocardial infarction.

Consistent with the results of classification of the original training set and of the total patient set, the mean percentage of patients classified correctly for the training sets, on the basis of KL features y_6, y_4 and y_{13} , was 10% lower than the percentage of correct classifications based on one KnY feature f_1 . (The mean percentages of correct classifications for the training sets in Tables 8.9–8.11 were comparable to those from the original training set presented in Tables 5.3 and 5.5, and for the total patient set in Tables 8.3 and 8.5. A notable difference was in the classification results between the original training set in chapter 5 and the calculated mean estimates for the two constituent groups based on the KL feature space. The percentage of VT patients who were correctly classified decreased from 88% in the original VT_{train} group to the average value of 82% for both bootstrap methods and cross validation.

In contrast, the average percentage of correctly-classified MI patients, as estimated by the two bootstrap methods and cross validation method, was better than the 69% correctly classified from the original MI group (cf. Table 5.3). The average error estimates of the diagnostic performance based on the KL feature space for the two groups were consistent with the results of the total patient set.

The results of classification for the training set, based on the KnY feature space, were consistent for the two bootstrap methods and cross validation. These average error estimates were comparable with the original training-set results and the results for the total patient set. There was a high sensitivity for the VT patients (93%), with a low variance associated with this value. The number of MI patients classified correctly was also consistent across all methods (84-86%). The variance estimates were similar for the both KL and KnY classification procedures; however, the variance estimates for the MI data were consistently higher than those for the VT data.

The error and variance estimates provided by the cross-validation method (Table 8.11) suggest that classifications based on a single KnY feature perform better, in every department, than classifications based on the three KL features. The results were the best for the KnY-feature-based classification of the training set, with 90% of the patients classified correctly and a 95% confidence limit ranging between 86-94%. Of particular importance was the VT sensitivity, with a 95% confidence limit ranging between 88-98%.

The test-set results were more variable and had a higher error rate than the training-set results for all three error estimates. The worst test-set result was the

sensitivity for the MI group, for classification based on the three KL features. The variance estimates obtained by the bootstrap method with replacement are noticeably higher, which in part can be explained by the smaller sample size ($\bar{n}=37.5$). The best test-set result was the VT sensitivity for the classification based on the KnY feature, as estimated by the cross-validation method (95% confidence limit ranging between 82–94%).

The difference between the test-set and training-set errors from the above procedures provided a measure of the error bias. The results of classification for the test-set, based on the KL feature space, were comparable to the training-set results for all three error estimates and the error bias for the classifications based on the KL features were 1-2%. The average test-set classification results, based on the KnY feature, were 7% lower than the training-set results as estimated by both bootstrap methods, and 5% lower according to cross-validation method. The error biases were slightly lower for the VT group than for the MI group, for all error estimates. While the error bias is higher for the classification based on the KnY feature, the number of correctly-classified patients who belonged to the VT_{test} group set was still on average 5-7% higher for this classification than for the one based on the KL feature space.

8.6 Number of features

The test-set results (chapter 6) and error estimates (section 8.5) provided evidence that the features derived from the QRST-integral maps contain important diagnostic information; however, the issue of tailoring the features to the training set was

further explored. The KL feature space was examined first to determine how many features could be used in the discriminant analysis before an overtraining effect was observed. Then the KnY feature space was examined, to evaluate the effect of 1 to 16 KL features on the diagnostic performance of classification based on the KnY transform. The two bootstrap methods and the cross validation were applied to the KL feature space and the KnY feature space, with 1 to 16 KL features employed in the analysis.

The discriminant analysis of the KL features illustrated that both the training-set and the test-set classification results improved as the number of features in the discriminant analysis was increased from 1 to 8. When more than 8 features were added to the discriminant analysis, the number of correctly classified patients improved only slightly for the training set and there was a slight deterioration for the test set. The decreased performance was mainly due to decreased sensitivity for the VT group. This suggests that up to 8 features could be used with minimal tailoring to the training set. The 8 features selected on the basis of stepwise discriminant analysis were: $y_6, y_4, y_{13}, y_5, y_1, y_2, y_{11}$ and y_{14} , corresponding to spatial patterns in Fig. 8.2. Table 8.12 provides a comparison of the results of the discriminant analysis based on 8 and 16 KL features.

The analysis of the classification based on KnY features demonstrated that the diagnostic performance improved for both the training and the test sets as the number of KL features included in the KnY transformation increased to 14. The results of the discriminant analysis of the single KnY feature based on 13 and 14 KL features are in Table 8.13. The results of the training-set classification improved

for the one KnY feature calculated from the 16 versus 13 KL features for the cross validation procedure, which may be indicative of a trend toward tailoring. However, it is evident that 13 to 16 KL features in the KnY procedure produced similar classification results for the test set, although the sensitivity for the MI group was slightly improved for the KnY feature calculated from the 16 KL features. The inclusion of the three extra KL features in the KnY calculation appears to have minimal effect on the diagnostic performance of that feature.

In general, there was a similarity between the diagnostic classification from the discriminant analysis of the 16 KL features and the discriminant analysis of the KnY feature space based on 16 KL features. The advantage of the latter is that a single feature that is easily displayed graphically contains the diagnostic information from the entire QRST-integral map.

8.7 Summary and discussion

The eigenvectors were calculated for the total patient set and low reconstruction errors were achieved using the 16 highest eigenvectors. The results of diagnostic classification for the total patient set were consistent with the results from the two-group training set. The three KL features identified as having the highest discriminating abilities corresponded to three nondipolar features: sixth, fourth and thirteenth. Consistent with previous results, the KnY feature provided the best classification (89% patients correctly classified), which was 10% better than the result based on the three KL features. The lower variability for the KnY feature

Table 8.12: Error and variance estimates of correct classifications for the 8- and 16-dimensional KL feature space

Group	KL (8 features)			KL (16 features)		
	BS1	BS2	CV	BS1	BS2	CV
	mean (\pm)	mean (\pm)	mean (\pm)	mean (\pm)	mean (\pm)	mean (\pm)
Training set <i>DP</i>	88 (5)	88 (5)	89 (4)	89 (5)	89 (5)	89 (4)
SE_{VT}	94 (6)	94 (5)	95 (4)	93 (6)	93 (6)	93 (5)
SE_{MI}	83 (7)	83 (7)	82(7)	85 (7)	85 (7)	85 (7)
Test set <i>DP</i>	84 (6)	84 (8)	85 (5)	82 (7)	82 (8)	84 (5)
SE_{TVT}	90 (8)	90 (10)	91 (6)	87 (10)	87 (12)	88 (6)
SE_{TMI}	78 (12)	78 (14)	78 (8)	77 (13)	77 (15)	79 (8)

Training set = set of data designated as the training set for each error-estimate procedure; Test set = set of data designated as the test set for each error-estimate procedure; BS1 = bootstrap without replacement; VT = the training-set group vulnerable to ventricular arrhythmia ($n=51$); MI = the training-set group with myocardial infarction ($n=51$); TVT = the test-set group vulnerable to ventricular arrhythmia ($n=51$); TMI = the test-set group with myocardial infarction ($n=51$). BS2 = bootstrap with replacement; VT = the training-set group vulnerable to ventricular arrhythmia ($\bar{n}=102$); MI = the training-set group with myocardial infarction ($\bar{n}=102$); TVT = the test-set group vulnerable to ventricular arrhythmia ($\bar{n}=37.5$); TMI = the test-set group with myocardial infarction ($\bar{n}=37.5$); CV = cross validation; $\pm = \pm 1.96$ SD.

Table 8.13: Error and variance estimates of correct classifications for one KnY feature based on 13 and 14 KL features

Group	13 KL features			14 KL features		
	BS1	BS2	CV	BS1	BS2	CV
	mean (\pm)					
Training set <i>DP</i>	87 (6)	87 (6)	87 (5)	88 (5)	88 (5)	87 (5)
<i>SE</i> _{VT}	92 (7)	92 (6)	92 (5)	93 (6)	93 (6)	91 (6)
<i>SE</i> _{MI}	82(8)	82 (7)	82 (7)	84 (8)	84 (7)	83 (7)
Test set <i>DP</i>	81 (6)	81 (8)	84 (5)	82(6)	82 (9)	84 (5)
<i>SE</i> _{TVT}	87 (10)	87 (12)	90 (6)	88 (10)	88 (11)	88(6)
<i>SE</i> _{TMI}	75 (13)	76 (14)	78 (8)	76 (14)	77 (15)	79 (8)

with the increased sample size indicated stability of the diagnostic classification based on this feature.

The reconstruction for the posttreatment VT group, based on the features derived from the total patient set, was fraught with high reconstruction errors. The results of classification demonstrated that the majority of patients remained classified, as in their pretreatment state, as vulnerable to ventricular arrhythmias—in both the KL and KnY feature space. This indicates that the features derived to separate the VT and MI categories were not effective in predicting the outcome of antiarrhythmic therapy (as assessed by programmed stimulation).

The error and variance estimates for the classification results were calculated by three methods: bootstrap without replacement, bootstrap with replacement and cross validation. All three procedures produced estimates of the mean classification error for the training set—based on both the KL feature space and the KnY feature

space—that were comparable to the results of discriminant analysis for the total patient set; therefore, doubling of the sample size seemed to have produced a stable set of features. The diagnostic sensitivity from these error estimates for the VT_{test} group was consistently better than that for the MI_{test} group. The poorer results for the MI data were also reflected in the greater variability associated with the classification for that group, compared to the VT group. The results of these error and variance estimates associated with the KL and KnY classifications provide a comprehensive evaluation of the expected performance of these features.

Finally, as the number of KL features used in the stepwise discriminant analysis increased to 8, there was little evidence of tailoring for the training set; this was reflected in the improved test-set results based on the error estimates. This suggests that the use of three KL features in the original analysis was a conservative number and thus for the sample size in this study a ratio of 1:13 was acceptable. There were similarities between the classification results based on the discriminant analysis of the 16 KL features and the results of the discriminant analysis of the one KnY feature calculated from the 16 KL features. Including all 16 KL features in the KnY procedure did not appear to tailor the training set, since the test-set performance was maintained or slightly improved. The advantage of using the KnY feature space for this diagnostic classification problem was the ease of representation of the data. The separation and confidence limits illustrated in Fig. 8.4 demonstrate that the KnY space for the VT and MI diagnostic categories was well defined.

Chapter 9

Discussion and conclusions

This study explored whether individuals at risk for malignant ventricular arrhythmias can be noninvasively detected by means of BSPM during sinus rhythm. Measurements analyzed for each subject consisted of QRST-integral values calculated from 117 ECG leads. The reason for selecting QRST integrals was that they reflect the distribution of ventricular repolarization properties (disparity of which creates arrhythmogenic conditions). A statistical empirical approach was used—first to extract characteristic features from measured data and then to perform diagnostic classification based upon discriminant analysis which employed selected features. The results demonstrate that *multiple body-surface ECGs contain valuable information that, if properly extracted, can identify an arrhythmogenic substrate in the myocardium.* This discussion addresses the significant results of this study as they relate to the objectives stated in chapter 1.

9.1 Spatial reduction of QRST-integral maps

The orthogonal expansion was applied in data reduction of ECG signals by several investigators [46,105,119,151,184]. In this study, the Karhunen-Loeve (KL) tech-

nique has been applied to represent each subject's measurements by 16 coefficients, and the Kittler and Young (KnY) method of feature selection further reduced the number of characteristic features to only one or two. The results of this study provide further evidence that the orthogonal expansion method is very effective in reducing dimensionality of BSPM data, while maintaining features necessary for accurate reconstruction.

Different criteria are being used to measure the quality of BSPM data reconstruction. The percent trace [119] provides a useful estimate of the expected errors associated with reconstructions based on varying number of eigenvectors (from one to twenty); this is illustrated in Figures 4.1, 5.1, 8.1. In agreement with the previously reported results for spatial reductions [46,119,151], the percent trace for all three training sets investigated in this study plateaued at around nine to twelve eigenvectors, with a 99% trace reached at 16 eigenvectors. Sixteen eigenvectors were included in the subsequent analysis, in an attempt to maintain the diagnostic information that may be contained in the higher-order eigenvectors—even though they contribute only very small percentages to the covariance matrix. The previously reported complexity of the spatial patterns of QRST-integral maps for the patient groups investigated in this study [65,154] was a deciding factor for including 16 eigenvectors.

Consistent with the results of other investigators [46,119,151], the first three eigenvectors were dipolar by definition and the fourth to sixteenth were nondipolar. This is illustrated in Figures 4.2, 5.2 and 8.2. The root-mean-squared errors and the peak errors calculated for the reconstructed maps, based on the 16 basis

functions derived from the eigenvector analysis of the training sets, were similar to previously reported results [119,184]. The magnitudes of these two error measures may seem smaller in this study in comparison with others; this is because QRST-integral values (μVs), rather than instantaneous potentials (μV) [119,184], were reconstructed. The mean peak and root-mean-squared errors were similar across groups of the training sets and the test sets; however, the mean and variability of the relative errors were higher for the patient groups compared to the group of normal subjects (see Table 4.1). This reflects the larger signal energy contained in the maps of normals. Even though the reconstructed patterns were somewhat smoother than the original measured maps, they maintained the principal spatial features with respect to location of maxima and minima and the areas of negative and positive QRST-integral values on the torso—even for the worst cases in terms of reconstruction errors. The increased smoothness of the reconstructed, compared to originally measured, patterns has been previously noted; it is conceivable that the difference between the measured and reconstructed maps is largely noise and that data-reduction procedure serves as a spatial filter [151].

The reconstruction errors for the training sets were in general lower than those for either the test set or the treatment set; this was expected, since the basis functions were derived from the training sets. The reconstruction errors for the test set, based on the training-set eigenvectors (from both the two-group and three-group training sets), were only slightly different from those of the training sets. Therefore, the features derived from the training set represented the test-set maps with only a very small additional error as demonstrated by the confidence limits asso-

ciated with the three quantitative measures. More important in this study was to establish an optimal classification space based on these features and choose suitable decision-making techniques for classification; however, accurate representation of the measured data was an essential prerequisite [119]. The reconstruction errors for the test set and training sets justified the use of 16 KL features derived from the training set in the diagnostic classification procedures. (The noticeably larger errors arose in the reconstruction of the posttreatment data, as will be discussed below.)

9.2 Nondipolar content of QRST-integral maps

The percent nondipolar content of QRST-integral maps—determined from higher-order KL coefficients—was significantly lower for the normal subjects than for the patient groups. This finding was consistent with the literature [9,46,134], as was the finding that a large variability accompanies this index for the patient groups (Figures 4.5 and 5.4). The nondipolar content percentages found in this study substantiated the qualitative observation that the QRST-integral maps of the normal subjects have dipolar spatial patterns (Figure 4.4) compared to the more complex maps of most VT and MI patients (some patients did have low nondipolar content). There was no significant difference between the VT and MI patient groups for this measure, calculated from either the two-group or three-group eigenvectors; therefore, this measure differentiated poorly between the two patient groups. Gardner et al. [65,66] found that some patients with MI and no clinical arrhythmias had multipolar QRST-integral distributions, but that long-term follow up was required to determine whether this reflected heterogeneity of repolarization associated with

VT. Similar to this study, Gardner et al. [65] also found that some patients with VT had a low multipolar index for their QRST-integral map.

A classification procedure based on nondipolar content was not even attempted in this study, since only the normal group was found to be different from the two patient groups. The nondipolar-content results in this study, and the poor results obtained by Periyalwar [151] for separating VT and MI groups based on nondipolarity, suggest that this index may not be specific enough for adequately separating these two patient groups. Although the percent contribution of nondipolar features to the QRST-integral map could be the same for both VT and MI groups, the percent contribution of each individual spatial pattern to the lumped nondipolar-content measure might be quite different. De Ambroggi et al. [46] showed that two of nine eigenvectors derived from QRST-integral maps (third and sixth) had coefficients that were significantly different between normals and patients with long QT syndrome (LQTS); however, the nondipolar content was also significantly different between the two groups. These findings suggest that *both* dipolar and nondipolar features may be valuable for differentiating between the LQTS patients and normals. Therefore, the difficulty in separating the two patient groups in the present study on the basis of merely nondipolar content of the QRST-integral map was not unexpected. Patients with myocardial infarction have structural alterations (fibrous amongst viable tissue) in the myocardium that have been associated with disturbances of the smooth propagation of electrical excitation [68,95]. The question is whether disturbances that are not reflective of an arrhythmogenic state can be differentiated from disturbances associated with the electrophysiological substrate for

arrhythmias. This very ability to differentiate between the two patient groups was considered important for evaluating the feature space for classification purposes, and therefore, the index of nondipolarity was not pursued any further as a means of solving the diagnostic classification problem. Instead, further interrogation of the individual KL features was attempted.

9.3 Analysis based on features from the three-group training set

The discriminant analysis of both the KL and KnY feature spaces derived from the three-group training set confirmed that the normal group was relatively easy to classify, whereas the two patient groups were still difficult to separate. This observation was similar to that made for the nondipolar-content results; however, a very noticeable improvement in diagnostic performance indicated that there was a discernible difference between the VT and MI groups.

The three features that best differentiated between the constituent groups of the three-group training set corresponded to coefficients y_1 , y_2 and y_4 (see chapter 4). Features one and two were smooth and dipolar by definition, whereas feature four was nondipolar. Although these features are not physiological themselves, the implicit assumption is that they represent the underlying cardiac generators [9] and therefore help to explain the differences noted between groups. Feature one (Figure 4.2) was strikingly similar to the measured maps from the normal subjects (cf. Figure 4.4) and it was the dominant pattern contributing to the QRST-integral maps of normal subjects. The mean magnitude of the weighting coefficient y_1 was substan-

tially higher for the NC group compared to both the VT_{train} and MI_{train} groups. The domination of this pattern reflects the large span in amplitude between the principal maxima and minima for many of the normal subjects compared to the VT and MI patients (Figure 4.4). The lower signal energy in QRST-integral maps for patients compared to normals has been previously observed and has been described as reflecting more disorganized repolarization process throughout the myocardium for patients [65,88,129]. The MI maps had a larger span between the two principal extrema than the VT maps; this difference was quantified by the coefficient associated with feature one. While this feature differed between groups, there were exceptions within each group; this explains why this single feature was not adequate to quantify differences in the organization of ventricular repolarization properties and thus did not differentiate between groups.

Feature two was also dipolar and the mean magnitude of coefficient y_2 was again higher for the NC group than for the VT_{train} and MI_{train} groups, although the polarity was negative for the normals and the MI patients, and positive for the VT patients. The effect of this particular pattern on the total map pattern would be a negative distribution over the right shoulder area for the normals as illustrated in Figure 4.4—a pattern that has been previously noted as characteristic of normal QRST-integral maps [88,129].

The third pattern was nondipolar and corresponded to coefficient y_4 ; this pattern differed in magnitude among the three groups. The greatest difference was between the normal subjects and the VT patients; the MI patients lay in between. The polarity of coefficient y_4 was negative for all three groups, indicating that the

pattern would be added with reverse polarity to what is depicted in Figure 4.2. The combined effect of these three KL patterns on the patient maps was more difficult to determine from the original maps, since their map patterns were much more diverse than for normals. In general, these features did not capture enough diagnostic information to differentiate satisfactorily among the three diagnostic groups. The poor test-set performance provides evidence that the features y_1 , y_2 and y_4 (see section 4.3) were to some extent reflective of differences between the groups of this specific training set and were not necessarily characteristic of the differences among the three diagnostic categories (in particular between the VT and MI categories). The classification results based on the three KL features were similar to those reported by Periyalwar [151] for the nondipolar content. This was not surprising, since two of the three features chosen in the present study were in fact dipolar by definition.

Including only three features (to obtain number-of-features to number-of-subjects ratio 1:17) in the discriminant analysis was a conservative *a priori* choice based on the sample size; such conservatism was considered necessary to minimize tailoring. The error estimates presented in chapter 8 show (for the total patient set with $n=204$) that eight features could be included in the analysis without tailoring them to the training set. Since the KnY feature space incorporates all KL features in weighted combination [102], it provides an indication of whether there would be an improvement in the diagnostic performance with an increase in the number of KL features.

The results for the training set were improved for the discriminant analysis based on the KnY feature space compared to the classification based on the three

KL features. As well, the diagnostic performance for the test set that included only the two patient groups was better for the KnY space than for the KL space. However, the error bias for the patient group was 16%. Inclusion of more features in the discriminant analysis produced an improvement in diagnostic classification; however, the diagnostic performance remained quite low. The plots of the two KnY features for both the training set (Figure 4.6) and the test set (Figure 6.3) clearly demonstrate the overlap among the diagnostic groups, with the MI group wedged between the VT_{train} and NC groups. A closer examination revealed that the patients with inferior MI in the MI_{test} group were more frequently missclassified as normals than were the patients with anterior MI. There was a larger proportion of anterior-MI patients in the training set, and this might have influenced the result of classification by making the features more specific to the training set rather than to the diagnostic categories in general.

Since 24% of the VT_{test} group and 51% of the MI_{test} group were missclassified, it was concluded that the KnY feature space defined from the three-group training set did not adequately solve the classification problem. The three training-set groups represent a continuum from presumably low risk to high risk for ventricular arrhythmias, and therefore, an overlap was expected; however, a sensitivity of only 76% for the VT_{test} group was considered unacceptable. The valuable finding was that the KnY approach that utilized the combined 16 KL features led to better results than the approach based on selecting only three best features from the KL space. This provided further evidence that the difference among the diagnostic groups, if any, would be based on a complex combination of characteristics.

One possible way to improve classification results was to increase the number of patients in each diagnostic group; however, that would not eliminate the dominant effect on both the feature space and classification space of the homogeneous group of normal subjects. The patient groups were more heterogeneous than the NC group with respect to their QRST-integral map patterns, and the larger differences in the dominant KL patterns were between the normals and patients than between the two patient groups. Therefore, it was doubtful whether increasing the number of patients alone would mitigate the dominant effect of the normal group on both the feature and classification space. Although the KnY feature space did have overlap, further analysis of these results based on nonparametric approaches such as those recently presented by Kozmann et al. [106] may improve the diagnostic performance since assumptions regarding normality of data are not required in these approaches.

9.4 Analysis based on features from the two-group training set

Based on the results of three-group classification, focus of this study shifted on *defining a classification space that would distinguish best between the two patient groups*. In many cases it was obvious from visual inspection that the patient maps differed from those for the normals and the three-group results showed that these differences were quantifiable on the basis of nondipolar content, KL features and KnY features. The two patient groups, however, were difficult to differentiate by mere visual inspection, or by the quantitative measures derived from the three-group training set. In contrast to the three-group results, the diagnostic performance of

classification based on the KL features and a single KnY feature derived from the two-group training set demonstrated that *differences between the QRS-integral maps from the VT and MI groups could be quantified with a good degree of accuracy.* Based on objective criteria, characteristics from maps of patients who were not vulnerable to arrhythmias were distinguishable from maps of patients who were vulnerable to arrhythmia.

For the two-group training set, the KL feature space was comprised of two nondipolar features, y_4 and y_6 , and one dipolar feature, y_2 —a very interesting difference from the three-group analysis. Since feature one was not chosen, the signal-energy difference between VT_{train} and MI_{train} groups was not one of the major features distinguishing between the two groups. *The more complex patterns were chosen as being more sensitive to the differences between the two patient groups.*

The value of the three KL features chosen for characterizing the two patient groups lies, in part, in the consistency of diagnostic classification based on these features when an independent test set was classified. The magnitude and polarity of feature two (y_2) differed between the VT_{train} and MI_{train} groups; however, this difference was not maintained for the test set (for which the coefficient associated with feature two for the VT_{test} group moved toward the MI_{train} value and the coefficient for the MI_{test} group moved toward the VT_{train} value). In contrast, the differences observed between the VT_{train} and MI_{train} groups for features six (y_6) and four (y_4) were consistent for the test set. The VT_{train} and MI_{train} groups, as well as corresponding test groups, had minimal overlap for these two KL features. From these observations, the value of feature two as a measure of the differences between the

VT and MI diagnostic categories was in doubt.

The physiological significance of the KL patterns and their contributions to the total QRST-integral map pattern for each diagnostic group was difficult to interpret. The additive effect of the average of these three features (y_2, y_4, y_6) would result in a large negative value of QRST integral on the anterior torso for the VT group; however, this distribution was also prominent on QRST-integral maps of some of the MI patients. The large areas of negative QRST-integral values have been previously observed on the anterior chest of patients who were vulnerable to ventricular arrhythmias [46]. It should be noted, however, that some patients from the VT_{train} and VT_{test} groups did not exhibit this pattern (i.e., there was a large variability among VT patients). The significance of certain patterns, such as the figure-of-eight pattern that appears in features four and six, is difficult to interpret, but perhaps worthy of further investigation. The combined effects of these three spatial features would be a complex spatial pattern for both patient groups.

Only six patients from the VT_{train} group were misclassified when the classification was based on the three KL features derived from the two-group training set. However, the poorer diagnostic performance was noted for the MI_{train} group; in particular, there was a large percentage of false positives (31%), which indicates that not all salient information necessary for differentiating between the two patient groups was identified. The test-set results confirmed this observation. The overall diagnostic performance was only slightly lower for the test set ($DP = 75\%$) than for the training set ($DP = 78\%$), which was a substantial improvement over the three-group results; however, 25% of patients were still misclassified. An interest-

ing finding was that the diagnostic performance of classification deteriorated for the VT_{test} group and actually improved for the MI_{test} group. The inconsistent behaviour of feature two provided a partial explanation for these results.

The diagnostic performance based on the one KnY feature clearly indicates that KnY transformation of the 16 KL features into one KnY feature captures a large amount of the diagnostic information contained in the QRST-integral maps. The KnY transform yielded a single index that performed very well in classifying the two patient groups (only 11% of patients were missclassified in training set). Compared to the plot of nondipolar content for the two patient groups, the plot of the KnY coefficient for both the training and test sets (Figure 6.5) demonstrates the advantage of the KnY approach over the nondipolar-content measure for quantifying differences between the VT and MI groups.

There was only a small deterioration in diagnostic performance between the training set ($DP = 89\%$) and the test set ($DP = 85\%$); this indicates potential value of the KnY feature for classifying future observations [54]. The sensitivity and predictive value for both the VT_{train} group (92% and 87%, respectively) and VT_{test} group (84% and 86%, respectively) were comparable with corresponding values in the literature and the predictive value was either higher than or comparable with predictive values reported for other noninvasive techniques [36,174,187]. Also, there was no distinct trend for higher classification errors associated with location of MI as was the case with the three-group classification.

Thus, *the KnY feature space was the best for classification and it was easy to visualize graphically*, since only one KnY feature contained a large percentage of

the diagnostic information extracted from the QRST-integral maps of two patient groups. The KnY coefficient reflected the weighted contributions of all KL features in Figure 5.2. The diagnostic performance and the stability between training-set and test-set results (error bias = 4%) for the KnY space provided further evidence that more than a few patterns were necessary to reflect the complexity of the difference between the VT and MI categories. Many different characteristics have been associated with the QRST-integral maps of patients with VT (such as maximum-to-minimum span, negativity on the anterior torso and multipolar distributions); it appears that the KnY feature might have captured and quantified these characteristics very well.

The results from chapters 4, 5 and 6 demonstrated the merit of the approaches based on the KL expansion, but the issue of applicability of the features to classifying future observations was only partially addressed by analysis of the test set. These findings provide the basis for quantifying those differences in the QRST-integral maps that reflect vulnerability to VT, but still a question remains whether the training-set features are characteristic of the differences between the VT and MI diagnostic categories. Some of the errors in classification may have been due to different composition of groups, e.g. the different percentages of patients with inferior MI and anterior MI in the MI_{train} and MI_{test} groups, or the different percentages of patients with sustained VT induced via EPS in the VT_{train} and VT_{test} groups.

To shed more light onto this problem, a classification space based on all available patient data (total patient set) was developed. This pooled data set yielded a more stable set of features and discriminant functions for classifying the VT and MI

categories. This quantified the variability that may have resulted from the initial (perhaps biased) assignment of patients to training and test sets.

When the total patient set was used, all three KL features chosen from the stepwise discriminant analysis (y_6 , y_4 and y_{13}) were nondipolar by definition (Figure 8.2). The patterns for features four and six were similar to those for features four and six derived for the two-group training set. Feature thirteen was similar to feature six with two lateral maxima on the left anterior torso. It was interesting that feature two was not chosen amongst the best three features in this discriminant analysis. This lends support to the suspicion that this feature's inconsistent behaviour between the training and test sets was reflective of a specific difference found in the training set and not necessarily one of the prominent differences between the two diagnostic categories. The diagnostic performance for the KL space was similar to that of the original two-group training set ($DP = 79\%$) and was 10% less than for the classification based on the KnY space ($DP = 89\%$), supporting the finding that the three KL features do not contain enough diagnostic information from the QRST-integral maps. The bootstrap and cross-validation procedures applied to this larger sample showed that the choice of only three features was perhaps overly conservative, and that up to eight features could be included in the analysis without a tailoring effect (see Table 8.6). The best eight features chosen (six of them nondipolar) reflected both complex patterns and (feature one) the difference in signal energy between the groups. The average sensitivities were good for the VT groups (95% confidence limits, based on cross validation, were 85–97%) for the classification based on the eight KL features; they were similar to those obtained in the KnY space (see

Table 8.6). Including more than eight KL features in this analysis did not improve the diagnostic results, since the test set result deteriorated.

The diagnostic performance of classification based on the KnY feature for the total patient set was consistent with that in the original training set; the box plot of the KnY coefficient (Figure 8.4) illustrates *a feature space with clearly defined separation between the two diagnostic groups*. An important observation was that the variability of the KnY feature for the VT_{total} group was lower than that of the original VT_{train} and VT_{test} groups. This reassuring finding indicates an increase in stability of diagnostic performance with the increase in sample size. The features of QRST-integral maps remained more variable for the MI_{total} group than for the VT_{total} group; this was a consistent finding throughout this study for MI and VT groups (which was reflected in higher missclassification errors for MI groups). An explanation for this diversity may be the inclusion of different proportions of inferior and anterior MIs in MI_{train} and MI_{test} groups (the variability estimates provide evidence of this). The VT group, however, had also very diverse clinical characteristics, since patients with anterior and inferior MI were present as well as patients with other causes for VT. The variance estimates provide an indication of the worst-case results that may be caused by the variation among patients.

The 92% sensitivity of diagnostic classification for the VT category demonstrated that the KnY classification space was particularly well defined for the VT group. In spite of the higher variability for the MI group, 86% of the QRST-integral maps were classified correctly in the feature space derived from the total patient set. Not only was there a high sensitivity for identifying patients at risk for ventricular arrhyth-

mias, but there was also a relatively low error associated with falsely classifying MI patients that were not at risk for arrhythmias. Many classification approaches based on electrocardiographic features have been shown to be very sensitive in identifying high risk for VT; however, their limitation has been the error associated with identifying incorrectly those not at risk [36]. An effective classifier should yield both high sensitivity and high predictive value.

Few studies have reported error and variance estimates, making it difficult to compare the results of this study with others. Papers which report only the training-set results provide an overly optimistic estimate of future diagnostic performance [55]. The error and variance estimates based on the two bootstrap procedures and the cross-validation procedure, were quite stable for overall diagnostic performance and sensitivity percentages—in particular for the VT group. The cross-validation estimates were slightly higher than those obtained by the two bootstrap methods, but, no large discrepancies were observed. Efron [54] found that the bootstrap with replacement provided the best estimate of the true error in the general classification problem, but the sample size in his experiments was very small compared to this study. The consistency of the error estimates from all three methods indicated that they reflected reasonably well the expected error for future observations.

The cross-validated sensitivity for the VT_{test} group was 88%, with a 95% confidence limit of 82–94%, and the MI_{test} sensitivity was 80%, with a 95% confidence limit of 72–88% (the bootstrap estimates were only slightly lower). These results compare favorably with a model recently proposed by Vatterott et al. [187], which incorporates both clinical variables and variables that examine the terminal QRS

complex of the ECG. They reported cross-validated sensitivities of 91% for predicting programmed stimulation outcomes in a similar patient population as VT_{total} group. Their sensitivity value was within the 95% confidence limits for VT sensitivity found in the present study; however, similar to many other studies that analyze the late QRS complex, they reported sensitivities of 59% (as estimated by cross-validation method) for patients not at risk of arrhythmias. Therefore, based on their logistic model, a large number of patients that were not at risk for VT were misclassified. One possible explanation for this poor sensitivity of signal-averaged ECGs for patients not at risk of arrhythmias is that high-frequency components at the terminal QRS complex are also associated with abnormalities other than VT [38,39,115]. Further refinement of signal-averaged ECG technique, to better identify features that are more specific to vulnerability to ventricular arrhythmias, are presently being pursued [36,39]. Since the difficulty in distinguishing VT from MI was also noted in studies examining the QRST-integral maps [65,66,151], the results of this present study indicate that an improvement was made on previous work.

In general, the diagnostic performance achieved in the present study compares favorably with reported sensitivities for VT achieved by other noninvasive approaches (such as signal-averaged ECG and ambulatory monitoring). Sensitivities 66–100% have been reported [36] for correctly predicting inducibility of VT on the basis of temporal and frequency analysis of signal-averaged ECG. In instances where the reported sensitivity was high, the specificity values were low. The exception was a study by Nalos et al., employing three criteria from signal-averaged ECG, which reported sensitivity of 93% and specificity of 94% for 100 patients [140]. These re-

sults stand out from all other reported results; unfortunately, no variance or error estimates were given. Therefore, it is difficult to ascertain whether these results were reflective of the unique sample in the study or a true indication of diagnostic performance based on the three proposed measures.

Recently, the association between delayed depolarization as the substrate for arrhythmias and the low-level potentials at the terminal portion of QRS complex has been questioned [36,39,57]. The criticism is that delayed ventricular activation may only be one possible anatomical/electrophysiological substrate for the development of VT and that analysis of the complete cardiac cycle—including both depolarization and repolarization—may be a more fruitful approach [39].

The diagnostic performance of Holter monitoring as a method of predicting risk for ventricular arrhythmias has been generally lower than that for signal-averaged ECGs. Better results were achieved when Holter monitoring was combined with either signal-average ECGs or radionuclide ventriculography [183,201]—with best diagnostic performance of combined methods in the 80% range compared to results of programmed stimulation. In both of these studies, the specificity values were higher than the sensitivity values, but the number of patients with their arrhythmia induced by programmed stimulation was relatively small (12 in reference [201] and 22 in reference [183]). Holter monitoring has been extensively used; however, recent studies have provided evidence that the presence of or the suppression of ectopic activity do not necessarily affect the vulnerability to ventricular arrhythmias [22,176].

In comparison with other noninvasive methods, only a few studies [9,18,65,66,151]

have addressed the problem of predicting risk for ventricular arrhythmias on the basis of assessment of disparate ventricular repolarization properties. This study contributes supportive evidence that a comprehensive examination of these properties yields valuable diagnostic information and that quantitative measures that differentiate between diagnostic groups can be extracted. Compared to some of the more simplistic approaches, body-surface potential mapping provides the comprehensive spatial information about ventricular repolarization properties [88,117]. A recent study by Benhorin et al. [18] evaluated the ability of electrocardiographic measures aimed at quantifying repolarization characteristics from 12-lead ECGs to classify patients with LQTS from normal subjects. They used a bootstrap technique with 100 randomizations and estimated the 95% confidence intervals for their sensitivity percentage as 81.6–100% and specificity percentages as 93–98%, based on five predictor variables. However, these high values reflected the low error in classifying 315 normal subjects, while the error rate for classifying the LQTS patients was 9.3/37 or 25%. More complex analysis, such as applying the 2-D FFT to the QRST-integral maps, has shown poor diagnostic performance for classifying VT and MI patient groups [153]; large overlap in the peak Fourier spectrum was found between these patient groups and only a slight improvement was noted over the extrema-count method reported by Gardner et al. [65].

The present study provides evidence that local disparities in repolarization properties can be quantified and used to identify individuals at risk for ventricular arrhythmias. The approaches employed in this study to identify features associated with arrhythmogenesis enhance previously used methods in that they incorporate a

large number of features in the analysis. Each feature has a distinctive pattern and assessing the combination of features appears to be necessary to accurately reflect the complex differences between the VT and MI groups. The classification space is well defined for the KnY feature and for the eight KL features; in these spaces it appears possible to discriminate between the two patient groups. However, the difference between the same patient groups is not easily quantifiable in feature spaces of smaller dimension. This intuitively makes sense, considering the complex interactions of factors that contribute to the inhomogeneity of refractoriness in ventricular arrhythmias.

Classification of posttreatment group

The objective of the analysis of posttreatment QRST-integral maps was to evaluate whether the prediction of successful treatment—such as that currently made by the invasive EPS studies—could be also made from the feature space that differentiated QRST-integral maps of patients that were at risk of ventricular arrhythmias from those that were not. The posttreatment maps, however, had larger reconstruction errors indicating that the features derived from the training sets did not provide all the salient information for reconstructing the posttreatment distributions. All error measures (both their mean values and the standard deviations) were higher for the posttreatment maps compared to the corresponding training-set values for the same patients. The relative errors were considerably higher than the training-set values; this was partly caused by the lower signal energy in the posttreatment maps compared to the pretreatment maps (see Figure 7.3). Over 60% of the posttreatment

maps had lower maximum-to-minimum differences than their pretreatment maps. The reconstruction errors were similar between the PET and nPET subgroups of the posttreatment set, indicating that the result of programmed stimulation was not an influential factor.

Previous studies [84,112,190] show changes in the ECGs following quinidine therapy, and perhaps the features characteristic of these alterations in the QRST-integral map were unique for the posttreatment group and were not represented in the set of eigenvectors derived from the training sets. Qualitative observations of the pretreatment and posttreatment maps for patients in the VT_{train} group (Figure 7.2) showed that, for many patients, there were noticeable differences between these maps; some of the posttreatment maps (e.g. PET_2) appeared to become less complex than their pretreatment maps, while others (e.g. $nPET_1$) appeared to become more complex. The inability to accurately reconstruct these maps provided quantitative evidence that differences existed between pretreatment and posttreatment maps.

The nondipolar content of the pretreatment and posttreatment QRST-integral maps for the VT_{train} group showed a trend toward a higher percentage of nondipolar features for the posttreatment maps. The slightly higher means after treatment were reflective of a general increase in complexity of maps, in particular those for the nPET group. This result was not statistically significant, however, nor were the differences between the PET and nPET subgroups (although the nPET subgroup's nondipolar content, based on eigenvectors from both the two-group and three-group training sets, was slightly higher). The increase in the variability of the nondipolar content for the posttreatment maps indicated that alterations in the maps were not

consistent for all patients. This complexity has been previously reported, with pretreatment and posttreatment difference found between PET and nPET subgroups, based on simple quantitative assessment of map features [131,132]. The small sample size, in particular for the PET subgroup, and the large variability may partially explain why the differences were not significant.

The disturbing finding was that the direction of the trend was toward a more complex QRST-integral map after treatment with quinidine. This was particularly evident for the nPET subgroup, although the PET subgroup also demonstrated more variability for this measure. These results are in concurrence with other studies that reported the proarrhythmic effects of quinidine [45,161]; also, the recent cessation of the CAST trial [20,21,150] because of the ineffectiveness of some class I antiarrhythmic agents (flecainide and encainide) suggests that quinidine's antiarrhythmic effects cannot be taken for granted. Several mechanisms associated with development of ventricular arrhythmias have been demonstrated in the presence of quinidine, including syncope and delayed repolarization [160], early afterdepolarization and triggered activity [45], abnormal automaticity [161] and reentry [170]. Alterations in postrepolarization refractoriness and action potential prolongation may be reflected in the posttreatment maps that were either lower in amplitude or more complex than the pretreatment maps.

The discriminant functions employing the KL and the KnY features derived from all three training sets were applied to classify posttreatment VT patients; very few patients actually moved from their pretreatment classification, i.e., in most instances they remained classified into the VT category. Both the KL and KnY features de-

rived from the training sets for classifying maps of individuals with the high risk for ventricular arrhythmias (VT category) from maps of individuals with the low risk for ventricular arrhythmias (MI and NC categories) detected a change in clinical state due to the quinidine treatment in very few patients. This change in classification to the nonvulnerable group was slightly higher in most instances for the PET subgroup, but these differences were not statistically significant. The difficulty in interpretation was to ascertain what was at fault—whether it was an insensitivity of the feature space to actual changes in the electrophysiological substrate, or an error in EPS studies' prediction of efficacy of therapy. This latter point has been an intensely debated issue [23,30,77,157] and few studies have addressed efficacy of EPS studies in randomized clinical trials [130]. In light of recent findings on class I antiarrhythmic agents [14], the efficacy of these agents for arrhythmia suppression is suspect. It is possible that the qualitative difference observed between the pretreatment and posttreatment maps was the quinidine effect, which may be reflective of a suppression of the substrate for ventricular arrhythmias in the PET group in some cases, but not for all patients. Therefore, if the classification space developed for the training sets contained the features associated with the arrhythmogenic substrate, the posttreatment results showed that the therapy was ineffective for the majority of patients. The posttreatment classification based on the total group data shows that only 14% of the patients in VT_{train} group moved to the nonvulnerable category after treatment (for both the KL and KnY feature spaces). The PET and nPET designations, based on the EPS studies, were not reflected in these values.

Noninvasive methods for evaluating the effectiveness of therapy are being pur-

sued and thus programmed stimulation, although it has limitations of its own, has been used as the standard for comparison [22]. Initial studies show that time-domain analysis of late QRS complex is not effective; on the other hand, frequency-domain analysis of the entire cardiac cycle has shown promise for evaluating effectiveness of treatment [36]. Further inquiry, to establish that the variables derived from the QRST-integral maps could evaluate effectiveness of therapy, will be required. Long-term follow up of patients may be needed to ascertain the true value of these techniques.

9.5 Summary

The stochastic pattern recognition approaches employed in this study identified spatial features from the QRST-integral maps that classified patients vulnerable to ventricular arrhythmias from those that were not vulnerable to arrhythmias. From a diagnostic-performance perspective, the more sophisticated methods based on the KL expansion and the KnY transformation outperformed the simple measure of nondipolar content. The KnY transform in particular had very good error estimates associated with applying KnY features to classify future observations. The KL classification space required 8 features to yield similar results. These results are promising, and the predictive values indicate that the measures extracted from evaluating the QRST-integral maps provide additional information for risk stratification of VT vulnerability. Based on the underlying assumption that the QRST integral measured from the body surface reflects the distribution of primary repolarization properties, these results demonstrate that spatial disparity of primary repolariza-

tion properties can be quantified as features derived from the QRST-integral maps. Although such features are not physiological themselves, they do reflect complexity of cardiac electrical generator and accurately represent the measured map. This study, therefore, provides empirical statistical evidence supporting the link between alterations in primary repolarization properties measured from the QRST-integral maps, and myocardium at risk for ventricular arrhythmias. It also provides quantitative support for other clinical studies in which more complex QRST-integral distributions were associated with the ECG patterns recorded from individuals at high risk for arrhythmias.

The value of the feature space developed for evaluating the arrhythmogenic substrate of the ventricles in assessing effectiveness of quinidine therapy was difficult to establish at this stage. From this study, the effect of quinidine treatment—measured in terms of features derived from the QRST-integral maps—was that only a small proportion of the VT patients in either the PET or nPET subgroups moved to a nonvulnerable diagnostic category.

9.6 Conclusions

The aim of this study—to extract the diagnostic information contained in QRST-integral maps that is associated with high risk for ventricular arrhythmias—has been achieved.

The pattern space for the QRST-integral maps acquired from training sets consisting of patients vulnerable to ventricular arrhythmias and those not vulnerable to arrhythmias were reduced to a feature space by orthogonal expansion methods.

The errors associated with reconstructing the map patterns, based on 16 principal eigenvectors, were low and justified the development of a classification criterion.

Features derived from the KL expansion were used to define a classification space that best differentiated between diagnostic groups of the training sets. The best results were obtained when the homogeneous group of normal subjects was removed from the analysis. The classification space based on the KnY transformation showed that this approach extracted a large portion of the diagnostic information contained in the QRST-integral maps.

The test-set results and the error estimates provided a rigorous estimate of the error associated with applying these approaches to classifying future observations. In general, the sensitivity for the VT patients was higher than that for the MI patients; however, the low number of MI patients missclassified indicated that the classification space was specific.

Increasing the number of maps in the classification space resulted in a stable feature space as evaluated by the error and variance estimates. Eight KL features were required in the classification space to yield results similar to the KnY transformed space.

Finally, the classification space derived from the training sets did not corroborate the results of the EPS studies for predicting effective therapy from the posttreatment maps following quinidine administration. Only a very small percentage of the patients in the PET subgroup were classified into a group considered nonvulnerable to arrhythmia after treatment.

The diagnostic performance for classifying individuals at risk for ventricular ar-

rhythmias achieved in this study provides further evidence that noninvasive methods can recognize cardiac states that are associated with vulnerability to arrhythmias.

Appendix A

Training-set groups

The training set was used to derive BSPM features suitable for diagnostic classification of patients vulnerable to ventricular arrhythmias. This Appendix provides demographic information about all members of the training set; this information comprises gender, age, heart rate and diagnosis according to the New York Heart Association [144]. BSPM data for all subjects listed in this Appendix are stored on the study tape MT222. The entire training set consists of 153 subjects: 51 patients vulnerable to ventricular arrhythmias (VT_{train} group); 51 normal subjects (NC group); and 51 patients with myocardial infarction and no arrhythmias (MI_{train} group). Mean age and gender characteristics of these three training-set groups are in Table A.1.

The VT_{train} group (Table A.2) was selected from the patient population treated for VT with quinidine as their first antiarrhythmic agent, at the Foothills Hospital in Calgary. All patients who belonged to the VT_{train} group underwent thorough clinical examination, the results of which are presented in Appendix C. As seen in Table A.2, 75% of the VT_{train} group had a prior myocardial infarction. Of those that had an infarction, 45% were inferior MIs, 42% were anterior MIs, 8% had both

Table A.1: Age and gender of the training-set groups

	VT _{train}	NC	MI _{train}
Age			
mean [yrs]	59.6	45.9	57.2
SD	12.2	8.5	11.1
males	47	47	45
females	4	4	6

an anterior and inferior MI and 3% had a lateral MI with 3% a nonspecified MI.

The NC group (Table A.3) and MI_{train} group (Table A.4) were selected from a population that underwent BSPM recording at the Victoria General Hospital in Halifax. Subjects who were selected for the NC group had no evidence of heart disease on history, 12-lead ECG, physical examination and echocardiographic examination. Patients in the MI_{train} group all had suffered an MI and were, based on their clinical assessment, without arrhythmias; 55% of these patients had an anterior MI and 45% had an inferior MI.

Table A.2: Training set: VT_{train} group

#	Subject	Session	Sex	Age	HR	Diagnosis
1	AD01	457	M	61/02	55	VT / Syncope / inferior MI
2	JD02	273	M	41/06	70	VT / Syncope / VPBs
3	GD03	601	M	28/10	69	VT / Cardiomyopathy
4	DE04	429	M	49/03	81	VT / anterior MI
5	RF05	176	M	52/10	62	VT / anterior MI
6	RG06	37	M	79/11	78	VT / anterior MI
7	WK07	430	M	79/06	50	VT / Syncope
8	MK08	540	F	68/06	75	VT / anterior MI
9	RL09	592	M	56/09	58	VT / Atherosclerosis / inferior MI / anterior MI
10	WM10	397	M	68/01	81	VT / Rheumatoid Arthritis
11	DM11	408	M	50/08	86	VT / Hypertension / inferior MI
12	GR12	59	M	54/01	105	VT / anterior MI / lateral MI
13	DW13	327	F	50/10	94	VT
14	HZ14	55	M	55/00	62	VT / Syncope / Cardiomyopathy
15	NA51	510	M	68/09	63	VT / Atherosclerosis / anterior MI
16	SB52	350	M	62/01	53	VT / Atherosclerosis / Syncope / inferior MI
17	OB53	431	M	58/08	82	VT / Cardiomyopathy
18	RB54	15	M	44/07	58	VT / inferior MI
19	RB55	276	M	54/02	68	VT / VPBs / inferior MI
20	JC56	271	M	64/09	57	VT / anterior MI / inferior MI
21	JC57	67	M	56/08	51	VT / anterior MI
22	WC58	615	M	69/00	47	VT / Atherosclerosis / VF
23	WC59	235	M	60/05	56	VT / inferior MI
24	LC60	58	M	61/03	71	VT / anterior MI / lateral MI
25	ED61	241	M	67/07	74	VT / Syncope / inferior MI
26	RE62	260	M	78/06	53	VT
27	AF63	91	M	64/04	70	VT / Syncope / anterior MI / 1 st degree AV block
28	NF64	481	M	68/03	70	VT / inferior MI
29	DG65	134	M	74/07	69	VT / inferior MI / lateral MI
30	PH66	360	M	62/01	72	VT / inferior MI
31	WI67	452	M	56/03	87	VT / anterior MI / inferior MI
32	EI68	513	M	58/10	72	VT / anterior MI / lateral MI
33	FK69	590	M	70/11	66	VT / anterior MI / lateral MI
34	KL70	534	M	69/03	82	VT / inferior MI
35	MM71	497	F	64/03	81	VT
36	OM72	191	M	70/11	70	VT / VPBs / inferior MI
37	RM73	198	M	50/09	83	VT / inferior MI / lateral MI
38	AN74	224	M	25/06	77	VT / WPW
39	JP75	395	M	61/08	83	VT / anterior MI
40	JP76	373	M	49/11	63	VT / anterior MI / lateral MI
41	RP77	522	F	51/01	87	VT / lateral MI
42	SP78	272	M	73/03	76	VT / Syncope / VPBs
43	LR79	57	M	78/06	58	VT / inferior MI
44	WR80	200	M	54/05	72	VT / anterior MI / lateral MI
45	OR81	494	M	74/05	66	VT / inferior MI
46	AR82	460	M	68/02	70	VT / inferior MI / lateral MI
47	AS83	111	M	63/06	68	VT / anterior MI / lateral MI
48	WS84	61	M	52/01	64	VT / inferior MI
49	AT85	64	M	49/02	75	VT / anterior MI / lateral MI
50	ZT86	292	M	65/09	61	VT / MI
51	JW87	609	M	33/08	74	VT

Table A.3: Training set: NC group

#	Session	Sex	Age	HR	Diagnosis
52	1419	M	33/00	55	normal
53	2304	M	53/11	80	normal
54	95	M	41/00	52	normal
55	97	M	43/06	55	normal
56	1897	M	45/09	37	normal
57	2863	M	39/03	58	normal
58	1915	M	37/05	63	normal
59	110	F	63/01	67	normal
60	2302	M	43/06	72	normal
61	23	M	44/01	62	normal
62	34	M	64/03	63	normal
63	2888	M	57/07	64	normal
64	2559	M	46/07	60	normal
65	1895	M	48/11	49	normal
66	25	M	50/06	67	normal
67	1923	M	38/08	73	normal
68	774	M	45/09	58	normal
69	2868	M	36/03	44	normal
70	2869	F	51/04	60	normal
71	28	M	50/03	61	normal
72	24	M	48/05	50	normal
73	2560	M	44/02	60	normal
74	90	M	42/03	50	normal
75	2043	M	42/01	60	normal
76	2279	F	51/09	68	normal / Obesity
77	1865	M	38/09	71	normal
78	21	M	46/08	57	normal
79	89	M	46/11	60	normal
80	104	M	51/07	68	normal
81	108	F	69/05	57	normal
82	2294	M	43/06	64	normal
83	102	M	43/10	49	normal
84	93	M	44/09	57	normal
85	71	F	49/11	60	normal
86	56	M	40/08	58	normal
87	17	M	55/01	68	normal
88	18	M	49/02	64	normal
89	954	M	30/10	63	normal
90	69	M	39/02	60	normal
91	952	M	47/09	65	normal
92	2202	M	51/05	57	normal
93	2201	M	66/06	71	normal
94	1678	M	39/09	47	normal
95	1003	M	30/03	65	normal
96	94	M	40/04	67	normal
97	29	M	54/00	57	normal
98	794	M	51/03	59	normal
99	820	M	36/02	61	normal
100	2866	M	36/09	55	normal
101	808	M	43/08	65	normal
102	2912	M	52/07	71	normal

Table A.4: Training set: MI_{train} group

#	Session	Sex	Age	HR	Diagnosis
103	1401	M	67/02	77	anterior MI
104	1756	M	46/11	59	inferior MI
105	1443	M	75/08	76	anterior MI
106	1575	M	41/11	68	inferior MI*
107	1177	M	74/10	56	anterior MI
108	868	M	44/10	74	anterior MI
109	866	M	44/01	73	anterior MI*
110	1397	M	54/05	66	anterior MI
111	1310	M	56/11	72	inferior MI
112	1361	M	55/06	71	inferior MI
113	1422	M	57/09	85	inferior MI
114	1958	M	72/03	82	anterior MI*
115	1327	F	63/05	59	inferior MI
116	1562	M	44/08	89	anterior MI*
117	1548	M	58/00	77	anterior MI*
118	1232	M	44/04	64	inferior MI
119	1519	F	69/06	80	anterior MI*
120	1306	M	52/05	63	anterior MI
121	2530	M	41/02	56	inferior MI
122	1663	M	59/01	70	inferior MI
123	1550	M	66/02	58	anterior MI*
124	1374	M	44/08	63	inferior MI
125	2662	M	67/10	62	anterior MI (nonQ)
126	1683	F	61/07	94	inferior MI*
127	1372	M	71/11	53	anterior MI
128	1601	M	70/09	63	inferior MI
129	1599	M	58/11	85	inferior MI
130	1539	M	63/00	54	anterior MI*
131	1586	M	60/04	87	inferior MI
132	1297	M	25/02	74	anterior MI
133	1080	F	57/05	53	anterior MI
134	2529	M	62/01	46	inferior MI
135	814	M	50/11	65	anterior MI
136	870	M	49/00	71	anterior MI
137	1225	M	54/09	87	inferior MI*
138	1079	F	68/05	70	anterior MI
139	1146	M	65/09	46	anterior MI*
140	1637	F	58/07	77	inferior MI
141	1675	M	49/08	69	anterior MI
142	1522	M	76/05	44	inferior MI
143	1582	M	70/10	69	inferior MI
144	1509	M	65/00	61	anterior MI
145	2164	M	62/01	72	inferior MI
146	1369	M	69/05	62	inferior MI
147	1135	M	66/05	69	anterior MI
148	2008	M	55/10	55	anterior MI*
149	2018	M	55/02	63	inferior MI*
150	2065	M	36/02	50	anterior MI*
151	2139	M	45/00	72	anterior MI*
152	2494	M	60/11	83	inferior MI (nonQ)
153	2557	M	48/00	69	anterior MI (nonQ)

Appendix B

Test-set groups

The general applicability of the feature-selection and classification procedures derived for the training set (Appendix A) was tested on an independent test set. This Appendix provides demographic information about all members of the test set; this information comprises gender, age, heart rate and diagnosis according to the New York Heart Association [144]. BSPM data for all subjects listed in this Appendix are stored on the study tape MT222. The entire test set consists of 102 subjects: 51 patients with recurrent ventricular tachycardia (VT_{test} group) and 51 patients with MI without arrhythmia (MI_{test} group). Mean age and gender characteristics of these two test-set groups are in Table B.1.

The VT_{test} group (Table B.2) was selected from the patient population treated for VT at the Foothills Hospital in Calgary, using the same inclusion criteria as for the VT_{train} group (Appendices A and C). The VT_{test} group was not restricted to one drug therapy, which was in this case irrelevant since no posttreatment evaluation was performed on BSPM data of these patients. Of the 51 patients in the VT_{test} group, 29 (57%) had a sustained VT induced by EPS and 9 (18%) had a nonsustained VT induced by EPS. Of the 13 remaining patients 9 had documented VT on Holter

Table B.1: Age and gender of the test-set groups

	VT_{test}	MI_{test}
Age		
mean [yrs]	58.5	54.7
SD	14.9	8.9
males	47	47
females	4	4

monitoring, with one patient having syncope of unknown origin and 3 patients had SVT induced by programmed stimulation. Of the 51 VT_{test} patients, 65% had a myocardial infarction with the percentage distribution of the location of the MIs as follows: 36% inferior MIs, 39% anterior MIs, 15% both anterior and inferior MIs, 6% lateral MIs and 3% unspecified MIs. The mean left ventricular ejection fraction was $36.9 \pm 13.7\%$ for this group.

The MI_{test} group (Table B.3) was selected from the patients who underwent BSPM recording in Victoria General Hospital in Halifax, using the same criteria as for the patients of MI_{train} group (Appendix A). In summary, 27% of the MI patients had anterior MI, 59% had an inferior MI, 4% had both anterior and inferior MI, and the remaining 10% had nonspecified MI.

The patient groups from the training and test sets were combined for the stochastic validation. For the $VT_{rmtotal}$, 71 patients had a prior myocardial infarction: 41% had an inferior MI, 41% had an anterior MI, 11% had both anterior and inferior MIs, 4% had a lateral MI and 3% had an unspecified MI location. For the $MI_{rmtotal}$ group of patients without VT ($n=102$): 52% had an inferior MI, 41% had an anterior MI, 2% had both an anterior and inferior MI and 5% had an unspecified MI location.

Table B.2: Test set: VT_{test} group

#	Session	Sex	Age	HR	Diagnosis
1	158	M	58/00	54	VT / anterior MI / inferior MI
2	181	M	36/09	69	VT
3	197	M	68/10	88	VT / VPBs / anterior MI / lateral MI
4	388	M	63/06	102	VT / Atherosclerosis / inferior MI / Ventricular Failure
5	102	M	61/04	109	VT / inferior MI / anterior MI
6	136	M	19/08	50	VT
7	16	M	76/11	79	VT / lateral MI / LBBB
8	403	M	50/01	49	VT / Atherosclerosis / inferior MI / anterior MI
9	68	M	56/03	77	VT / Atherosclerosis
10	435	M	55/04	52	VT
11	412	M	70/09	55	VT / inferior MI / Obesity
12	179	M	49/00	55	VT / anterior MI / lateral MI / Mitral Regurgitation / LA enlargement
13	135	M	70/09	122	VT / Mitral Regurgitation
14	22	M	76/10	70	VT / anterior MI / Hypertension
15	160	M	49/04	89	VT / inferior MI / Atherosclerosis
16	413	F	74/07	76	VT / anterior MI / Ventricular aneurysm / inferior MI
17	184	M	61/02	69	SVT / VPBs / anterior MI
18	182	M	69/04	81	VT / anterior MI / VPBs
19	186	M	85/04	50	VT / VPBs / Atherosclerosis / inferior MI / anterior MI
20	13	M	26/04	65	VT
21	219	M	69/02	87	VT / Atherosclerosis / Hypertension / lateral MI
22	129	M	74/01	83	VT / VPBs / anterior MI
23	488	M	50/04	64	VT / inferior MI
24	254	M	31/05	57	VT
25	277	M	56/08	67	VT / inferior MI
26	159	M	80/09	40	VT / anterior MI / Hypertrophy
27	407	M	64/07	66	VT / inferior MI / LV Hypertrophy
28	137	M	59/06	76	VT / lateral MI / anterior MI / Atherosclerosis
29	368	M	53/01	88	VT / Atherosclerosis / Diabetes / inferior MI
30	36	M	76/11	75	VT / Valvular obstruction / MI
31	374	M	65/03	99	VT / anterior MI / Ventricular aneurysm
32	297	M	15/09	67	SVT / LV Hypertrophy / VPBs / Mitral valve prolapse
33	251	M	61/05	78	VT / Atherosclerosis / VPBs
34	255	M	55/08	78	VT / Atherosclerosis / anterior MI
35	458	M	64/11	70	VT
36	304	M	62/09	98	VT / LBBB / Atherosclerosis
37	113	M	44/05	66	VT
38	17	M	43/10	62	VT / anterior MI / Ventricular aneurysm / lateral MI
39	462	M	55/11	78	VT / anterior MI / lateral MI / Atherosclerosis
40	21	M	68/00	55	VT / lateral MI
41	311	M	55/09	91	VT / Cardiomyopathy
42	237	F	64/00	64	VT / Atherosclerosis / anterior MI / lateral MI
43	8	F	60/04	71	VT / inferior MI
44	171	M	60/08	76	VT / inferior MI
45	165	M	75/10	74	VT / Atherosclerosis / inferior MI
46	54	M	37/10	87	VT / Atrial fibrillation / Cardiomyopathy / Obesity
47	152	M	71/02	66	VT / Atherosclerosis / inferior MI
48	4	M	67/06	56	VT / Atherosclerosis
49	56	F	55/01	82	VT / VPBs
50	336	M	61/02	97	VT
51	381	M	62/11	55	SVT

Table B.3: Test set: MI_{test} group

#	Session	Sex	Age	HR	Diagnosis
52	1483	M	47/08	62	inferior MI
53	1318	M	60/06	56	anterior MI
54	2789	M	43/03	47	anterior MI (nonQ)
55	2773	F	67/09	68	MI / Obesity
56	2790	M	48/07	60	MI / Obesity
57	2781	M	48/11	54	anterior MI (nonQ)
58	1413	M	67/02	56	anterior MI
59	1803	M	54/00	67	inferior MI
60	2762	M	67/10	57	anterior MI (nonQ)
61	2250	M	57/07	79	anterior MI / inferior MI (nonQ)
62	1676	M	54/07	65	inferior MI
63	1716	M	49/08	57	inferior MI
64	1314	M	31/11	59	anterior MI
65	2277	F	68/06	94	anterior MI / Obesity
66	1308	M	54/01	47	anterior MI
67	1313	M	60/10	55	inferior MI
68	1605	M	48/01	40	inferior MI
69	1738	M	48/11	73	inferior MI
70	1415	M	50/06	57	inferior MI
71	2918	M	51/08	54	anterior MI / anterior MI
72	1161	M	64/03	77	inferior MI
73	1730	M	47/01	54	inferior MI
74	1785	M	54/03	77	inferior MI
75	2685	M	56/04	68	MI
76	3090	M	69/09	70	inferior MI
77	1809	M	61/11	70	inferior MI
78	2676	M	55/07	54	inferior MI (nonQ)
79	2799	M	52/08	63	anterior MI / inferior MI
80	1777	M	55/09	54	inferior MI
81	1345	M	51/10	74	anterior MI
82	1846	M	53/09	66	inferior MI
83	1360	M	68/00	80	anterior MI
84	2697	M	42/10	43	inferior MI (nonQ)
85	1797	M	47/01	51	inferior MI
86	1441	M	48/04	59	inferior MI
87	1773	M	51/04	68	inferior MI
88	1747	M	53/08	69	inferior MI
89	1446	M	53/04	62	inferior MI
90	1111	M	47/05	56	inferior MI
91	3109	M	54/09	60	anterior MI
92	1816	M	59/02	67	inferior MI
93	2782	M	52/02	52	inferior MI (nonQ)
94	2804	M	55/06	51	MI / Obesity
95	2150	M	48/09	48	inferior MI (nonQ)
96	1712	M	58/10	65	inferior MI
97	2172	F	67/06	55	anterior MI
98	1771	M	77/03	55	inferior MI
99	1107	M	69/07	88	anterior MI
100	1687	M	37/05	69	inferior MI
101	2753	F	54/10	66	MI
102	1829	M	62/07	75	inferior MI

Appendix C

Posttreatment group

The posttreatment group consisted of the members of the VT_{train} group, in their posttreatment state (i.e., after they were treated with an antiarrhythmic agent, quinidine). This Appendix contains tables of the individual clinical characteristics, summary data and statistical results for the comparisons between the two subgroups (referred to as PET and nPET subgroups) of the entire posttreatment group.

The electrophysiological studies (EPS) were used to support VT diagnosis and to determine the effectiveness of the antiarrhythmic therapy; all patients were free of any antiarrhythmic agent at the time of the pretreatment EPS. Cycle lengths and durations of the induced arrhythmia were measured. According to the results for the duration of the VT induced by the EPS, 84% of the members of this group had a sustained VT, while the remaining 16% had a nonsustained VT. Patients were monitored by an ambulatory device for at least 24 hours during their drug-free state and the records were analyzed to determine the frequency and duration of abnormal sequences. The baseline BSPM data were acquired during normal sinus rhythm in a drug-free state. Summary statistics for age, left ventricular ejection fraction, quinidine blood levels and VT cycle lengths induced in the drug-free state

for each group are in Table C.1.

An antiarrhythmic agent, quinidine, was administered to the patients who belonged to the VT_{train} group; the quinidine blood levels for the total sample are in Table C.1. On the same day, the EPS studies were repeated. On the basis of the posttreatment EPS, the 51 patients of the VT_{train} group were divided into two subgroups. The PET subgroup ($n=14$) consisted of those patients for whom quinidine was the predicted effective therapy (since the EPS studies could not induce VT after treatment). The nPET subgroup ($n=37$) consisted of those patients who remained susceptible to ventricular arrhythmias (since the VT remained inducible by programmed stimulation even after treatment). The criterion for determining predicted effective therapy (PET) was that no more than 4 VPDs occur in response to the programmed stimulation protocol.

A Bartlett test for homogeneity of variance between PET and nPET subgroups was performed on the four variables in Table C.1, using the SYSTAT (SYSTAT, Inc.) software package. The results of this analysis indicate that homogeneity of variance could be assumed and thus an independent t-test, using pooled variances, was performed between the two subgroups (see t-statistic for each variable in Table C.1. These results indicate that there were no statistically significant differences ($p \geq 0.05$) between PET and nPET subgroups for these four variables. Tables C.2 and C.3 provide, respectively, the individual characteristics for the PET and nPET subgroups. Comparisons between PET and nPET subgroups on several clinical pretreatment characteristics were performed; the results are presented in Tables C.4-C.6. There were no statistically significant differences ($p \geq 0.05$) between

Table C.1: Summary statistics for VT_{train} group and posttreatment subgroups

	Total	PET	nPET	t-stat	p
Age					
mean [yrs]	59.6	56.7	60.7	1.040	NS
SD	12.2	13.8	11.5		
LVEF					
mean [%]	38.1	44.1	35.8	1.676	NS
SD	16.1	19.4	14.3		
Quin					
mean [μ mole/l]	9.3	9.9	9.1	0.896	NS
SD	2.6	2.4	2.6		
EPS-RR					
mean [ms]	246.8	252.6	244.5	0.468	NS
SD	54.1	58.7	52.9		

t-stat = calculated t-statistic for independent test between the PET and nPET subgroups; p = probability value for t-statistic; NS = nonsignificant at the $p \leq 0.05$; LVEF = left ventricular ejection fraction at rest; Quin = blood serum levels of quinidine after treatment; EPS-RR = cycle length of ventricular tachycardia induced with programmed stimulation.

groups for the quantitative measures.

Since fibrillation was coded as a 1 for the VTS-RR, these data were ranked for nonparametric-comparison purposes. A Mann-Whitney U statistic was calculated for AFC, DFC and VTS-RR, using the SYSTAT statistical package. The summary results for the rank sum and U statistic for these three variables are in Table C.4. No statistically significant differences were found between the subgroups for these three variables.

A Bartlett test on the VPB, CPLT and GE3 data showed that the variances between subgroups could not be assumed to be homogeneous. The VPB data were transformed using a natural log transformation and the CPLT and GE3 data were transformed using a sine transformation. The Bartlett test was recalculated on

Table C.2: Clinical characteristics for PET subgroup

Subject	AFC	DFC	Pres	VTS-RR	HM	VPB	CPLT	GE3	PES
AD01	2	0	suo	-	-	156.8	4.7	0.25	ns
JD02	0	0	weak	350	sus	107	0	0	sus
GD03	0	3	sync	380	sus	68	2.5	.08	sus
DE04	2	2	nsscd	1	sus	69	3.2	.04	sus
RF05	0	0	nmscd	1	sus	.780	0	0	ns
RG06	0	0	suo	-	-	2.8	0	0	ns
WK07	1	0	sync	400	ns	1.7	0	0.8	ns
MK08	2	2	weak	400	sus	193.5	1.68	2	ns
RL09	2	2	weak	500	ns	89	2.5	.04	sus
WM10	0	0	weak	270	sus	3.4	.43	.08	sus
DM11	1	1	palps	400	sus	379	.82	.27	sus
GR12	4	4	sync	240	sus	1	0	.08	sus
DW13	1	1	weak	370	sus	100	16	69	ns
HZ14	0	1	sync	360	ns	7	0	0	sus

AFC = angina functional class; DFC = dyspnea functional class; PRES = presenting symptoms; VTS-RR = spontaneous ventricular tachycardia cycle length; HM = ventricular tachycardia duration from Holter monitoring; VPB = ventricular premature beats per hour; CPLT = ventricular couplets per hour; GE3 = runs of 3 or more consecutive ventricular beats per hour; PES = duration of induced ventricular arrhythmia in drug-free state from electrophysiological study; suo = syncope of unknown origin; sync = syncope; nmscd = near miss sudden cardiac death; palps = palpitations; ns = nonsustained; sus = sustained.

the transformed data and the results showed that homogeneity of variance could be assumed for all three sets of transformed data. An independent t-test was performed; the summary results are presented in Table C.5, together with the original mean and standard deviations for each variable.

All nominal variables (Table C.6) were calculated as a percent of each subgroup. Both the percentages and actual numbers are shown, because of the difference in n between the two subgroups. As illustrated, there were large percentage differences between subgroups on some of the variables. For example, a larger proportion of the nPET subgroup had ischemic heart disease, MI, near-miss sudden cardiac death and sustained VT induced during programmed stimulation. A larger proportion of subgroup PET had no dominant heart disease. Statistical comparisons between subgroups were not performed on these variables, because of the small sample size.

Table C.3: Clinical characteristics for nPET subgroup

Subject	AFC	DFC	Pres	VTS-RR	HM	VPB	CPLT	GE3	PES
NA51	1	1	nmscd	1	sus	390.7	0	0.5	sus
SB52	3	0	suo	-	-	.02	0	0	sus
OB53	0	0	suo	-	-	.2	0	0	sus
RB54	1	0	weak	430	sus	357	.04	0	sus
RB55	2	2	sync	215	ns	359	35	.08	sus
JC56	2	1	nmscd	1	sus	8	.22	.13	sus
JC57	3	0	weak	300	sus	554	0	0	sus
WC58	1	1	nmscd	1	sus	13	.04	0	sus
WC59	1	1	weak	320	sus	19	0	0	ns
LC60	0	0	nmscd	300	sus	7.3	.04	0	sus
ED61	0	0	suo	-	-	40	.04	0	sus
RE62	0	0	weak	380	ns	31.6	1.8	0	sus
AF63	3	2	sync	400	ns	44.3	.740	.17	sus
NF64	2	2	weak	300	sus	8	0	0	sus
DG65	0	2	sync	280	ns	56	.04	0	sus
PH66	0	0	weak	460	sus	238	24	2	sus
WI67	1	3	nmscd	1	sus	121	8.3	.2	sus
EI68	1	1	weak	250	sus	.9	0	0	sus
FK69	3	3	weak	400	sus	287.16	20.5	6	sus
KL70	1	1	weak	461	sus	341	10.67	0	sus
MM71	0	0	nmscd	1	sus	41.4	0	0	sus
OM72	1	4	sync	360	sus	135	5.3	1.03	sus
RM73	0	0	nmscd	1	sus	1.13	0	0	sus
AN74	0	0	weak	260	sus	10	0	0	sus
JP75	1	1	nmscd	350	sus	431	1	0	sus
JP76	0	0	suo	-	-	47	0	0	sus
RP77	0	0	nmscd	190	sus	0.04	0	0	sus
SP78	0	0	suo	-	-	56	130	4	sus
LR79	2	1	weak	320	sus	1050	19.1	1.4	sus
WR80	2	2	nmscd	1	sus	0.17	0	0	sus
OR81	3	3	nmscd	320	sus	112.8	.48	0	sus
AR82	2	1	nmscd	277	sus	37.49	0	0	sus
AS83	1	2	weak	280	sus	119	4.6	.35	sus
WS84	0	2	palps	315	sus	607	111	26	sus
AT85	2	1	nmscd	300	sus	48	.26	.04	sus
ZT86	4	2	palps	500	ns	56.26	2.5	1	sus
JW87	0	0	weak	320	sus	204	10	.29	sus

Table C.4: Summary statistics for ranked clinical data

Variable	PET		nPET		U-stat	PROB
	count	rank sum	count	rank sum		
VTS-RR	12	282.0	32	708.0	204	NS
AFC	14	350.5	37	975.5	246	NS
DFC	14	368.0	37	958.0	263	NS

U-stat = calculated Mann-Whitney U statistic; PROB = probability; NS = non-significant.

Table C.5: Summary statistics for transformed data

Variable		PET		nPET		t-stat	PROB
		\bar{X}	SD	\bar{X}	SD		
VPB	o	84.2	105.7	159.0	227.3		
	t	3.1	2.2	3.4	2.7	.477	NS
CPLT	o	2.274	4.2	10.4	27.95		
	t	.142	.497	-.002	.531	.908	NS
GE3	o	5.1	18.4	1.2	4.4		
	t	.122	.247	.125	.341	.975	NS

\bar{X} = mean; SD = standard deviation; t-stat = calculated t statistic; PROB = probability; NS = non significant; o = original data; t = transformed data.

Table C.6: Summary statistics for nominal clinical data

Variable	PET (<i>n</i> =14)	nPET (<i>n</i> =37)
HD1		
IHD	57.1 (8)	86.5 (32)
other	21.5 (3)	11.8 (4)
none	21.4 (3)	2.7(1)
HD2		
MI	57.1 (8)	81.1 (30)
WPW	7.14 (1)	2.7 (1)
none	35.7 (5)	16.2 (6)
PRES		
nmscd	7.1 (1)	35.1 (13)
sync	28.6 (4)	10.8 (4)
suo	14.3 (2)	13.5 (5)
other	50.0 (7)	40.6 (15)
HM		
ns	21.4 (3)	13.5 (5)
sus	64.3 (9)	73.0 (27)
nd	14.3 (2)	13.5 (5)
PES		
ns	42.9 (6)	2.7 (1)
sus	57.1 (8)	97.3 (36)
Sex		
M	85.7 (12)	94.6 (35)
F	14.3 (2)	5.4 (2)

()=actual values; HD1 = dominant heart disease; HD2= secondary heart disease; HD3 = tertiary heart disease; WPW = Wolff-Parkinson-White syndrome; IHD = ischemic heart disease; HM = Holter monitor results; PES = programmed stimulation results; M = male and F = female.

Appendix D

Interpolation procedure

To obtain the complete set of 117 body-surface potential values for each subject, the bad leads in the data files from individual subjects had to be interpolated. (The number of bad leads per map varied between none and twenty.) The approach proposed by Oostendorp, van Oosterom and Huiskamp [145] was used to perform a 3D interpolation of potentials on the body surface. The Dalhousie boundary-element model of the torso was used; the model has 352 nodes and 700 surface triangles [121]. A detailed description of the interpolation procedure which simultaneously minimizes Laplacian of electric potential at all nodes by solving the set of equations in a least-squares sense is elsewhere [141]. The program INTERPVAR2.f, written by J. Nenonen performed this procedure; interpolation results presented by Nenonen [141] were very good, even when large number of leads were removed. These results illustrate that the procedure can be applied to measured BSPM data with a variable number of randomly placed bad leads.

The ability of this procedure to interpolate bad leads in a measured data set was tested by comparing the interpolated values of leads with the actual measured data values. Three good leads (60, 80 and 106) from a normal subject were designated

Table D.1: Mean error, percent error and correlation coefficients of measured versus interpolated leads for a normal subject

Lead	$e_{\text{mean}}[\mu\text{V}]$	Perr[%]	CC
60	6.4	6.8	.999
80	3.4	3.6	.999
106	8.4	7.0	.998

e_{mean} = mean error; Perr = percent error; CC= correlation coefficient.

as bad leads and were interpolated by the program INTERPVAR2.f. The mean error (e_{mean}), percent error and correlation coefficient were calculated to compare the original data and the interpolated data for these three leads (Table D.1). The mean error was defined as the sum of the absolute differences between the measured and the interpolated values divided by the number of data points:

$$e_{\text{mean}} = \frac{\sum_{i=1}^{nsamp} |v_i - \hat{v}_i|}{nsamp} \quad (\text{D.1})$$

where e_{mean} is the mean error, v_i is the measured potential in lead i , \hat{v}_i is the interpolated potential in lead i , $nsamp$ is the number of samples interpolated for one lead. The percent error is a ratio of the mean error with respect to the mean signal magnitude:

$$Perr = \frac{e_{\text{mean}}}{\frac{\sum_{i=1}^{nsamp} |v_i|}{nsamp}} \times 100, \quad (\text{D.2})$$

where Perr is the percent error. The correlation coefficients were calculated using a NAG library routine G02BAF (Numerical Algorithms Group, Inc.).

Applying this interpolation procedure to the BSPM data for two randomly selected VT patients illustrates the fit of the interpolated ECG complexes to the surrounding leads (Figures D.1 and D.2).

TAPE: 222 FILE: 19 CODE: 0

540 1988/06/27 09.56.45

diagnosis 3.1.53 2.53 23.2 seconds skipped(*10): seconds averaged(*10)

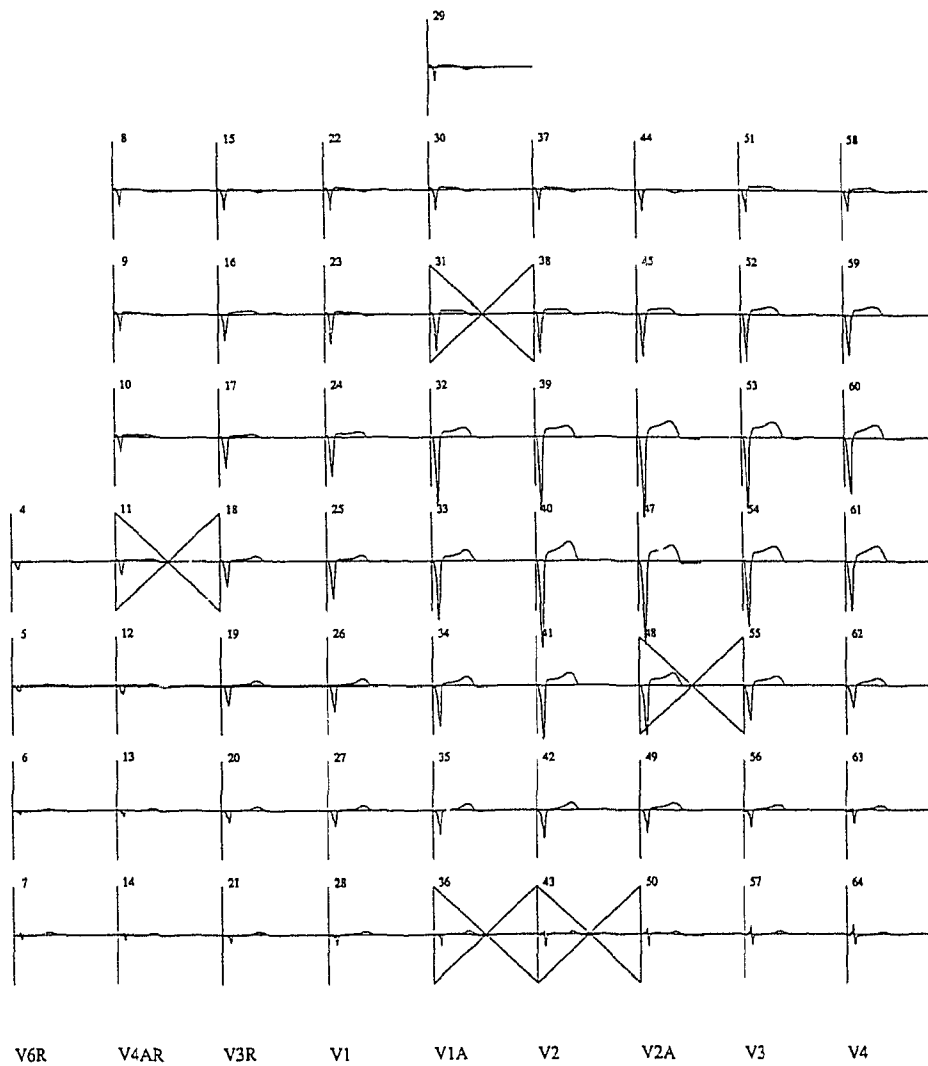


Figure D.1: Interpolation results for a VT patient. Plot of 61 signal-averaged ECGs following the 3D interpolation procedure. The x indicates leads that were judged as bad before the interpolation.

TAPE: 222 FILE: 12 CODE: 0

176 1985/05/22 13 26 34

diagnosis 3 1.5.3 2.5.3 1.1 2.3.2 1.1.3 seconds skipped(*10) seconds averaged(*10)

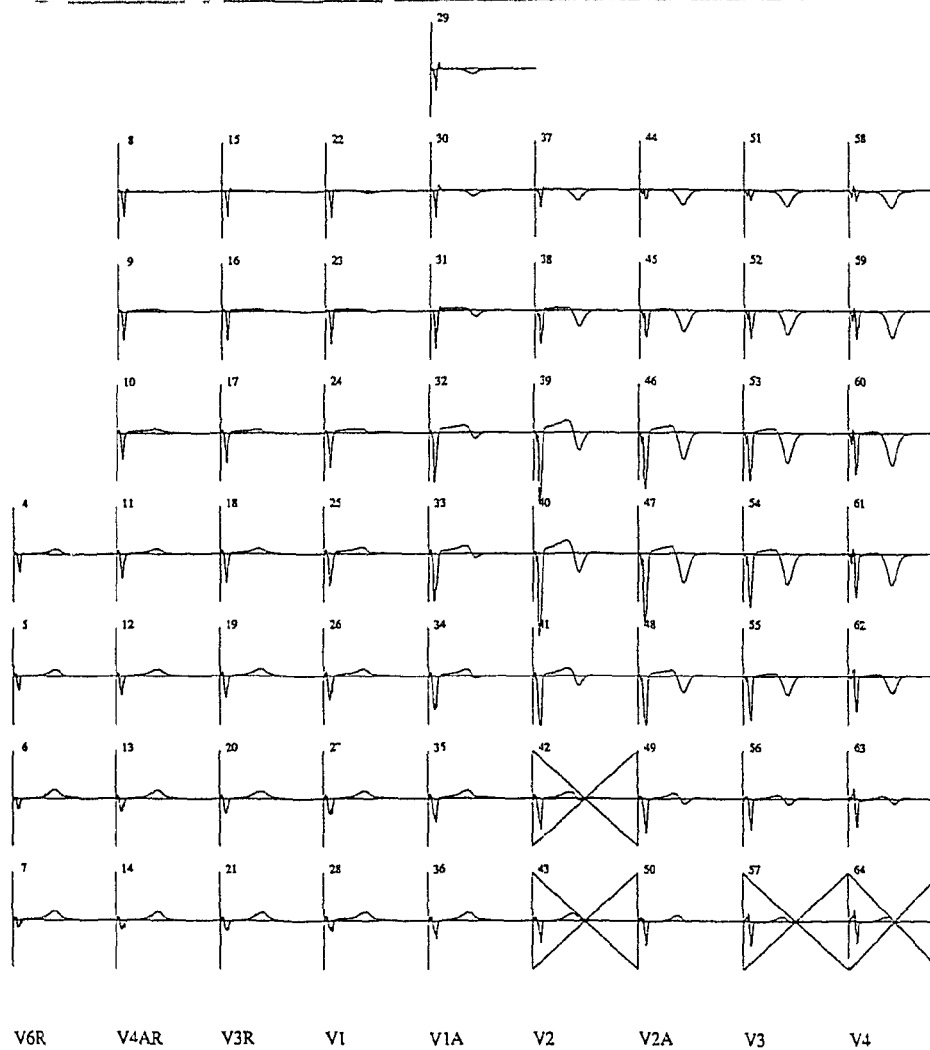


Figure D.2: Interpolation results for a VT patient.

This 3D interpolation was performed on the designated bad leads for all data files in this study. These data files were then stored as 352 values (corresponding to potential values at 352 nodes of the three-dimensional torso model) for each time instant. This allowed easy retrieval of the 117 lead potentials for use in the data-reduction analysis.

Bibliography

- [1] J.A. Abildskov. Adrenergic effects on the QT interval of the electrocardiogram. *Am Heart J*, 92:210–216, 1976.
- [2] J.A. Abildskov, M.J. Burgess, I. Ershler, R.L. Lux, and P. Urie. Electrocardiographic recognition of states at high risk of ventricular arrhythmias. *Circulation*, 58 (suppl II):II–153, 1978.
- [3] J.A. Abildskov, M.J. Burgess, R.L. Lux, R.F. Wyatt, and G.M. Vincent. The expression of normal ventricular repolarization in the body surface distribution of T potentials. *Circulation*, 54:901–905, 1976.
- [4] J.A. Abildskov, M.J. Burgess, K. Millar, R.F. Wyatt, and G. Baule. The primary T wave – a new electrocardiographic waveform. *Am Heart J*, 81:242–249, 1971.
- [5] J.A. Abildskov, M.J. Burgess, P. Urie, R.L. Lux, and R.F. Wyatt. The unidentified information content of the electrocardiogram. *Circ Res*, 40:3–7, 1977.
- [6] J.A. Abildskov, A.K. Evans, R.L. Lux, and M.J. Burgess. Direct evidence relating QRST deflection area and ventricular recovery properties. *Circulation*, 60:100–110, 1979.
- [7] J.A. Abildskov, A.K. Evans, R.L. Lux, and M.J. Burgess. Ventricular repolarization properties and QRST area in cardiac electrograms. *Am J Physiol*, 239:227–231, 1981.
- [8] J.A. Abildskov, L.S. Green, A.K. Evans, and R.L. Lux. The QRST deflection area of electrograms during global alterations of ventricular repolarization. *J Electrocardiol*, 15:103–108, 1982.
- [9] J.A. Abildskov, L.S. Green, and R.L. Lux. Detection of disparate ventricular repolarization by means of the body surface electrocardiogram. In D.P. Zipes and J. Jalife, editors, *Cardiac electrophysiology and arrhythmias*, pages 495–499, Grune & Stratton, New York, 1985.
- [10] J.A. Abildskov, P.M. Urie, R.L. Lux, M.J. Burgess, and R.F. Wyatt. Body surface distribution of QRST area. *Adv Cardiol*, 21:59–64, 1978.

- [11] D.R. Adam, J.M. Smith, S. Akselrod, S. Nyberg, A.O. Powell, and R.J. Cohen. Fluctuations in T-wave morphology and susceptibility to ventricular fibrillation. *J Electrocardiol*, 17:209–218, 1984.
- [12] H.C. Andrews. *Mathematical techniques in pattern recognition*. Wiley-Interscience, Toronto, Ontario, 1972.
- [13] C. Anzelevitch, S. Sicouri, S.H. Litovsky, A. Lukas, S.C. Krishnan, J.M. Di Diego, G.A. Gintant, and D-W. Liu. Heterogeneity within the ventricular wall: Electrophysiology and pharmacology of epicardial, endocardial, and m cells. *Circ Res*, 69:1427–1449, 1991.
- [14] J.R. Balsler, P.B. Bennett, L.M. Hondeghem, and D.M. Roden. Suppression of time-dependent outward current in guinea pig ventricular myocytes: Actions of quinidine and amiodarone. *Circ Res*, 69:519–529, 1991.
- [15] R.C. Barr, T.C. Pilkington, J.P. Boineau, and M.S. Spach. Determining surface potentials from current dipoles, with application to electrocardiography. *IEEE Trans Biomed Eng*, BME-13:88–92, 1966.
- [16] R.C. Barr, M. Ramsey, and M.S. Spach. Relating epicardial to body surface potential distributions by means of transfer coefficients based on geometry measurements. *IEEE Trans Biomed Eng*, BME-24:156–166, 1977.
- [17] R.C. Barr, M.S. Spach, and G.S. Herman-Giddens. Selection of the number and positions of measuring locations for electrocardiography. *IEEE Trans Biomed Eng*, BME-18:125–138, 1971.
- [18] J. Benhorin, M. Merri, M. Alberti, E. Locati, A.J. Moss, W.J. Hall, and L. Cui. Long QT syndrome: New electrocardiographic characteristics. *Circulation*, 82:521–527, 1990.
- [19] R.M. Berne and M.N. Levy. *Physiology*. C.V. Mosby Company, St. Louis, second edition, 1988.
- [20] J.T. Bigger Jr. Cardiac electrophysiological effects of moricizine hydrochloride. *Am J Cardiol*, 65 (suppl D):15D–20D, 1990.
- [21] J.T. Bigger Jr. Implications of the Cardiac Arrhythmia Suppression Trial for antiarrhythmic drug treatment. *Am J Cardiol*, 65 (suppl D):3D–10D, 1990.
- [22] J.T. Bigger Jr. Pharmacologic prevention of sudden cardiac death: role of antiarrhythmic drugs. In J.B. Kostis and M. Sanders, editors, *The prevention of sudden cardiac death*, pages 155–195, Wiley-Liss, New York, 1990.
- [23] J.T. Bigger Jr. and J. Coromilas. Identification of patients at risk for arrhythmic death: role of Holter ECG recording. In M.E. Josephson, editor, *Sudden cardiac death*, pages 131–143, F.A. Davis, Philadelphia, 1985.

- [24] S.S. Bloomfield, D.W. Romhilt, T-C. Chou, and N.O. Fowler. Natural history of cardiac arrhythmias and their prevention with quinidine in patients with acute coronary insufficiency. *Circulation*, 47:967-973, 1973.
- [25] S.S. Bloomfield, D.W. Romhilt, T-C. Chou, and N.O. Fowler. Quinidine for prophylaxis of arrhythmias in acute myocardial infarction. *New Eng J Med*, 285:979-986, 1971.
- [26] H. Boudoulas, P. Geleris, S.F. Schaal, C.V. Leier, and R.P. Levis. Comparison between electrophysiological studies and ambulatory monitoring in patients with syncope. *J Electrocardiol*, 16:91-96, 1983.
- [27] L. Breiman and D. Freedman. How many variables should be entered into a regression equation? *J Am Stat Assoc*, 78:131-136, 1983.
- [28] G. Breithardt, M. Borggrefe, U. Karbenn, R. Abendroth, H. Yeh, and L. Seipel. Prevalence of late potentials in patients with and without ventricular tachycardia: Correlation with angiographic findings. *Am J Cardiol*, 49:1932-1937, 1982.
- [29] G. Breithardt, M.E. Cain, N. El-Sherif, N.C. Flowers, V. Hombach, M. Janse, M.B. Simson, and G. Steinbeck. Standards for analysis of ventricular late potentials using high-resolution or signal-averaged electrocardiography: A statement by a task force committee of the European Society of Cardiology, the American Heart Association, and the American College of Cardiology. *JACC*, 17:999-1006, 1991.
- [30] P. Brugada and H.J.J. Wellens. Programmed electrical stimulation of the human heart: General principles. In M.E. Josephson and H.J.J. Wellens, editors, *Tachycardias: Mechanisms, diagnosis, treatment*, pages 61-89, Lea & Febiger, Philadelphia, 1984.
- [31] M. J. Burgess. Relation of ventricular repolarization to electrocardiographic T wave-form and arrhythmia vulnerability. *Am J Physiol*, 236:H391-H402, 1979.
- [32] M.J. Burgess. Ventricular repolarization and electrocardiographic T wave form and arrhythmia vulnerability. In M.N. Levy and M. Vassalle, editors, *Excitation and neural control of the heart*, pages 181-202, American Physiological Society, Bethesda, Md, 1982.
- [33] M.J. Burgess, L.S. Green, K. Millar, R.F. Wyatt, and J.A. Abildskov. The sequence of normal ventricular recovery. *Am Heart J*, 84:660-669, 1972.
- [34] M.J. Burgess, K. Harumi, and J.A. Abildskov. Application of a theoretic model to experimentally induced T-wave abnormalities. *Circulation*, 34:669-678, 1966.

- [35] M.J. Burgess and R.L. Lux. Physiologic basis of the T wave. In R.C. Schlant and J.W. Hurst, editors, *Advances in electrocardiography*, pages 327–337, Grune & Stratton, New York, 1976.
- [36] M.E. Cain, H.D. Ambos, R.M. Arthur, and B.D. Lindsay. Signal-averaged electrocardiography: Methods of analysis and clinical impact. In W.W. Parmley and K. Chatterjee, editors, *Cardiology Vol. 1, Physiology, pharmacology, diagnosis*, Lippincott, Philadelphia, 1992. Chapter 72.
- [37] M.E. Cain, H.D. Ambos, and B.D. Lindsay. Fast Fourier transform analysis of signal averaged electrocardiograms in the management of patients with or prone to ventricular tachycardia or fibrillation. In P. Brugada and H.J.J. Wellens, editors, *Cardiac arrhythmias: Where to go from here?*, pages 311–328, Futura Publishing Co, Mount Kisco, NY, 1987.
- [38] M.E. Cain, H.D. Ambos, J. Markham, A.E. Fischer, and B.E. Sobel. Quantification of differences in frequency content of signal averaged electrocardiograms in patients with compared to those without sustained ventricular tachycardia. *Am J Cardiol*, 55:1500–1505, 1985.
- [39] M.E. Cain, H.D. Ambos, J. Markham, B.D. Lindsay, and R.M. Arthur. Diagnostic implications of spectral and temporal analysis of the entire cardiac cycle in patients with ventricular tachycardia. *Circulation*, 83:1637–1648, 1991.
- [40] M.E. Cain, H.D. Ambos, F.X. Witkowski, and B.E. Sobel. Fast Fourier transform analysis of signal-averaged electrocardiograms for identification of patients prone to sustained ventricular tachycardia. *Circulation*, 69:711–720, 1984.
- [41] R. Cardinal, P. Savard, D.L. Carson, J.B. Perry, and P. Pagé. Mapping of ventricular tachycardia induced by programmed stimulation in canine preparations of myocardial infarction. *Circulation*, 70:136–148, 1984.
- [42] N.H. Carliner, W.G. Crouthamel, M.L. Fisher, M.A. Mugmon, D.L. Vassar, P.K. Narang, and G.D. Plotnick. Quinidine therapy in hospitalized patients with ventricular arrhythmias. *Am Heart J*, 98:708–715, 1979.
- [43] P.B. Corr, B. Pitt, B.H. Natelson, D.J. Reis, K.I. Shine, and J.E. Skinner. Task force 3: Sudden cardiac death. Neural-chemical interactions. *Circulation*, 76(suppl I):I-208–I-214, 1987.
- [44] P.B. Corr, K.A. Yamada, and F.X. Witkowski. Mechanisms controlling cardiac autonomic function and their relation to arrhythmogenesis. In H.A. Fozzard, E. Huber, R.B. Jennings, A.M. Katz, and H.E. Morgan, editors, *The heart and cardiovascular system: Scientific foundations, Vol. 2*, pages 1343–1403, Raven Press, New York, 1986.

- [45] J.M. Davidenko, L. Cohen, R. Goodrow, and C. Antzelevitch. Quinidine-induced action potential prolongation, early afterdepolarizations, and triggered activity in canine purkinje fibers. Effects of stimulation rate, potassium, and magnesium. *Circulation*, 79:674–686, 1989.
- [46] L. De Ambroggi, T. Berton, E. Locati, M. Stramba-Badiale, and P.J. Schwartz. Mapping of body surface potentials in patients with the idiopathic long QT syndrome. *Circulation*, 74:1334–1345, 1986.
- [47] L. De Ambroggi, E. Musso, and B. Taccardi. Body-surface mapping. In *Comprehensive electrocardiology*, Vol. 2, page , Pergamon Press, New York, 1989.
- [48] L. De Ambroggi, B. Taccardi, and E. Macchi. Body-surface maps of heart potentials: Tentative localization of pre-excited areas in forty-two Wolff-Parkinson-White patients. *Circulation*, 54:251–263, 1976.
- [49] P. Denes, P. Santarelli, R.G. Hauser, and E.F. Uretz. Quantitative analysis of the high-frequency components of the terminal portion of the body-surface QRS in normal subjects and in patients with ventricular tachycardia. *Circulation*, 67:1129–1138, 1983.
- [50] E. Downar, I.D. Parson, L.L. Mickleborough, D.A. Cameron, L.C. Yao, and M.B. Waxman. On-line epicardial mapping of intraoperative ventricular arrhythmias; Initial clinical experience. *JACC*, 4:703–714, 1984.
- [51] H.J. Duff, W.M. Lester, and M. Rahmberg. Amiloride: Antiarrhythmic and electrophysiological activity in the dog. *Circulation*, 78:1469–1477, 1988.
- [52] Jr. D.W. Benson, R. Sterba, J.J. Gallagher, A. Walston II, and M.S. Spach. Localization of the site of ventricular preexcitation with body surface maps in patients with Wolff-Parkinson-White syndrome. *Circulation*, 65:1259–1268, 1982.
- [53] B. Efron. The 1977 Rietz Lecture: Bootstrap methods: another look at the jackknife. *Ann Stat*, 7:1–26, 1979.
- [54] B. Efron. Estimating the error rate of a prediction rule: improvement on cross-validation. *J Am Stat Assoc*, 78:316–331, 1983.
- [55] B. Efron. *The jackknife, the bootstrap and other resampling plans*. Society for Industrial and Applied Mathematics, Philadelphia, 1982.
- [56] N. El-Sherif. Electrophysiology of ventricular arrhythmias in myocardial infarction. In N. El-Sherif and C.V. Ramana Reddy, editors, *The pathophysiology and pharmacotherapy of myocardial infarction*, pages 187–240, Academic Press, Orlando, Fl, 1986.
- [57] T. Engel. High frequency electrocardiography: diagnosis of arrhythmia risk. *Am Heart J*, 118:1302–1316, 1989.

- [58] A.K. Evans, R.L. Lux, M.J. Burgess, R.F. Wyatt, and J.A. Abildskov. Redundancy reduction for improved display and analysis of body surface potential maps. II Temporal compression. *Circ Res*, 49:197-203, 1981.
- [59] G. Faugère, P. Savard, R.A. Nadeau, D. Derome, M. Shenasa, P.L. Page, and R. Guardo. Characterization of the spatial distribution of late ventricular potentials by body surface mapping in patients with ventricular tachycardia. *Circulation*, 74:1323-1333, 1986.
- [60] G. Fontaine, G. Guiraudon, and R. Frank. Mechanism of ventricular tachycardia with and without associated chronic myocardial ischemia: Surgical treatment based on epicardial mapping. In O.S. Narula, editor, *Innovations in diagnosis and management of cardiac arrhythmias*, pages 516-545, Williams & Wilkins, Baltimore, Md, 1979.
- [61] G. Fontaine, G. Guiraudon, R. Frank, Y. Tereau, A. Pavie, C. Cabrol, G. Chomette, and Y. Grosgeat. Surgical management of ventricular tachycardia not related to myocardial ischemia. In M.E. Josephson and H.J.J. Wellens, editors, *Tachycardias: Mechanisms, diagnosis, treatment*, pages 451-474, Lea & Febiger, Philadelphia, 1984.
- [62] G.E. Forsythe, M.A. Malcolm, and C.B. Moler. *Computer methods for Mathematical Computations*. Prentice-Hall Inc., Englewood Cliffs, NJ, 1977.
- [63] H.A. Fozzard and M.F. Arnsdorf. Cardiac electrophysiology. In H.A. Fozzard, E. Huber, R.B. Jennings, A.M. Katz, and H.E. Morgan, editors, *The heart and cardiovascular system: Scientific foundations*, pages 63-99, Raven Press, New York, 1991.
- [64] K.J. Friday and R. Lazzara. Mechanisms and management of myocardial infarction arrhythmias. In N. El-Sherif and C.V. Ramana Reddy, editors, *The pathophysiology and pharmacotherapy of myocardial infarction*, pages 269-316, Academic Press, Orlando, Fl, 1986.
- [65] M.J. Gardner, T.J. Montague, C.S. Armstrong, B.M. Horáček, and E.R. Smith. Vulnerability to ventricular arrhythmia: Assessment by mapping of body surface potential. *Circulation*, 73:684-692, 1986.
- [66] M.J. Gardner, T.J. Montague, B.M. Horáček, D.A. Cameron, C.S. Flemington, and E.R. Smith. Vulnerability to ventricular dysrhythmia: Assessment by body-surface mapping. *Circulation*, 64 (suppl IV):IV-328, 1981.
- [67] M.J. Gardner, S.S. Periyalwar, S.T. Nugent, and B.M. Horacek. Assessment of vulnerability to ventricular arrhythmia by mathematical analysis of body surface potential maps. *Clin Invest Med*, 13 (suppl C):C-49, 1990.
- [68] P.I. Gardner, P.C. Ursell, J.J. Fenoglio Jr., and A.L. Wit. Electrophysiologic and anatomic basis for fractionated electrograms recorded from healed myocardial infarcts. *Circulation*, 73:596-611, 1985.

- [69] P.I. Gardner, P.C. Ursell, T.D. Pham, J.J. Fenoglio Jr., and A.L. Wit. Experimental chronic ventricular tachycardia: anatomic and electrophysiologic substrates. In M.E. Josephson and H.J.J. Wellens, editors, *Tachycardias: Mechanisms, diagnosis, treatment*, pages 29–60, Lea & Febiger, Philadelphia, 1984.
- [70] J.J. Gerbrands. On the relationship between SVD, KLT and PCA. *Pattern Recognition*, 14:375–381, 1981.
- [71] D.B. Geselowitz. Use of time integrals of the ECG to solve the inverse problem. *IEEE Trans Biomed Eng*, BME-32:73–75, 1985.
- [72] D.B. Geselowitz. The ventricular gradient revisited: Relation to the area under the action potential. *IEEE Trans Biomed Eng*, BME-30:76–77, 1983.
- [73] R.F. Gilmore and D.P. Zipes. Abnormal automaticity and related phenomenon. In H.A. Fozzard, E. Huber, R.B. Jennings, A.M. Katz, and H.E. Morgan, editors, *The heart and cardiovascular system: Scientific foundations*, pages 1239–1257, Raven Press, New York, 1986.
- [74] J.A. Gomes, R. Mehra, P. Barreca, N. El-Sherif, R. Hariman, and R. Holtzman. Quantitative analysis of the high-frequency components of the signal-averaged QRS complex in patients with acute myocardial infarction: a prospective study. *Circulation*, 72:105–111, 1985.
- [75] J.A. Gomes, S.L. Winters, D. Stewart, S. Horowitz, M. Milner, and P. Barreca. A new noninvasive index to predict sustained ventricular tachycardia and sudden death in the first year after myocardial infarction: Based on signal averaged electrocardiogram, radionuclide ejection fraction and Holter monitoring. *J Am Coll Cardiol*, 10:349–357, 1987.
- [76] R.C. Gonzalez and P. Wintz. *Digital image processing*. Addison-Wesley, Reading, Ma, 1977.
- [77] C. Gottlieb and M.E. Josephson. The preference of programmed stimulation-guided therapy for sustained ventricular arrhythmias. In P. Brugada and H.J.J. Wellens, editors, *Cardiac arrhythmias: Where to go from here?*, pages 421–434, Futura Publishing Co, Mount Kisco, NY, 1987.
- [78] L.S. Green, R.L. Lux, and C.W. Haws. Detection and location of coronary artery disease with body surface mapping in patients with normal electrocardiograms. *Circulation*, 76:1290–1297, 1987.
- [79] L.S. Green, R.L. Lux, D. Stilli, C.W. Haws, and B. Taccardi. Fine detail in body surface potential maps: accuracy of maps using a limited lead array and spatial and temporal data representation. *J Electrocardiol*, 20:21–26, 1987.
- [80] The Multicenter Post-Infarction Research Group. Risk stratification and survival after myocardial infarction. *New Eng J Med*, 309:331–336, 1983.

- [81] J. Han, J. De Traglia, D. Millet, and G.K. Moe. Incidence of ectopic beats as a function of basic rate in the ventricle. *Am Heart J*, 72:632–639, 1966.
- [82] J. Han, P. Garcia de Jalon, and G.K. Moe. Fibrillation threshold of premature ventricular responses. *Circ Res*, 18:18–25, 1966.
- [83] J. Han and B.S. Goel. Electrophysiologic precursors of ventricular tachyarrhythmias. *Arch Intern Med*, 129:749–755, 1972.
- [84] B.F. Hoffman, M.R. Rosen, and A.L. Wit. Electrophysiology and pharmacology of cardiac arrhythmias: VII. Cardiac effects of quinidine and procaine amide. *Am Heart J*, 89:804–808, 1975.
- [85] S. Holmberg and H. Bergman. Prophylactic quinidine treatment in myocardial infarction. *Acta Med Scand*, 181:297–304, 1967.
- [86] B.M. Horáček, R.G. deBoer, L.J. Leon, and T.J. Montague. Human epicardial potential distributions computed from body-surface-available data. In K. Yamada, K. Harumi, and T. Musha, editors, *Advances in body surface potential mapping*, pages 47–54, University of Nagoya Press, Nagoya, 1983.
- [87] B.M. Horáček, W.J. Eifler, H. Gewirtz, R.K. Helppi, P.B. Macaulay, J.D. Sherwood, E.R. Smith, J. Tiberghien, and P.M. Rautaharju. An automated system for body-surface potential mapping. In H.G. Ostrow and K.L. Ripley, editors, *Computers in Cardiology*, pages 399–407, IEEE Computer Soc., Long Beach, CA, 1977.
- [88] B.M. Horáček, T.J. Montague, M.J. Gardner, and E.R. Smith. Arrhythmogenic conditions. In D.M. Mirvis, editor, *Body surface electrocardiographic mapping*, pages 167–189, Kluwer Academic Publishers, Boston, MA, 1988.
- [89] B.M. Horáček, E.R. Smith, D.A. Cameron, H. Gewirtz, and P.M. Rautaharju. Iso-integral analysis of body surface potential maps. In P.W. Macfarlane, editor, *Progress in electrocardiology*, pages 22–27, Pitman Medical, Kent, 1979.
- [90] B.M. Horáček, E.R. Smith, D.A. Cameron, H. Gewirtz, and P.M. Rautaharju. Iso-integral analysis of body-surface potential maps. In P.W. Macfarlane, editor, *Progress in Electrocardiology*, pages 22–27, Pitman Medical, Kent, 1979.
- [91] L.N. Horowitz, S.R. Spielman, A.M. Greenspan, and C.R. Webb. The selection of antiarrhythmic regimes by electrophysiologic studies: techniques and results. In M.E. Josephson, editor, *Sudden cardiac death*, pages 187–197, F.A. Davis, Philadelphia, 1985.
- [92] R.E. Ideker, A.S.L. Tang, and J.P. Daubert. On the trail of ventricular tachycardia or the adventure of the unspeckled band. *PACE*, 11:650–655, 1988.
- [93] SAS Institute Inc. *SAS user's guide: statistics*. SAS Institute Inc., Carey, NC, 1982.

- [94] T. Iwa and T. Magara. Correlation between localization of accessory conduction pathway and body surface maps in the Wolff-Parkinson-White syndrome. *Jpn Circ J*, 45:1192-1198, 1981.
- [95] M.J. Janse. Reentrant arrhythmias. In H.A. Fozzard, E. Huber, R.B. Jennings, A.M. Katz, and H.E. Morgan, editors, *The heart and cardiovascular system: Scientific foundations*, pages 2055-2094, Raven Press, New York, 1991.
- [96] D.T. Jones, W.J. Kostuk, and R.W. Gunton. Prophylactic quinidine for the prevention of arrhythmias after acute myocardial infarction. *Am J Cardiol*, 33:655-660, 1974.
- [97] M.E. Josephson, F.E. Marchlinski, A.E. Buxton, H.L. Waxman, J.U. Doherty, M.G. Kienzle, and R. Falcone. Electrophysiologic basis for sustained ventricular tachycardia: Role of reentry. In M.E. Josephson and H.J.J. Wellens, editors, *Tachycardias: Mechanisms, diagnosis, treatment*, pages 305-324, Lea & Febiger, Philadelphia, 1984.
- [98] M.E. Josephson and S.F. Seides. *Clinical cardiac electrophysiology: Techniques and interpretations*. Lea & Febiger, Philadelphia, 1979.
- [99] M.E. Josephson, M.B. Simson, A.H. Harken, L.N. Horowitz, and R.A. Falcone. The incidence and clinical significance of epicardial late potentials in patients with recurrent sustained ventricular tachycardia and coronary artery disease. *Circulation*, 66:1199-1204, 1982.
- [100] W.B. Kannel and D.L. McGee. Epidemiology of sudden death: Insight from the Framingham study. In M.E. Josephson, editor, *Sudden cardiac death*, pages 93-105, F.A. Davis, Philadelphia, 1985.
- [101] H.L. Kennedy, M.K. Sprague, K.K. Shriver, S.C. Smith, J.A. Whitlock, and R.D. Wiens. Real-time ambulatory electrocardiography - clinical evaluation of cardiac arrhythmias by Aegis system. *J Electrocardiol*, 20:247-254, 1987.
- [102] J. Kittler and P.C. Young. A new approach to feature selection based on the Karhunen-Loeve expansion. *Pattern Recognition*, 5:335-352, 1973.
- [103] G.J. Klein, R.E. Ideker, W.M. Smith, L.A. Harrison, J. Kasell, A.G. Wallace, and J.J. Gallagher. Epicardial mapping of the onset of ventricular tachycardia initiated by programmed stimulation in the canine heart with chronic infarction. *Circulation*, 60:1375-1384, 1979.
- [104] C. Klersy, M. Vigano, L. Martinelli, M. Chimienti, and J.A. Salerno. Body surface map and location of origin of ventricular tachycardia. Comparison with epicardial map. In R.Th. van Dam and A. van Oosterom, editors, *Electrocardiographic body surface mapping*, pages 105-108, Martinus Nijhoff, Dordrecht, 1986.

- [105] F. Kornreich, P.M. Rautaharju, J.W. Warren, B.M. Horáček, and M. Dramaix. Effective extraction of diagnostic ECG waveform information using orthonormal basis functions derived from body surface potential maps. *J Electrocardiol*, 18:341–350, 1985.
- [106] G. Kozmann, L.S. Green, and R.L. Lux. Nonparametric identification of discriminative information in body surface maps. *IEEE Trans Biomed Eng*, BME-38:1061–1068, 1991.
- [107] I. Kubota, R.L. Lux, M.J. Burgess, and J.A. Abildskov. Relation of cardiac surface QRST distributions to ventricular fibrillation threshold in dogs. *Circulation*, 78:171–177, 1988.
- [108] D.L. Kuchar, C.W. Thornburn, and N.L. Samuel. Prediction of serious arrhythmic events after myocardial infarction: signal averaged electrocardiograms, holter monitoring and radionuclide ventriculography. *J Am Coll Cardiol*, 9:531–538, 1987.
- [109] C.-S. Kuo, C.P. Reddy, K. Munakata, and B. Surawicz. Arrhythmias dependent predominantly on dispersion of repolarization. In D.P. Zipes and J. Jalife, editors, *Cardiac electrophysiology and arrhythmias*, pages 277–286, Grune & Stratton, New York, 1985.
- [110] P.A. Lachenbruch. *Discriminant analysis*. Hafner Press, New York, 1975.
- [111] D. Lacroix, P. Savard, M. Shenasa, W. Kaltenbrunner, R. Cardinal, P. Pagé, D. Joly, D. Derome, and R. Nadeau. Spatial domain analysis of late ventricular potentials: Intraoperative and thoracic correlations. *Circ Res*, 55–68, 1990.
- [112] B. Lecocq, P. Jaillon, V. Lecocq, A. Ferry, M.E. Gardin, C. Jarreau, R. Leroyer, M. Pays, and F.X. Jarreau. Clinical pharmacology of hydroxy-3(S)-dihydroquinidine in healthy volunteers following oral administration. *J Cardiovasc Pharmacol*, 12:445–450, 1988.
- [113] W. Lengfelder, J. Senges, I. Rizos, R. Jauernig, J. Brachmann, K. von Ohlshausen, and W. Kubler. Intraindividual comparison of intravenous ajmaline and quinidine in patients with sustained tachycardia: effects on normal myocardium and on arrhythmia characteristics. *Eur Heart J*, 6:312–322, 1985.
- [114] J. Liebman, Y. Rudy, P. Diaz, C.W. Thomas, and R. Plonsey. The spectrum of right bundle branch block as manifested in electrocardiographic body surface potential maps. *J Electrocardiol*, 17:329–346, 1984.
- [115] B.D. Lindsay, J. Markham, K.B. Schechtman, H.D. Ambos, and M.E. Cain. Identification of patients with sustained ventricular tachycardia by frequency analysis of signal-averaged electrocardiograms despite the presence of bundle branch block. *Circulation*, 77:122–130, 1988.

- [116] R.L. Lux. Electrocardiographic body surface potential mapping. *CRC Crit Rev Biomed Eng*, 8:253-279, 1982.
- [117] R.L. Lux. Mapping techniques. In P.W. Macfarlane and T.D.V. Lawrie, editors, *Comprehensive electrocardiology*, pages 1001-1014, Pergamon Press, Oxford, 1989.
- [118] R.L. Lux, M.J. Burgess, R.F. Wyatt, A.K. Evans, G.M. Vincent, and J.A. Abildskov. Clinically practical lead systems for improved electrocardiography: Comparison with precordial grids and conventional lead systems. *Circulation*, 59:356-363, 1979.
- [119] R.L. Lux, A.K. Evans, M.J. Burgess, R.F. Wyatt, and J.A. Abildskov. Redundancy reduction for improved display and analysis of body surface potential maps. I. Spatial compression. *Circ Res* 49:186-196, 1981.
- [120] R.L. Lux, C.R. Smith, R.F. Wyatt, and J.A. Abildskov. Limited lead selection for estimation of body surface potential maps in electrocardiography. *IEEE Trans Biomed Eng*, BME-25:270-276, 1978.
- [121] R. S. MacLeod. *Percutaneous transluminal coronary angioplasty as a model of cardiac ischemia: Clinical and modelling studies*. PhD thesis, Dalhousie University, 1990.
- [122] R.S. MacLeod, B.K. Hoyt, J.D. Sherwood, P.J. MacInnis, R.V. Potter, and B.M. Horáček. A body surface mapping unit for recording during coronary angioplasty. In *Proc 10th Ann Conf IEEE Eng Med Biol Soc*, pages 97-98, New Orleans, 1988.
- [123] F.E. Marchlinski, A.E. Buxton, H.L. Waxman, and M.E. Josephson. Role of electrophysiologic study in predicting sudden death following myocardial infarction. In M.E. Josephson and H.J.J. Wellens, editors, *Tachycardias: Mechanisms, diagnosis, treatment*, pages 497-505, Lea & Febiger, Philadelphia, 1984.
- [124] J.W. Mason and R.A. Winkle. Accuracy of the ventricular tachycardia-induction study for predicting long-term efficacy and inefficacy of antiarrhythmic drugs. *New Eng J Med*, 303:1073-1077, 1980.
- [125] D.D. McPherson, B.M. Horáček, D.J. Sutherland, C.S. Armstrong, C.A. Spencer, and T.J. Montague. Exercise electrocardiographic mapping in normal subjects. *J Electrocardiol*, 18:351-360, 1985.
- [126] M. Merri, J. Benhorin, M. Alberti, E. Locati, and A.J. Moss. Electrocardiographic quantification of ventricular repolarization. *Circulation*, 80:1301-1308, 1989.

- [127] B.J. Messinger-Rapport and Y. Rudy. The inverse problem in electrocardiography: A model study of the effects of geometry and conductivity parameters on the reconstruction of epicardial potentials. *IEEE Trans Biomed Eng*, EME-33:667-676, 1986.
- [128] J.M. Miller, F.E. Marchlinski, A.E. Buxton, and M.E. Josephson. Relationship between the 12-lead electrocardiogram during ventricular tachycardia and endocardial site of origin in patients with coronary artery disease. *Circulation*, 77:759-766, 1988.
- [129] D.M. Mirvis. Body surface distribution of repolarization forces during acute myocardial infarction. I. Isopotential and isoarea mapping. *Circulation*, 62:878-887, 1980.
- [130] L.B. Mitchell, H.J. Duff, D.E. Manyari, and D.G. Wyse. A randomized clinical trial of the noninvasive and invasive approaches to drug therapy of ventricular tachycardia. *New Eng J Med*, 317:1681-1687, 1987.
- [131] L.B. Mitchell, C. Hubley-Kozey, E.R. Smith, D.G. Wyse, H.J. Duff, A.M. Gillis, and B.M. Horáček. Electrocardiographic body surface mapping in patients with ventricular tachycardia: Assessment of utility in the identification of effective pharmacologic therapy. *Circulation*, 1992. (accepted).
- [132] L.B. Mitchell, C. Kozey, E.R. Smith, D.G. Wyse, H.J. Duff, A.M. Gillis, and B.M. Horáček. Body surface potential mapping: Identification of effective drug therapy in patients with ventricular tachycardia. *Circulation*, 84 (suppl II):II-597, 1991.
- [133] D.M. Monro, P.J. Bones, R. De L. Stanbridge, and R.W. Jones. Comparison of epicardial and body surface ECG potentials in man. *Cardiovasc Res*, 20:201-207, 1986.
- [134] D.M. Monro, R.A.L. Guardo, P.J. Bourdillon, and J. Tinker. A Fourier technique for simultaneous electrocardiographic surface mapping. *Cardiovasc Res*, 8:688-700, 1974.
- [135] T.J. Montague, E.R. Smith, D.A. Cameron, P.M. Rautaharju, G.A. Klassen, C.S. Flemington, and B.M. Horáček. Isointegral analysis of body surface maps: Surface distribution and temporal variability in normal subjects. *Circulation*, 63:1166-1172, 1981.
- [136] T.J. Montague, E.R. Smith, D.E. Johnstone, C.A. Spencer, L.D. Lalonde, R.M. Bessaudo, M.J. Gardner, R.N. Anderson, and B.M. Horáček. Temporal evaluation of body surface map patterns following acute inferior myocardial infarction. *J Electrocardiol*, 17:319-328, 1984.
- [137] J. Morganroth and L.N. Horowitz. Incidence of proarrhythmic effects from quinidine in the outpatient treatment of benign or potentially lethal ventricular arrhythmias. *Am J Cardiol*, 56:585-587, 1985.

- [138] E. Musso, D. Stilli, E. Macchi, G. Regoliosi, C. Brambilla, P. Fancescon, M. Bo, A. Rolli, G. Botti, and B. Taccardi. Surface maps in left bundle branch block uncomplicated or complicated by myocardial infarction, left ventricular hypertrophy or myocardial ischemia. *J Electrocardiol*, 20:1–20, 1987.
- [139] K. Nademanee, W.G. Stevenson, J.N. Weiss, V.B. Frame, M.G. Antimisiaris, T. Suithichaiyakul, and C.M. Pruitt. Frequency-dependent effects of quinidine on the ventricular action potential and qrs duration in humans. *Circulation*, 81:790–796, 1990.
- [140] P.C. Nalos, E. S. Gang, W.J. Mandel, M.L. Ladenheim, Y. Lass, and T. Peter. The signal-averaged electrocardiogram as a screening test for inducibility of sustained ventricular tachycardia in high risk patients: A prospective study. *J Am Coll Cardiol*, 9:539–548, 1987.
- [141] J. Nenonen. *Biomagnetic functional localization*. PhD thesis, Helsinki University of Technology, 1990.
- [142] T.L. Nichols and D.M. Mirvis. Frequency content of the electrocardiogram spatial features and effects of myocardial infarction. *J Electrocardiol*, 18:185–194, 1985.
- [143] B.J. Northover. A comparison of the effects of bethanidine, meobentine or quinidine on the electrical activity of rat hearts in vivo and in vitro. *Br J Pharmacol*, 84:755–763, 1984.
- [144] The Criterion Committee of the New York Heart Association. *Nomenclature and criterion for diagnosis of diseases of the heart and great vessels*. Little, Brown and Co., Boston, Ma, 1979.
- [145] T.F. Oostendorp, A. van Oosterom, and G. Huiskamp. Interpolation on a triangulated 3D surface. *J Comp Physics*, 80:331–343, 1989.
- [146] A.V. Oppenheim and R.W. Schaffer. *Digital signal processing*. Prentice-Hall Inc., Englewood Cliffs, NJ, 1975.
- [147] E. Page. Cardiac gap junctions. In H.A. Fozzard, E. Huber, R.B. Jennings, A.M. Katz, and H.E. Morgan, editors, *The heart and cardiovascular system: Scientific foundations*, pages 1003–1048, Raven Press, New York, 1991.
- [148] P.L. Pagé, R. Cardinal, P. Savard, and M. Shenasa. Sinus rhythm mapping in a canine model of ventricular tachycardia. *PACE*, 11:632–644, 1988.
- [149] I.P. Panidis and J. Morganroth. Initiating events of sudden cardiac death. In M.E. Josephson, editor, *Sudden cardiac death*, pages 81–92, F.A. Davis, Philadelphia, 1985.
- [150] Y. Pawitan and A. Hallstrom. Statistical interim monitoring of the Cardiac Arrhythmia Suppression Trial. *Statistics in Medicine*, 9:1081–1090, 1990.

- [151] S.S. Periyalwar. *Two-dimensional Fourier and eigenvector analysis of body surface potential maps*. Master's thesis, Technical University of Nova Scotia, Halifax, N.S., Canada, 1987.
- [152] S.S. Periyalwar, S.T. Nugent, and B.M. Horáček. Classification of QRST integral maps using the Kittler-Young transform. Unpublished manuscript.
- [153] S.S. Periyalwar, S.T. Nugent, and B.M. Horáček. Two-dimensional Fourier spectrum of QRST integral maps in classification of patients prone to ventricular arrhythmia. *IEEE Trans Biomed Eng*, BME-36:493-496, 1989.
- [154] H. Pham-Huy, R.M. Gulrajani, F.A. Roberge, R.A. Nadeau, G.E. Mailloux, and P. Savard. A comparative evaluation of three different approaches for detecting body surface isopotential map abnormalities in patients with myocardial infarction. *J Electrocardiol*, 14:43-56, 1981.
- [155] R. Plonsey. A contemporary view of the ventricular gradient of Wilson. *J Electrocardiol*, 12:337-341, 1979.
- [156] P.J. Podrid. The role of antiarrhythmic drugs in prevention of sudden cardiac death. In M.E. Josephson, editor, *Sudden cardiac death*, pages 265-286, F.A. Davis, Philadelphia, 1985.
- [157] E.N. Prystowsky, J.J. Heger, E.A. Lloyd, and D.P. Zipes. Clinical electrophysiology of ventricular tachycardia. In D.P. Zipes, editor, *Cardiology clinics*, pages 253-273, W.B. Saunders, Philadelphia, 1983.
- [158] W.L. Quan and Y. Rudy. Unidirectional block and reentry of cardiac excitation: a model study. *Circ Res*, 66:367-382, 1990.
- [159] E.W. Reynolds and C.R. van der Ark. An experimental study on the origin of T-waves based on determinations of effective refractory period from epicardial and endocardial aspects of the ventricle. *Circ Res*, 8:943-949, 1959.
- [160] E.W. Reynolds and C.R. van der Ark. Quinidine syncope and the delayed repolarization syndromes. *Mod Concepts Cardiovasc Dis*, 45:117-122, 1976.
- [161] D.M. Roden and B.F. Hoffman. Action potential prolongation and induction of abnormal automaticity by low quinidine concentrations in canine Purkinje fibers. Relationship to potassium and cycle length. *Circ Res*, 56:857-867, 1985.
- [162] D.M. Roden, R.L. Woosley, and D. Bostick. Quinidine-induced long QT syndrome: Incidence and presenting features. *Circulation*, 68 (suppl III):III-276, 1983.
- [163] M.R. Rosen. The links between basic and clinical cardiac electrophysiology. *Circulation*, 77:251-263, 1988.

- [164] D. Roy, F.E. Marchlinski, J.U. Doherty, A.E. Buxton, and M.E. Josephson. Pharmacologic therapy for survivors of sudden death based on programmed stimulation. In M.E. Josephson, editor, *Sudden cardiac death*, pages 179–185, F.A. Davis, Philadelphia, 1985.
- [165] D. Roy, F.E. Marchlinski, J.U. Doherty, A.E. Buxton, H.L. Waxman, and M.E. Josephson. Electrophysiological testing of survivors of cardiac arrest. In M.E. Josephson, editor, *Sudden cardiac death*, pages 171–177, F.A. Davis, Philadelphia, 1985.
- [166] Y. Rudy and B.J. Messinger-Rapport. The inverse problem in electrocardiography: Solutions in terms of epicardial potentials. *CRC Crit Rev Biomed Eng*, 16:215–268, 1988.
- [167] H. Scholz. Antiarrhythmische und kardiodepressive Wirkungen antiarrhythmischer Substanzen. *Z Kardiol*, 77 (suppl 5):113–119, 1988.
- [168] P.J. Schwartz, M. Periti, and A. Malliani. The long QT syndrome. *Am Heart J*, 89:378–390, 1975.
- [169] P.J. Schwartz and S. Wolf. QT interval prolongation as predictor of sudden death in patients with myocardial infarction. *Circulation*, 57:1074–1077, 1978.
- [170] X. Shen and C. Antzelevitch. Mechanisms underlying the antiarrhythmic and arrhythmogenic actions of quinidine in a Purkinje fiber–ischemic gap preparation of reflected reentry. *Circulation*, 73:1342–1353, 1986.
- [171] J.D. Sherwood, B. Hoyt, P.J. MacInnis, R. Potter, and B.M. Horáček. A high performance data acquisition system for body surface potential mapping. In *Proc 10th Can Med & Biol Eng Conf*, pages 99–100, CMBES, Ottawa, 1984.
- [172] L.A. Siddoway, D.M. Roden, and R.L. Woosley. Clinical pharmacology of old and new antiarrhythmic drugs. In M.E. Josephson, editor, *Sudden Cardiac Death*, pages 199–248, F.A. Davis, Philadelphia, 1985.
- [173] M.B. Simson. Use of signals in the terminal QRS complex to identify patients with ventricular tachycardia after myocardial infarction. *Circulation*, 64:235–242, 1981.
- [174] M.B. Simson, M. Kanovsky, R.A. Falcone, C. Dresden, and M.E. Josephson. Noninvasive methods of predicting patients at risk for malignant ventricular arrhythmias. In M.E. Josephson and H.J.J. Wellens, editors, *Tachycardias: Mechanisms, diagnosis, treatment*, pages 507–518, Lea & Febiger, Philadelphia, 1984.
- [175] M.B. Simson, M.S. Kanovsky, C.A. Dresden, R.A. Falcone, and M.E. Josephson. Signal averaging methods to select patients at risk for lethal arrhythmias. In M.E. Josephson, editor, *Sudden cardiac death*, pages 145–153, F.A. Davis, Philadelphia, 1985.

- [176] M.S. Smith and L.C. Pritchett. Electrocardiographic monitoring in ambulatory patients with cardiac arrhythmias. In D.P. Zipes, editor, *Cardiology clinics*, pages 293–304, W.B. Saunders, Philadelphia, 1983.
- [177] J.R. Sommer and R.B. Jennings. Ultrastructure of cardiac muscle. In H.A. Fozzard, E. Huber, R.B. Jennings, A.M. Katz, and H.E. Morgan, editors, *The heart and cardiovascular system: Scientific foundations*, pages 3–50, Raven Press, New York, 1991.
- [178] G. Sun. *Event detection, data reduction, and classification of body surface potential maps*. PhD thesis, Case Western Reserve University, Cleveland, Oh, 1989.
- [179] K. Suzuki, S. Toyama, K. Yoshino, and Y. Fudemoto. Relation between the location of the infarcted area in body surface isopotential mapping and the location of the myocardial infarction in vectorcardiography. *J Electrocardiol*, 17:47–54, 1984.
- [180] P.A. Sytkowski, W.B. Kannel, and R.B. D'Agostino. Changes in risk factors and the decline in mortality from cardiovascular disease. *N Engl J Med*, 322:1635–1641, 1990.
- [181] B. Taccardi. Distribution of heart potentials on the thoracic surface of normal human subjects. *Circ Res*, 12:341–352, 1963.
- [182] B. Taccardi, L. De Ambroggi, and C. Viganotti. Body surface mapping of heart potentials. In C.V. Nelson and D.B. Geselowitz, editors, *The theoretical basis of electrocardiology*, pages 436–466, Clarendon Press, Oxford, 1976.
- [183] G. Turitto, J.M. Fontaine, and S.N. Ursell. Value of the signal averaged electrocardiogram as a predictor of the results of programmed stimulation in non-sustained ventricular tachycardia. *Am J Cardiol*, 61:1272–1278, 1988.
- [184] G.J.H. Uijen, A. Heringa, and A. van Oosterom. Data reduction of body surface potential maps by means of orthogonal expansions. *IEEE Trans Biomed Eng*, BME-31:706–714, 1984.
- [185] G.J.H. Uijen, A. Heringa, A. van Oosterom, and R.Th. van Dam. Body surface maps and the conventional 12-lead ECG compared by studying their performances in classification of old myocardial infarction. *J Electrocardiol*, 20:193–202, 1987.
- [186] P. Urie, M.J. Burgess, R.L. Lux, R.F. Wyatt, and J.A. Abildskov. The electrocardiographic recognition of cardiac states at high risk of ventricular arrhythmias: an experimental study in dogs. *Circ Res*, 42:350–358, 1978.
- [187] P.J. Vatterott, K.R. Bailey, and S.C. Hammill. Improving the predictive ability of the signal-averaged electrocardiogram with a linear logistic model incorporating clinical variables. *Circulation*, 81:797–804, 1990.

- [188] G.M. Vincent, L.S. Green, R.L. Lux, M.H. Merchant, and J.A. Abildskov. Use of QRST area distributions to predict vulnerability to cardiac death following myocardial infarction. *Circulation*, 68(suppl III):III-352, 1983.
- [189] B. Vondenbusch, J. Silny, R.V. Essen, B. Ludwig, G. Rau, and S. Effert. ECG-mapping during coronary dilatation: improvement of diagnosis and therapy control. *IEEE Trans Biomed Eng*, BME-32:43-46, 1985.
- [190] S. Vozech, T. Uematsu, T.W. Guentert, H.R. Ha, and F. Follath. Kinetics and electrocardiographic changes after oral 3-OH-quinidine in healthy subjects. *Clin Pharmacol Ther*, 37:575-581, 1985.
- [191] H.L. Waxman, A.E. Buxton, F.E. Marchlinski, and M.E. Josephson. Pharmacologic therapy of sustained ventricular tachyarrhythmias. In M.E. Josephson and H.J.J. Wellens, editors, *Tachycardias: Mechanisms, diagnosis, treatment*, pages 399-412, Lea & Febiger, Philadelphia, 1984.
- [192] H.J.J. Wellens and P. Brugada. Value of programmed stimulation of the heart in patients with the Wolff-Parkinson-White syndrome. In M.E. Josephson and H.J.J. Wellens, editors, *Tachycardias: Mechanisms, diagnosis, treatment*, pages 199-221, Lea & Febiger, Philadelphia, 1984.
- [193] H.J.J. Wellens and P. Brugada. Value of programmed stimulation of the heart in patients with the Wolff-Parkinson-White syndrome. In M.E. Josephson and H.J.J. Wellens, editors, *Tachycardias: Mechanisms, Diagnosis, Treatment*, pages 199-221, Lea & Febiger, Philadelphia, 1984.
- [194] H.J.J. Wellens, D.R. Durrer, and K.I. Lie. Observations on mechanisms of ventricular tachycardia in man. *Circulation*, 54:237-244, 1976.
- [195] H.J.J. Wellens, K.I. Lie, and D. Durrer. Further observations on ventricular tachycardia as studied by electrical stimulation of the heart. Chronic recurrent ventricular tachycardia and ventricular tachycardia during acute myocardial infarction. *Circulation*, 49:647-653, 1974.
- [196] L. Wilkinson. *SYSTAT: The system for statistics*. SYSTAT Inc., Evanston, IL, 1987.
- [197] E.M. Vaughan Williams. Electrophysiological basis for a rational approach to antidysrhythmic drug therapy. *Adv drug research*, 9:69-101, 1974.
- [198] R.A. Winkle. Ambulatory electrocardiography and the diagnosis, evaluation, and treatment of chronic ventricular arrhythmias. *Prog Cardiovasc Dis*, 23:99-128, 1980.
- [199] R.A. Winkle. Clinical pharmacology of new antiarrhythmic drugs. In M.E. Josephson and H.J.J. Wellens, editors, *Tachycardias: Mechanisms, diagnosis, treatment*, pages 387-397, Lea & Febiger, Philadelphia, 1984.

- [200] R.A. Winkle, A.H. Gradman, and J.W. Fitzgerald. Antiarrhythmic drug effect assessed from ventricular arrhythmia reduction in the ambulatory electrocardiogram and treadmill test: Comparison of propranolol, procainamide, and quinidine. *Am J Cardiol*, 42:473, 1978.
- [201] S.L. Winters, D. Stewart, and J.A. Gomes. Signal averaging of surface qrs complex predicts inducibility of ventricular tachycardia in patients with syncope of unknown origin: A prospective study. *J. Am Coll Cardiology*, 10:775-781, 1987.
- [202] A.L. Wit and M.R. Rosen. Afterdepolarizations and triggered activity. In H.A. Fozzard, E. Huber, R.B. Jennings, A.M. Katz, and H.E. Morgan, editors, *The heart and cardiovascular system: Scientific foundations*, pages 1449-1487, Raven Press, New York, 1986.
- [203] A.L. Wit and M.R. Rosen. Cellular electrophysiology of cardiac arrhythmias. In M.E. Josephson and H.J.J. Wellens, editors, *Tachycardias: Mechanisms, diagnosis, treatment*, pages 1-27, Lea & Febiger, Philadelphia, 1984.
- [204] M. Zehender, A. Geibel, S. Hohnloser, T. Meinertz, and H. Just. Standardization of noninvasive and invasive studies in the assessment of patients with ventricular arrhythmias. In P. Brugada and H.J.J. Wellens, editors, *Cardiac arrhythmias: Where to go from here?*, pages 435-455, Futura Publishing Co, Mount Kisco, NY, 1987.
- [205] D.P. Zipes. Autonomic innervation of the heart: Role in arrhythmia development during ischemia and in the long QT syndrome. In H.A. Fozzard, E. Huber, R.B. Jennings, A.M. Katz, and H.E. Morgan, editors, *The heart and cardiovascular system: Scientific foundations*, pages 2095-2112, Raven Press, New York, 1991.